The role of AgRax1p, AgRax2p, AgBud7p and AgBud10p in mycelial development of the filamentous fungus *Ashbya gossypii*

Inauguraldissertation

zur
Erlangung der Würde eines Doktors der Philosophie
vorgelegt der
Philosophisch-Naturwissenschaftlichen Fakultät
der Universität Basel

von

Kamila Wojnowska-Boudier
aus Gdynia, Polen

Basel, 2005

Genehmigt von der Philosophisch-Naturwissenschaftlichen Fakultät auf Antrag von Prof. M. Primmig, Dr. M.-P. Gulli und Prof. P. Philippsen

Basel, den 27. Juni 2005

Prof. Dr. Hans-Jakob Wirz
Dekan

Table of Contents

Summary 6

General Introduction 7

Chapter1: AgRax1p and AgRax2p are involved in spatial and temporal control of branching

Introduction 12

Results 12

The *A. gossypii* homologues of the *S. cerevisiae RAX1* and *RAX2* genes 12

AgRax1p and AgRax2p might be required for the selection of a new axis of polarity 14

AgRax1p and AgRax2p are involved in maintenance of polar growth and temporal regulation of branch emergence 16

Selection of branch and septum sites take place in Agrax2 mutant but is not always followed by polarity establishment 18

AgRax1p and AgRax2p are involved in the maintenance of polarity at the tip 19

AgRax1p and AgRax2p play a role in focusing actin patches to the tip region 20

Absence of AgRax1p and AgRax2p do not have an impact for microtubule cytoskeleton organization 22

Absence of AgRax1p and AgRax2p do not influence chitin deposition 22

AgRax1p and AgRax2p may function in the same pathway 22

AgRax1p and AgRax2p act downstream of AgSep7p in the septation process 22

AgRax1p and AgRax2p do not have an impact on the localization of the polarisome marker AgSpa2p at the tip but may have an impact on the protein abundance at the septum 23

AgSpa2p acts independently on AgRax1p and AgRax2p to maintain a new axis of polarity 25

AgRax2p acts independently of AgBud10p to maintain a new axis of polarity 26

A functional GFP fusion to AgRax2p locates to the tip and the septum region 29

AgRax2p localizes permanently to sites of polarized growth 29

AgRax2p is continuously delivered to the tip 32

AgRax2p delivery to the tip is actin dependent 32

A functional GFP fusion to AgRax2p only partially co-localizes with Spitzenkörper 33

A signal sequence is essential for the localization of AgRax2p 34

AgRax1p is essential for the proper AgRax2p deposition at the tip and septum 35

AgBud10p stabilizes AgRax2p at the tip 35

AgCdc24p is essential for the cortical localization of AgRax2p at new growth sites 36

AgBni1p not essential for the AgRax2p initial polarization 36

A functional GFP fusion of AgRax2p locates to the septum region 38

AgRax2p co-localize only with the single actin ring and its localization to the septum region depends on actin 40

AgBni1p is not essential for the AgRax2p initial localization at the septum 41

AgCyk1p dependent actin ring formation is essential for the initial deposition of AgRax2p at the septum 41

Discussion 43

Regulation of cell polarity 43

AgRax1p and AgRax2p are potential candidates for control of polarity in *A.gossypii* 43

Organization of polarization at the tip in *A.gossypii* 45

Organization of polarization at the septum in *A.gossypii* 46

AgRax proteins are likely part of a landmark complex – Model 47

Chapter 2: AgBud7p help maintaining sustained polar growth

Introduction 49

Results 49

The *A. gossypii* homologue of the *S. cerevisiae* twin genes *ScBUD7* and *ScBCH1* 49

ScBud7p and ScBch1p may be involved in the final step of cell wall synthesis at the septum 49

ScBud7p and ScBch1p are involved in budding of diploid *S. cerevisiae* 52

*Agbud7*Δ deletion influenced the average growth speed of the mycelium 52

*Agbud7*Δ plays a role in selection of sites for germ tube formation at the cortex of germinating spores 52

AgBud7p could be required for the maintenance of hyphal tip shape 53

Actin rings are formed with a delay in *Agbud7*Δ 55

AgBud7p is involved in sporulation 56

A functional GFP fusion to AgBud7p locates to vesicle-like structures 56

AgBud7-GFP oscillations most probable depend on the flow of cytoplasm 58

Part of AgBud7-GFP signal co-localizes with Spindle Pole Bodies 58

Discussion 60

ScBud7p andScBch1p are involved in the budding pattern of *S.cerevisiae* 60

AgBud7p maintains polar growth likely by supporting the cell wall construction 60

Chapter3: Heterologous complementation in *S.cerevisiae* by *A.gossypii* genes

Introduction 62

Results and Discussion 62

A.gossypii RAX1, *RAX2* and *BUD8* complement deletions of *S.cerevisiae RAX1*, *RAX2* and *BUD8* genes 62

The evolutionary rearranged *ScBUD9* promoter does not allow complementation of the *ScBUD9* deletion by the *A.gossypii* homologue 64

Chapter4: Materials and Methods

A.gossypii and *E.coli* strains used in this work 66

Growth conditions 66

Genomic DNA isolation 66

Cytoskeletal staining 66

Tubulin staining 66

Hoechst staining 67

Calcofluor staining 67

FM 4-64 staining 67
Image acquisition and processing 67
Analysis of sequences and standard procedures 68
Construction of the deletion mutants; Transformation of *A. gossypii* strains 68
Generation of C-Terminal GFP fusions to different genes 69
Plasmid isolation 69
Yeast strains, growth conditions, and genetic methods 69
Cloning 69
Cloning of pRS415_*RAX1* 69
Construction of N-terminal GFP fusion to pRS415_*RAX1* 70
Cloning of pRS415_*RAX2* 70
Construction of pRS415_*RAX2*_GFP 70
Construction of pRS415_*RAX2*_DSP and pRS415_*RAX2*_DSP-GFP 70
Cloning of pRS415_*BUD7* 70
Construction of a N-terminal GFP fusion of pAg*BUD8* and cloning of pRS415_*BUD8*_NTGFP 71
Cloning of pRS415_*SEC4*-RFP 71
Table 1. Oligonucleotides used for the construction of the deletions and GFP fusions in *A.gossypii* 72
Table 2. *A.gossypii* strains used in these studies 73
Table 3. Oligonucleotides used to create the *S.cerevisiae* mutants 75
Table 4. *S.cerevisiae* strains used in these studies 76
Table 5. Oligonucleotides used for cloning 77
Table 6. Plasmids used in these studies 77

Curriculum vitae 81
Appendix: Additional gene analyses 83
Abbreviations 87
Acknowledgments 88
References 89

Summary

Polarized growth is essential for hyphal and mycelial morphogenesis. The diversity of fungal morphology and development raises many questions considering the mechanism involved in selection of new polar growth sites. Landmark events of fungal growth include the emergence of germ tubes from a germinated spore, sustained hyphal tip extensions, lateral and apical branching and septation. The basis for each of these events is the polarized growth machinery and in contrast to the well studied polarized growth pattern in the budding yeast *S.cerevisiae*, the molecular requirements for the development of a fungal mycelium are not well known.

The filamentous fungus *Ashbya gossypii* and the budding yeast *S. cerevisiae* have different life styles despite very similar gene contents and conserved domain compositions of gene products.

In this work, I was investigating the role of several homologues of *S.cerevisiae* genes involved in the budding pattern in the filamentous ascomycete *A.gossypii.* Since *A.gossypii* does not grow by budding, it was interesting to search for the function of *S.cerevisiae BUD* gene homologues. It was hypothesized that genes controlling the budding pattern of this yeast could be landmarks involved in polarized growth control, branching or the stabilization of growth axis in the filamentous fungus *A.gossypii.*

The goal of Chapter one was to describe the role of AgRax1p and AgRax2p, homologues of the *S.cerevisiae* genes *ScRAX1* and *ScRAX2*. AgRax1p and AgRax2p are implicated in maintenance of cell polarity. They play important roles in emergence of germ tubes and lateral branches as well as in maintenance of permanent hyphal tip extension during tip branching. A related role was also suggested for ScRax2p in *S.cerevisiae*. Yeast Rax2p was implicated in the maintenance of the bipolar budding pattern but not in its establishment, in diploid *S.cerevisiae* cells (Chen, et al. 2000). AgSpa2-GFP, a polarity marker was maintained at the hyphal tip in *Agrax1*Δ and *Agrax2*Δ strain during polarized growth as described before for the wild type. Thus AgRax1p and AgRax2p might not be permanently required during polarized growth but only in response to distinct events. Such events might be the initiation of a second germ tube or a lateral branch, which cause the hyphal tip growth speed to temporary slow down even though polarization at the tip is maintained. Thus, AgRax1p and AgRax2p might be required for reinforcement of polarization in response to branching in order to maintain permanent hyphal tip extension.

I show here that AgRax2p is involved in the temporal regulation of branch emergence by maintenance of polarity at selected branch sites. Furthermore, we prove that AgRax1p and AgRax2p signal peptide are essential for the proper localization of AgRax2p. AgRax2p might be placed at the tips in response to a lateral branching or septation event. Additionally, I demonstrate that AgRax2p has a role in the septation process where it may persist to direct future branching events. The first chapter also contains information about the probable role of AgBud10p in polarity maintenance.

In the second Chapter, I describe a possible role of AgBud7p in the maintenance of sustained polar growth and for the sporulation process. The fact that the *AgBUD7* gene has two homologues in *S.cerevisiae* gave this work a more interesting dimension. I verified the role of both homologues in *S.cerevisiae* and performed in addition experiments with a number of double deletions. The phenotypes obtained helped to analyse the role of AgBud7p in filamentous growth. GFP fluorescence of AgBud7p-GFP transformants was highly enriched in small organelles, which were constantly oscillating with about the same amplitude in young and in old mycelium. Moreover, I present evidence that the observed AgBud7-GFP movements rather depend on the flow of cytoplasm than on actin-based structures. Co-localization studies indicated that a small number of AgBud7p-vesicles co-localize with Spindle Pole Bodies. Studies done in *S.cerevisiae* indicated a colocalization of ScBud7p with late Golgi structures. Presently, late Golgi structures cannot be visualized in *A.gossypii* to allow a comparison with the *S.cerevisiae* data. The 40% decrease in maximal radial growth speed determined from *Agbud7*Δ colonies and significant deviations from the growth axis suggest that AgBud7p could be required for the maintenance of hyphal tip shape by delivering certain substances to the cortical membrane. In the absence of AgBud7p an insufficient amount of building materials is transported to the growing tips leading to a decrease in hyphal diameter and to changes in growth direction.

The last chapter presents the results of heterologous complementation experiments done in *S.cerevisiae*. The goal was to analyze whether *A.gossypii* proteins involved in diverse polar growth events can complement *S.cerevisiae* deletions of homologous genes. In these cases the *A.gossypii* and the *S.cerevisiae* gene diverged from a common ancestral gene over 100 million years ago. In all of the cases tested full or at least partial complementation was found. This chapter again shows the power of knowledge about *A.gossypii* genomics in understanding the degree of evolutionary conservation of protein functions and of gene promoters.

These and other results highlight common themes for the genetic regulation of growth guidance in eukaryotic cells and make filamentous fungi powerful model systems to elucidate the molecular mechanisms that regulate these processes.

General Introduction

A central feature of cellular morphogenesis is cell polarization, which involves the asymmetric organization of the cytoskeleton, secretory system and plasma membrane components along an appropriate axis (Drubin and Nelson 1996). The ability of cells to polarize is essential to mediate functions as diverse as vectorial transport in epithelial cells, directed cell movement in amoeba or leukocytes, cell shape development in early embryogenesis, neurite outgrowth or mycelium development in fungi.

The cell polarity consists of three hierarchical and interdependent steps. First a response to intra and/or extracellular signals and selection of polar sites, second the generation of an axis of polarity in response to this signal and third the subsequent asymmetric distribution of cellular components along this axis. Feedback loops reinforce the ordering of these events resulting in the maintenance of cell polarity.

Polar growth requires selection of specific sites, establishment of polarity at those sites and finally it requires mechanisms that control the stability of growth axis. Although hyphal tip growth has been correlated with turgor pressure (Wessels, 1986), with pH gradient (Robson, Prebble et al. 1996) and with Ca gradient (Regalado 1998), the molecular mechanisms responsible for the hyphal development are largely unknown.

Many of the conserved proteins that have been implicated in cell polarity in a variety of other organisms contribute to filamentous growth of *A.gossypii*. However, still relatively little is known about the molecular nature of putative landmark proteins involved in the selection of polar sites.

The goal of this work was to find the potential landmarks that control polarity in the filamentous fungus *A.gossypii.*

Cell polarity has been most intensively investigated in the budding yeast *S.cerevisiae*. This yeast exhibits two distinct patterns of polarization-axis selection and oriented cell division depending on the cell type (Freifelder, 1960; Hicks *et al*., 1977; Chant and Pringle, 1995) **(Fig. 1)**. It has been shown, that the position of bud emergence and thus the position of the cleavage plane, is determined by landmark proteins. A specific set of genes seems to be required for either the diploid-specific bipolar bud site selection or the haploid-specific axial budding pattern (Chant *et al*., 1996).

Bipolar budding relies on persistent cues at the poles. Of the gene products identified as required for bipolar budding, three have hallmarks of such cues. Interestingly, ScBud8p is at the distal pole and its loss prevents budding from that pole, whereas ScBud9p localizes to the proximal pole (the former bud neck when the cell was still a bud), and its loss prevents budding from that pole (Zahner, Harkins et al. 1996; Taheri, Kohler et al. 2000; Harkins, Page et al. 2001). These results suggest that ScBud8p and/or ScBud9p contribute to the signalling that recruits the bud initiation machinery to the respective poles. ScRax2p, is deposited at the cell surface with each cell division, which results in its appearance at both poles. This highly stable protein is not required for positioning a new cell‘s first bud, but it is required to maintain bipolar budding over multiple generations (Chen, Hiroko et al. 2000), suggesting it stabilizes the ScBud8p/ScBud9p-dependent cues (Pruyne, Legesse-Miller et al. 2004).

Axial budding relies on cues associated with the previous bud site. The axial program depends on a ring of septin filaments that are assembled prior to bud emergence and remain at the bud neck throughout the cell cycle. Among proteins identified as important for this pathway, a transmembrane protein, the bud neck-associated ScAxl2p/ScBud10p (Halme,

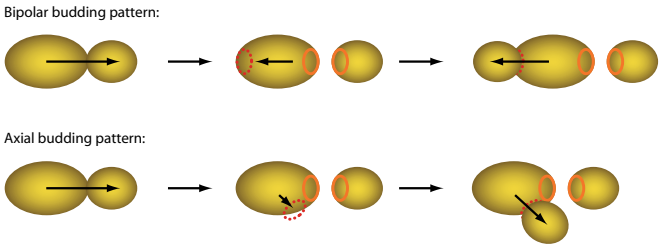

Figure 1
Budding patterns of *S.cerevisiae*.

Michelitch et al. 1996; Roemer, Vallier et al. 1996; Kang, Sanson et al. 2001) appears to be the most critical for axial budding (Fujita, Oka et al. 1994; Lord, Inose et al. 2002). In the absence of the axial program, haploids revert to the bipolar pattern (Chant and Herskowitz 1991).

The axial and bipolar budding programs feed into a common pathway - a module composed of a ras-related GTPase, ScRsr1p/ScBud1p (Bender and Pringle 1989; Chant and Herskowitz 1991; Park, Chant et al. 1993), its regulatory GTPase-activating protein (GAP) ScBud2p (Park, Chant et al. 1993) and guanine-nucleotide exchange factor (GEF) ScBud5p (Chant et al. 1991). All three are cortical proteins that become enriched at the nascent bud site (Michelitch and Chant 1996; Marston, Chen et al. 2001) suggesting they are physically recruited by the budding pattern cues. However, several studies recently examined how singularity of polarity can be achieved without cortical cues (Gulli, Jaquenoud et al. 2000; Caviston, Tcheperegine et al. 2002; Irazoqui, Gladfelter et al. 2003; Wedlich-Soldner, Altschuler et al. 2003).

Landmarks from previous budding cycles are interpreted by the bud site-selection protein Bud1p that provides a spatial cue for Cdc24p/Cdc42p/Bem1p polarity establishment proteins, likely through direct interactions with all three (Kozminski, Beven et al. 2003; Pruyne, Legesse-Miller et al. 2004) **(Fig. 2)**.

Studies on cell polarity in other eukaryotic organisms as the fission yeast *S.pombe*, *C.elegans*, *Drosophila* or cultured mammalian cells suggest that the molecular mechanism underlying cell polarity is conserved among eukaryotes.

A variety of studies from all of these systems demonstrate that the Cdc42p GTPase and other Rho-type GTPases are key players in the establishment and maintenance of cell polarity.

The activity of Cdc42p is controlled via its nucleotide bound state. Cdc42p bound to GTP is active whereas Cdc42p bound to GDP is inactive. Guanine nucleotide exchange factors (GEFs) and GTPase activating proteins (GAPs) are regulators of Cdc42p. GEFs catalyse the transition from the GDP to the GTP bound form, thereby activating Cdc42p whereas GAPs activate the intrinsic GTPase activity of Cdc42p, which leads to a hydrolysis of the bound GTP to GDP and a subsequent inactivation of Cdc42p. The regulators of Cdc42p respond to intra and/or extracellular signals to activate or inactivate Cdc42p (Hall 1998; Johnson 1999). Locally activated Cdc42p signals act with a variety of effectors to assemble polarized cytoskeleton.

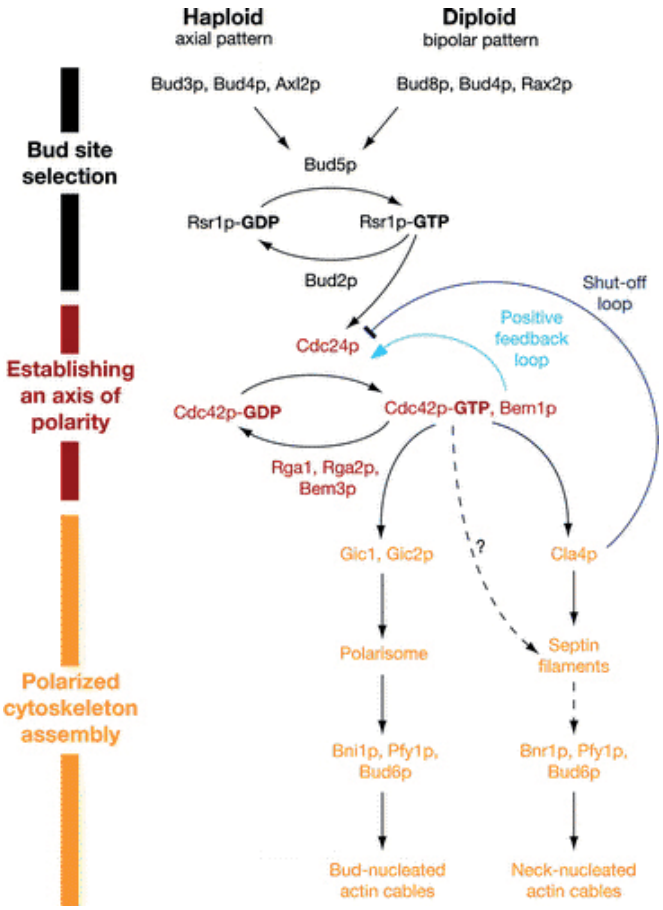

Figure 2
Simplified overview of the signalling pathways that lead to the establishment of a polarized cytoskeleton early in the cell cycle. Black arrows indicate direct physical interactions, whereas dotted arrows indicate pathways that may not be direct. Additional components and interactions exist and were omitted for simplicity. *AXL2* is also known as *BUD10*, and *RSR1* is also know as *BUD1*. Pathways operating later in the cell cycle are not included (Pruyne et al., 2005).

In filamentous fungi, cell polarity is the basis for hyphal morphogenesis. In 1926 Ashby and Nowell have described for the first time *Ashbya gossypii*, a plant pathogen that causes stigmatomycosis in fruit such as cotton (*Gossypium hirsutum*) or subtropical citrus fruits.

A. gossypii does not develop specialized infection structures such as penetrational hyphae. It relies on heteropterous insects for dispersal of spores or mycelial fragments. The spread of the disease is therefore readily controlled with insecticides, which might be one of the reasons why *A. gossypii* is not a devastating plant pathogen.

This fact together with the developmental pattern being similar to other pathogenic fungi and several properties and established techniques make *A.gossypii* an interesting model organism to study cell polarity. For example, homologous recombination that functions as the main mechanism for DNA integration (Steiner, Wendland et al. 1995) and replicative plasmids bearing CEN/ARS elements from *S.cerevisiae* are maintained under appropriate conditions (Wright and Philippsen 1991). The PCR based gene targeting works as an efficient tool for the generation of deletions and gene fusions (Wendland et al., 2000). Several selectable marker genes for dominant selection (antibiotic resistance) and strains auxotrophic for *LEU2* (leucine biosynthesis) and *THR4* (threonine biosynthesis) have been developed. Additionally, the green fluorescent protein (GFP) used for protein localization studies and a number of fluorescent dyes can be used in *A. gossypii* to stain the actin cytoskeleton, vacuoles, nuclei and mitochondria. And finally, the genome is completely sequenced and annotated (Dietrich, Voegeli et al. 2004).

The completion of a whole genome sequencing approach in *A.gossypii* revealed a relatively small genome of only 9 Mbp encoding about 4700 genes with very few gene duplications (Dietrich, Voegeli et al. 2004). Interestingly, 96 % of all genes identified had a homologue in the budding yeast *S.cerevisiae* and for nearly all genes implicated in cell polarity in *S.cerevisiae* orthologues could be identified in *A.gossypii*. This included Rho-type and Ras GTPase modules, regulators of these modules, scaffold proteins, formin homologues and PAK kinases and proteins involved in bud site selection in haploid and diploid *S.cerevisiae* cells (Madden and Snyder 1998; Chant 1999; Johnson 1999; Pruyne and Bretscher

2000; Pruyne and Bretscher 2000; Gulli and Peter 2001; Casamayor and Snyder 2002; Pruyne, Legesse-Miller et al. 2004).

It was unexpected that such distinct cellular morphogenesis as budding in *S.cerevisiae* and filamentous growth in *A.gossypii* requires a very similar set of genes.

The developmental pattern of *A.gossypii* starts with an isotropic growth phase **(Fig 3A-B)**. Polarized growth leads to the initiation of the first germ tube to form the unipolar germling **(Fig 3C)**. A second site of polarisation is established at the periphery of the germ bubble to induce a second germ tube and this generates the bipolar germling **(Fig 3D)**. Further, the establishment of cell polarity directs polarized growth spatially which initiates germ tubes and lateral branches **(Fig 3E)**. Filamentous fungi maintain cell polarity at tips of hyphae resulting in a permanent apical extension.

Hyphal tubes elongate and new hyphal tips are formed by lateral branching, which requires new polar site selection. This generates a juvenile mycelium. About 20-24 hours post-germination, a mature state of mycelial growth is reached and the edges of *A. gossypii* colonies produce new tips exclusively using a dichotomous branching pattern (Y-shaped hyphal filaments) **(Fig 3F)**. The life cycle ends when the mycelium has produced new spores **(Fig 3G)**. This occurs in the older parts of the mycelium and requires entry into a different developmental phase.

Furthermore, a polarization within hyphae directs the formation of a septum, the incomplete cytokinesis in *A.gossypii* that lacks cell-cell separation (Ayad-Durieux, Knechtle et al. 2000; Wendland and Philippsen 2000; Wendland and Philippsen 2001; Knechtle, Dietrich et al. 2003).

All presented events, like branching, permanent polarized growth and septation are landmarks of filamentous growth (Harris, Hamer et al. 1997; Momany and Hamer 1997; Spohr, Dam-Mikkelsen et al. 1998; Lengeler, Davidson et al. 2000; Momany and Taylor 2000; Wendland and Philippsen 2001). It was hypothesized that *A.gossypii* homologues that are implicated in polarized growth in *S.cerevisiae*, could guide the process of filamentous growth.

A number of studies with *A.gossypii* have characterized potential players involved in regulation of polar growth in this filamentous fungus. The table below summarizes our knowledge about proteins important for the *A.gossypii* morphogenesis. All indicated proteins have homologues in budding yeast and their role in most of the cases is already proposed.

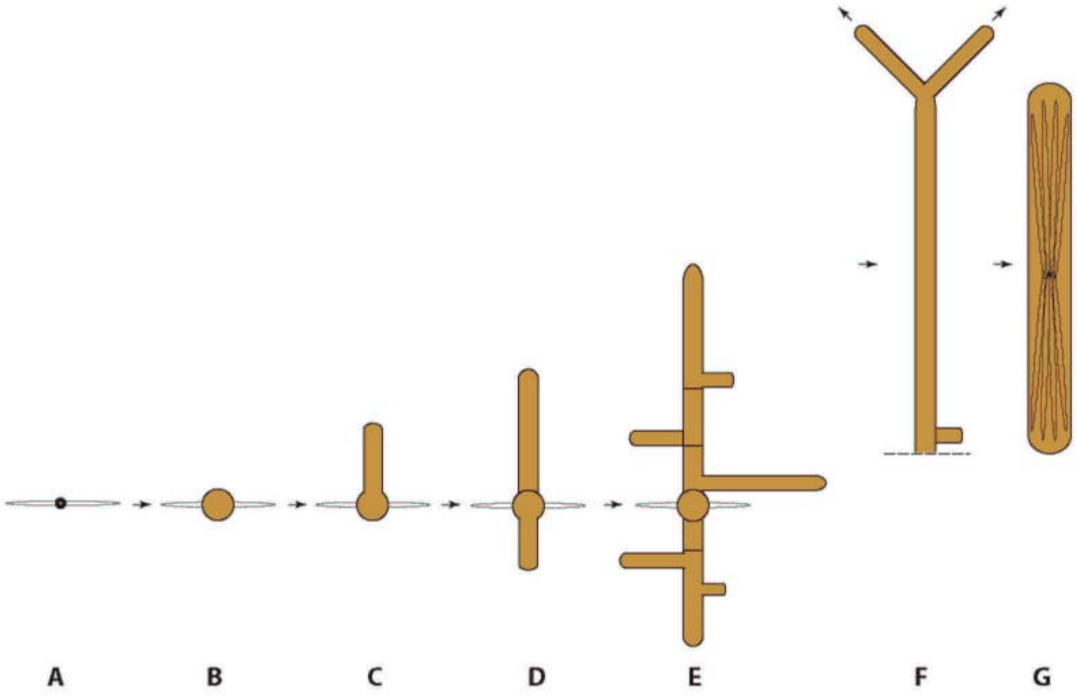

Figure 3
Schematic developmental pattern of *Ashbya gossypii*. For more details, please see the text.

Protein	Phenotype of the deletion in *A.gossypii*	Proposed role in *A.gossypii*
Bud1	Deletion of *BUD1* reduces the growth rate dramatically. Pausing and resumption of growth indicates that alternative routes of Cdc42 activation exist which could explain the zig-zag phenotype of *bud1* hyphal growth. Bud1 does not seem to have a role in the early phases of germination and the generation of the bipolar germination pattern.	The Bud1 is required for maintenance of hyphal growth and determination of the site of polarized growth. It governs the localization of the polarizome component Spa2. Bud1 module activates the polarizome through the Cdc42 module.
Bud2	Deletion of *BUD2* shows similar phenotype to *bud*1Δ	Part of Bud1 GTPase module.
Bud5	Wild type like phenotype	Part of Bud1 GTPase module.
Cdc24 and Cdc42	Deletion of a *CDC42* or its putative GEF *CDC24*, still allowed isotropic growth of the spore but prevented the establishment of cell polarity. These germ cells failed to polarize the cortical actin patches and never formed germ tubes.	Cdc24 and Cdc42 are required for correct cell polarization.
Bem2	*bem2* germ cells have a prolonged isotropic growth phase, generate enlarged germ cells that fail to produce the bipolar germination pattern. Hyphae were swollen and the cortical actin patches were delocalized. Loss of polarity in the swollen hyphal tips of *bem2* mutants was overcome by establishing new cell polarities to form new hyphal tips at random positions.	Bem2 determines cell polarity in germinated spores and hyphal tips. Bem2 regulates the activity of Cdc42.
Rho1	Mutant *Rho1* strains were non-viable, as hyphae lysed at the microcolony stage	Rho1 controls functions of the cell-wall-integrity pathway for polarized growth.
Rho3	*RHO3* deletion mutants showed defects in polarized morphogenesis. First, during the hyphal growth phase, swellings occurred at the hyphal tips. Second, where recurrent polarized growth occurred, the direction of growth was maintained in the axis of previous cell polarity. Finally, during germination at elevated temperatures, deletion of *RHO3* resulted in lethality and lysis of the primary germ tube.	Rho3 is important for polarity maintenance.
Spa2	*spa2* mutant hyphae growth was slowed down, but the organization of the actin cytoskeleton was not disturbed.	Spa2 delimit the region of hyphal tip growth, therefore determining the diameter of the hyphae. *SPA2* deletion did not eliminate either polarisome or formin activity.
Bni1	Deletion of *BNI1* is *l*ethal	Bni1 is essential factor for elongation of hyphae and for symmetric hyphal tip branching.
Cla4	The *cla4* mutation showed defects in hyphal growth as well as defects in septation.	A member of the p21 activated kinases, Cla4 is downstream target of Rho-protein signalling pathway. A potential effector of Cdc42 was shown to be required for hyphal maturation. Cla4 might be involved in a tip-based process of positioning early septal protein complexes at regular intervals along the hyphal tube.
Bud3	*bud3* mutant show partial defects in septum formation. Some septa seemed normal, whereas at malformed septal sites, aberrant deposition of chitin occurred. The actin cytoskeleton in *bud3* mutants was defective for actin-ring formation (linear actin filaments, attached to the cell cortex, were formed).	Bud3 protein transiently localizes to septal sites. This localization might be sufficient to serve as positional information for lateral branching. Bud3 is upstream of Cyk1.
Cyk1	Cyk1 is essential for actin ring formation.	Linear actin rings co-localized with linear Cyk1 filaments. Cyk1 filaments also undergo ring constriction, which indicates that Cyk1 is not only required for the formation of the actin ring but also for the dynamic processes of the ring.

Wal1	Disruption of *WAL1* in led to slow and bulbous growth of hyphae, which failed to produce septa. The tips lack both cortical actin patches and early endosomes. Instead, a subapical accumulation of patches was observed. Movement of endosomes and vacuoles is greatly reduced.	Wal1 functions to co ordinate the positioning of cortical actin patches and endocytosis. Wal1 is a downstream target of Rho-protein signalling pathway.
Boi	Deletion of *BOI* caused lysis of germinated spores at elevated temperature. At the same hyphal length the boi strain displayed less lateral branches compared to wildtype.	Boi1 is required for establishment of cell polarity to initiate germ tubes and lateral branches and for maintenance of cell polarity to allow a permanent hyphal tip extension.

The majority of discovered potential signal cascades that regulate polarized hyphal growth and septation are presented below **(Fig. 4)**. Many of the conserved proteins that have been implicated in cell polarity in a variety of other organisms contribute to filamentous growth of *A.gossypii*. However, still relatively little is known about the molecular nature of putative landmark proteins involved in the selection of polar sites. In order to find potential landmarks of filamentous growth, I compared *A.gossypii* proteins with their orthologues in *S.cerevisiae*.

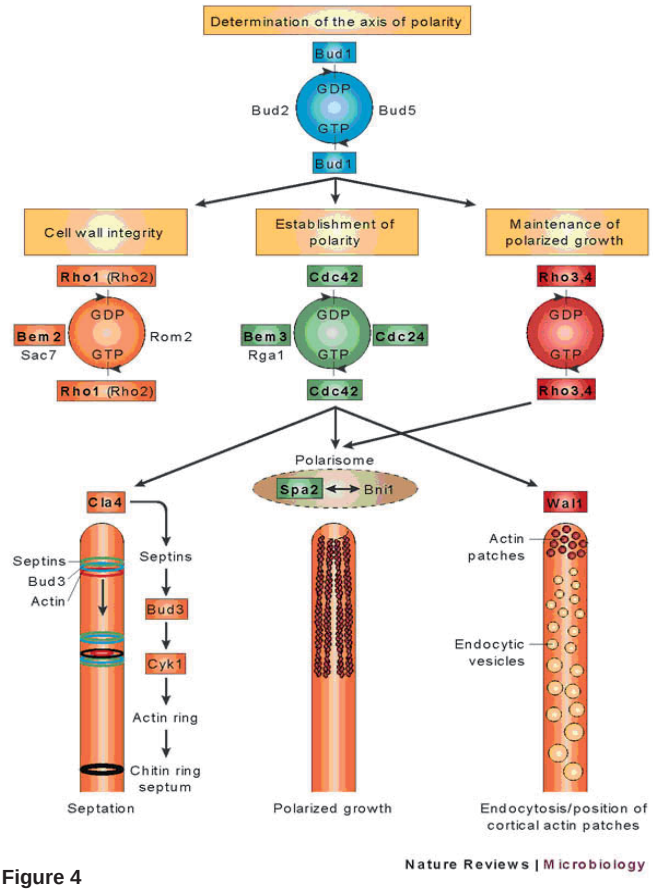

Figure 4
Potential signal cascades that regulate polarized hyphal growth and septation in *Ashbya gossypii*. Several GTPase modules have been identified in *A. gossypii*, mainly based on homology to those in *Saccharomyces cerevisiae*. Proteins shown in bold type correspond to genes that have been analysed in *A. gossypii*. The modules were found to be involved specifically in one of the indicated processes, which are important steps leading to polarized hyphal growth. This is a schematic model of a protein network that controls septation, polarized growth and endocytosis. (Wendland et al., 2005).

In this work I investigated the function of AgRax1p, AgRax2p, AgBud7p, AgBud10p and AgBud9p proteins in the filamentous ascomycete *Ashbya gossypii*, mainly focusing on the function of AgRax1p, AgRax2p and AgBud7p.
In Chapter 1 and Chapter 2, I describe the identification of 4 genes that are involved in polarized growth and I highlight their role as factors important for filamentous growth. At the end of the first two chapters I conclude where these proteins act in polar growth in *A.gossypii*.
In the final Chapter 3 I describe the results of complementation of *S.cerevisiae* bud gene deletions with *A.gossypii* homologues of the deleted genes.
This work contains as well a description of all tools that were established for the functional analysis of the genes investigated in the three chapters and a complete list of strains created for this work and for future use is presented here.

AgRax1p and AgRax2p are involved in spatial and temporal control of branching

Introduction

To extend our investigations about polarity control we screened the genome of the filamentous fungus *A. gossypii* (Ashby and Nowell, 1926), for the candidate genes implicated in the regulation of this process. Interestingly, we identified orthologues of the *S.cerevisiae* ScRax1p and ScRax2p in *A.gossypii* that exhibits a completely different morphological development than yeast.

ScRax1p and ScRax2p were implicated in bipolar budding in diploid *S. cerevisiae* cells. The genes encoding these proteins were originally identified by mutations that appeared to suppress the loss of axial budding in an *axl1* mutant (Fujita *et al.*, 1994; Chen *et al.*, 2000). A deletion of any of these genes causes similar phenotypes. Analysis of *Scrax1*Δ and *Scrax2*Δ budding patterns indicated that both proteins were involved in the selection of the bud sites at both the distal and proximal poles of daughter cells, as well as near previously used division sites on mother cells. ScRax1p and ScRax2p both appear to be integral membrane proteins. In the *S. cerevisiae* ScRax1p and ScRax2p were both observed at the distal pole as well as at the division site on both mother and daughter cells; localization to the division sites was persistent through multiple cell cycles.

In the *A. gossypii* AgRax1p and AgRax2p were found to be involved in the branch formation in young mycelium (placement and timing of newly formed branches) and in the maintenance of the straight axis of growth in mature mycelium.

The *A. gossypii* homologues of the *S. cerevisiae RAX1* and *RAX2* genes

We identified the potential transmembrane proteins AgRax1p and AgRax2p based on amino acid comparisons with *S. cerevisiae* proteins **(Fig.1)**. *A. gossypii* homologues of both ScRax1p and ScRax2p are conserved with respect to size and domain structure. AgRax1p and AgRax2p share 45% and 38% identity on amino acid level with its *S. cerevisiae* homologue, respectively. AgRax1p encodes a 48,624 kDa and AgRax2p 132,140 kDa-polypeptide. Apparently, AgRax1p and AgRax2p appear to be integral membrane proteins. AgRax1p contains 3 transmembrane domains near its C-terminus (280-302; 317-339; 396-418 aa), which are conserved with the *S. cerevisiae* homologue up to 45%, 56,2%, and 63,6% respectively, and one potential regulator of G-protein signalling domain (19-260 aa) conserved with the *S. cerevisiae* homologue up to 40,6%. AgRax2p contains one potential transmembrane domain near its C-terminus (1144-1166 aa), which is conserved with the *S. cerevisiae* homologue (66,7%). Additionally, the TM-Pred program searching for membrane topology (Hoffman and Stoffel, 1993) predicts that the short hydrophobic region at the N-terminus of AgRax2p (1-21 aa) may be a signal sequence (23,8% identity on amino acid level with the *S. cerevisiae* homologue).

The plasmids *p*RS*415RAX1* and *p*RS*415RAX2* carrying one copy of *AgRAX1* and *AgRAX2*, respectively, are able to complement the deletion of *ScRAX1* and *ScRAX2* as measured by a 68% and 66% restoration of the bipolar budding pattern in the respective mutants. The *Scrax1*Δ and *Scrax2*Δ mutants displayed a severe disruption of bipolar budding. Cells exhibited a rather non-random budding pattern (heterogeneous), however there was a strong bias in most cases for one end of the chain of bud scars to originate from the proximal pole. The presence of plasmid *pRS415RAX1* rescued the deletion phenotype observed for the diploid *Scrax1/Scrax1* strain. The majority of the cells carrying this plasmid exhibited the first bud at the distal position. Interestingly in almost 25% the third bud appeared in the equatorial region, which is slightly different from the wild type pattern. A similar budding pattern to the one described above was observed for the *Scrax2*Δ*/Scrax2*Δ deletion strain carrying the plasmid *p*RS*415RAX2* (for more details please see Materials and Methods).

To investigate the functions of AgRax1p and AgRax2p we deleted the whole ORF´s from start to stop codon using standard PCR-based gene targeting. For the single deletions we used the cassette coding for the resistance against the drug G418. To obtain *Agrax1*Δ*rax2*Δ mutants we deleted the entire *AgRAX2* ORF with a cassette coding for resistance against the drug clonNAT in the *Agrax1*Δ strain. Examination of single deletions showed that *AgRAX1* together with *AgRAX2* produced similar phenotypes. To explore the function of both genes we carefully analysed the development of the deletion mutants.

Interestingly, over 40% of *Agrax1*Δ and *Agrax2*Δ spores showed different morphology than wild type spores **(Fig. 2)**. Mutant spores often produced additional germ bubbles at the end and close to the centre of the needle-shaped spore. Sporulation in various osmolarity media did not change the abnormal shape of the mutant spores. The staining of the nuclei did not show any differences between the position of the nuclei in the abnormal and the wild type spore, where it was placed in the middle of the spore needle. Only 62% of *Agrax1*Δ (n=100) and 64% of *Agrax2*Δ (n=100) germlings formed a second germ tube. The majority of them emerged at the +/-90° or

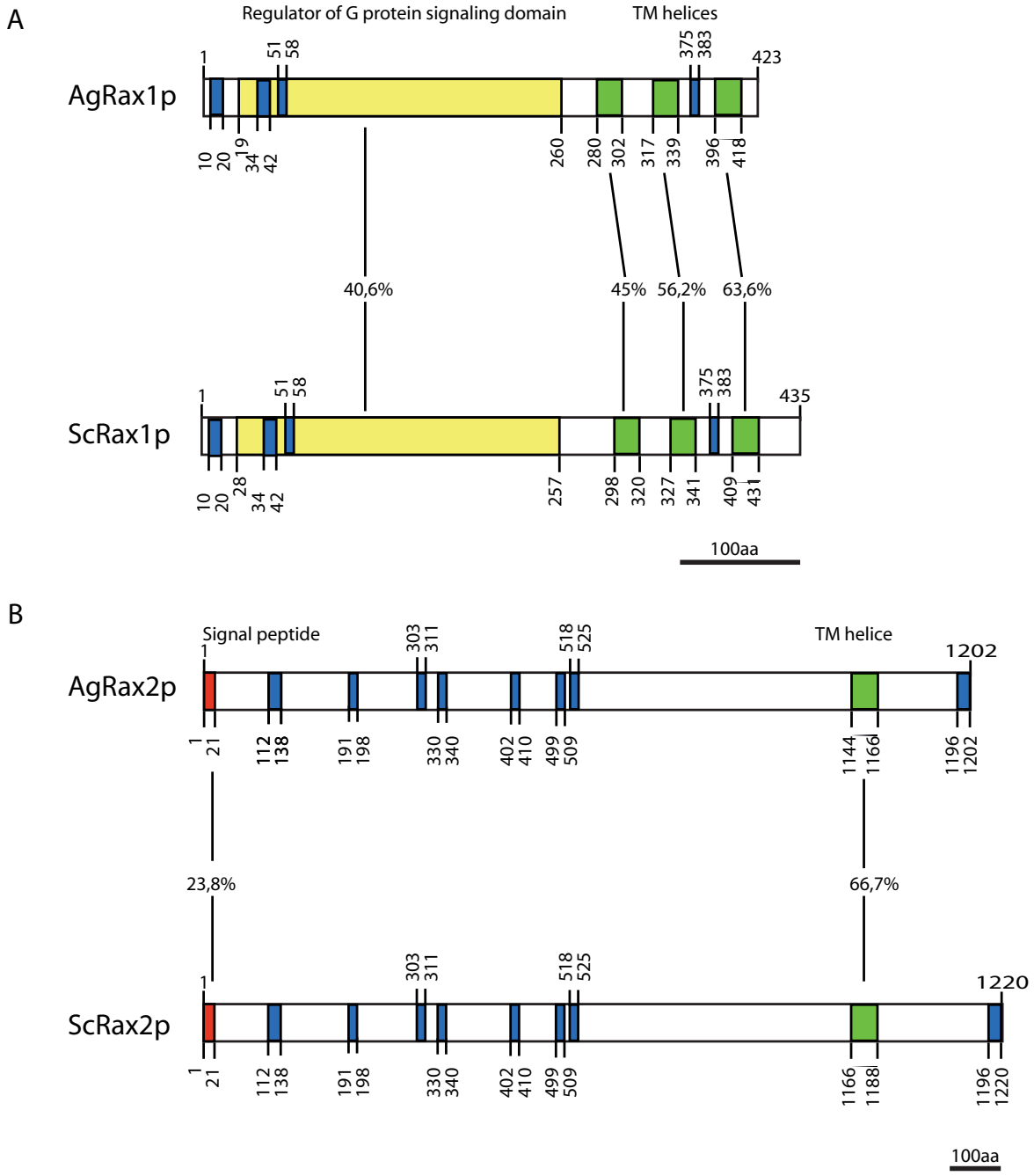

Figure 1
Comparison of protein domains of *A.gossypii* AgRax1p and AgRax2p with *S.cerevisiae* ScRax1p and ScRax2p, respectively. Blocks of homology on the amino acid level are indicated. All domains predicted by SMART are shown. Amino acid positions of the conserved regions are indicated. Additionally, domains with 100% identity are indicated in blue. The % identity of the domains was scored according to a „Smith-Waterman" alignments. Corresponding domains carry the same colors. A comparative bioinformatic analysis revealed 45% identity between AgRax1p and ScRax1p and 38% identity between AgRax2p and ScRax2p.

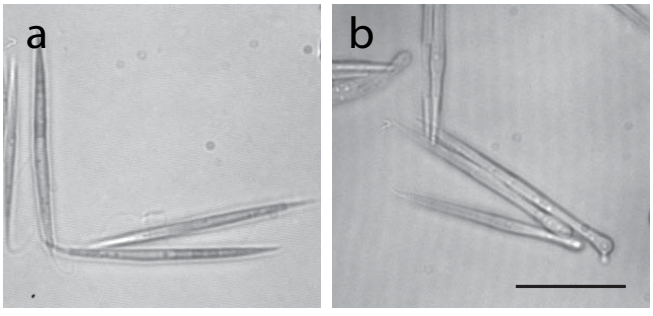

Figure 2
Spore morphology. (a) Usual needle-shaped WT spores after washing with Triton 0.03% in order to decrease aggregation. (b) Round deformations at ends of spores needle of *Agrax2*Δ. Bar,10 µm.

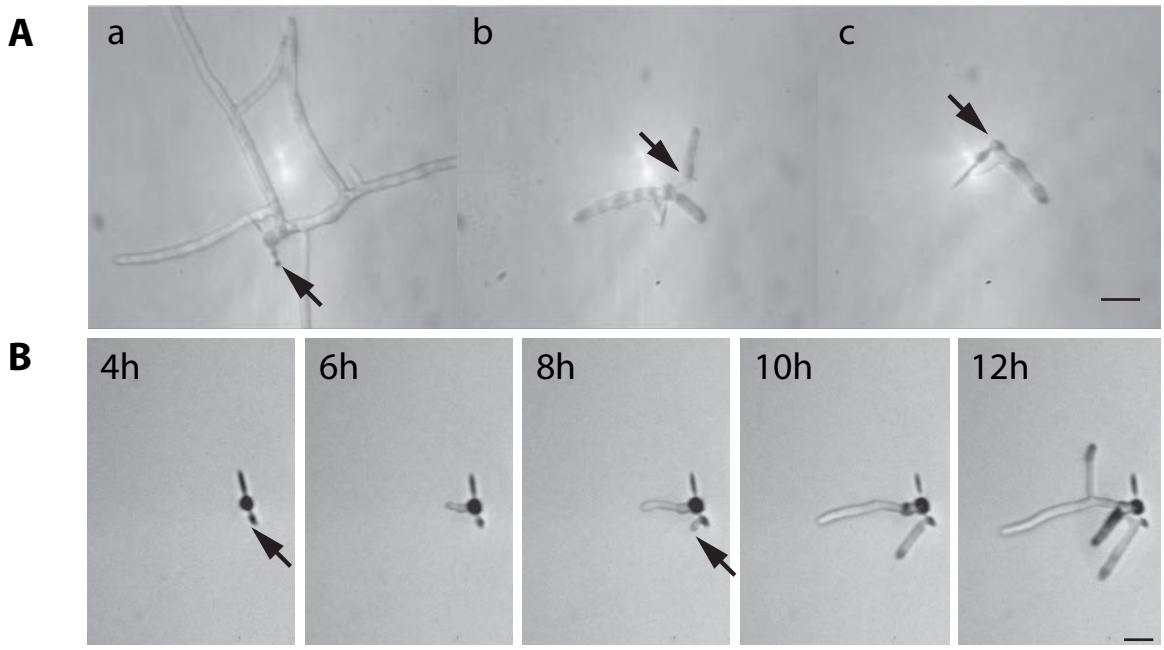

Figure 3
(A) Spore development patterns. **(a)** WT-like development of *Agrax2*Δ. **(b)** Round deformation of *Agrax2*Δ spore gives rise to additional hyphae. **(c)** First hypha develops from round deformation of a spore needle. **(B)** Time-lapse acquisition of *Agrax2*Δ during aberrant spore germination. Spores were inoculated on complete solid medium at 30°C. The time-lapse was carried out at 30°C. Growth of the spore started with an initial isotropic growth phase generating a germ bubble followed by germ tube formation. Similar pattern of growth was observed starting at the round deformations of a spore needle. Black arrows indicate spores of different than wild type morphology. Bar, 20 μm.

even more random with respect to the previous germination site. Interestingly, in 10-12% of cases the second germ tube initiated from the abnormal bubble at the end of the needle-shaped spore **(Fig. 3)**.

Both, *Agrax1*Δ and *Agrax2*Δ mutants produced a random germination pattern, which suggests that AgRax1p and AgRax2p could be required for the selection of subsequent polar growth sites in respect to the existing ones.

AgRax1p and AgRax2p might be required for the selection of a new axis of polarity

Analysis of the radial growth speed of *AgRAX1* and *AgRAX2* deletions at different temperatures revealed a 40% decrease compared to the wild type **(Fig. 4)**. To further explore these differences in growth rate we employed *in vivo* time-lapse microscopy. All quantitative data representing essential parameters of growth guidance were determined using movies **A**, **B** and **C (Fig. 5)** (Supplementary Materials), and at least 3 additional movies for each strain.

First we monitored in 5 min intervals the development of *A. gossypii* wild type on the solid full medium starting from germinating spores to multi-branched young mycelia **(Fig. 5A)**. Spores were pregrown for 8 h on solid medium at 30°C prior to

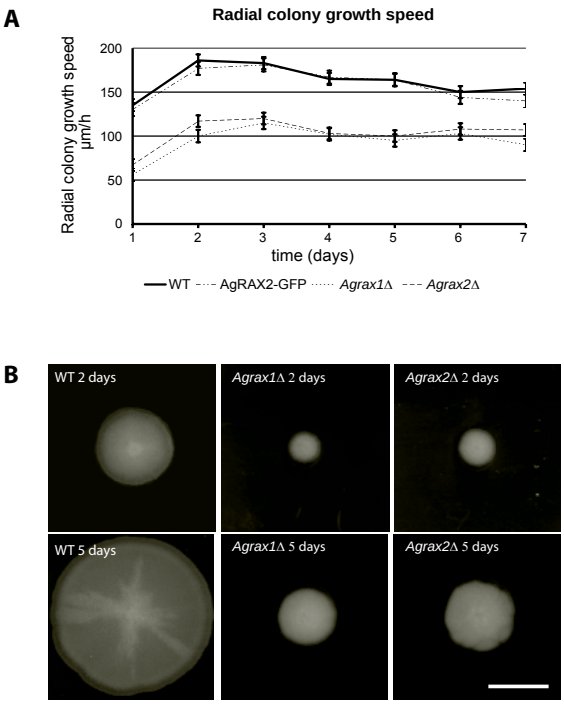

Figure 4
(A) Radial growth speed of WT, AgRax2-GFP, *Agrax1*Δ and *Agrax2*Δ strains. The x-axis represents the time in days, the y-axis the radial growth speed in μm/h. The value measured after the first day was the difference between the inoculums (1 mm in diameter) and the radial growth distance after 1 day divided by 24 h. The inoculums were taken from plates that had already been growing for 3 days and should have reached the maximal radial growth speed. Bar, SEM.**(B)** Colony diameter after 2 and 5 days for the WT, *Agrax1*Δ and *Agrax2*Δ Bar, 1 cm.

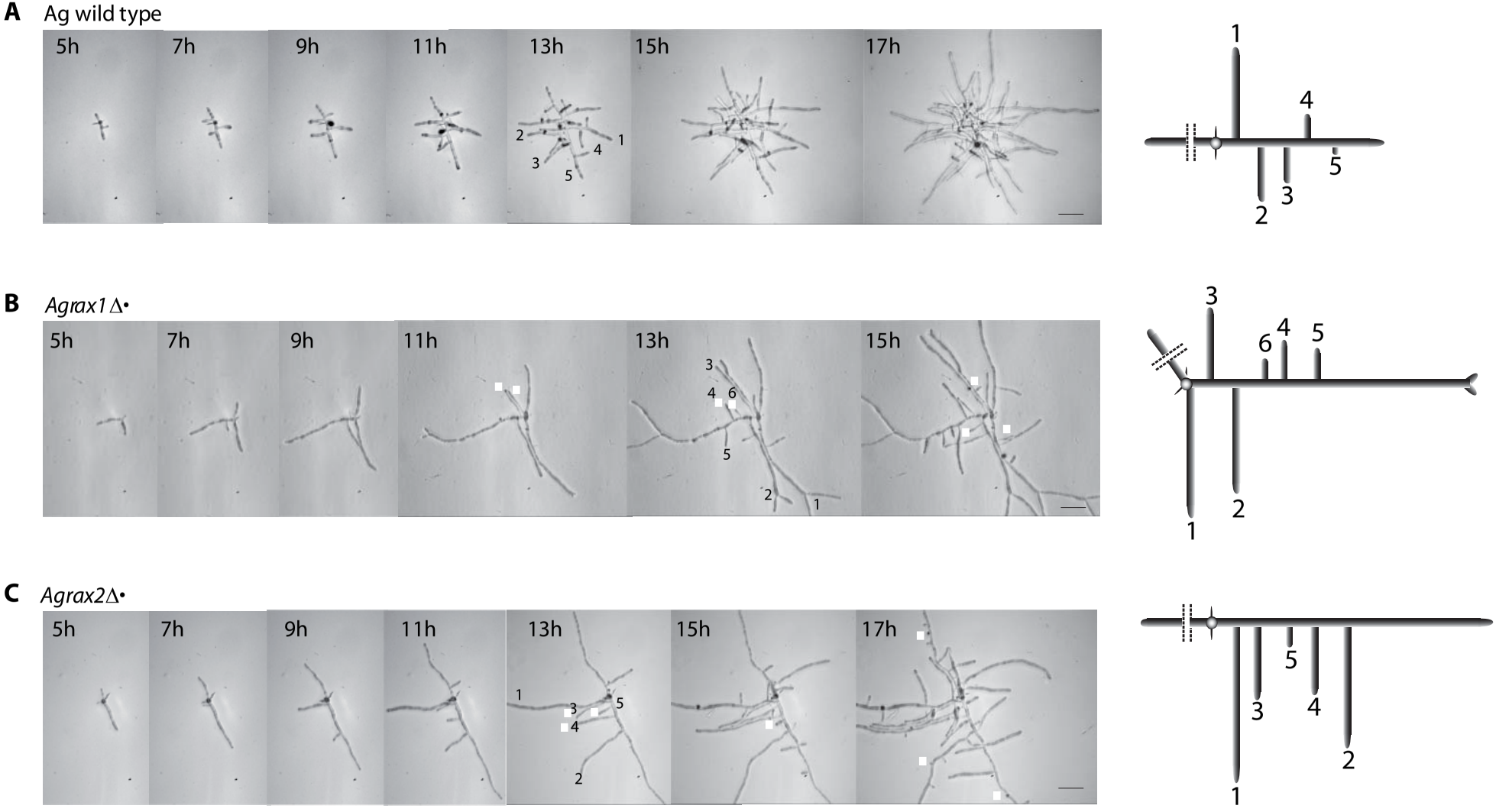

Figure 5
Development of WT, *Agrax1*Δ and *Agrax2*Δ young mycelium monitored by in vivo time-lapse microscopy. Spores were pregrown for 10h (5h prior and 5 h after germination) on solid medium at 30°C prior to mounting for video microscopy. Digital images were collected at 5 min intervals for all movies. The time-lapse was carried out at room temperature (25°C). **(A)** Representative frames taken at 2 h intervals show the development of WT, **(B)** *Agrax1*Δ and **(C)** *Agrax2*Δ mycelium. The numbers indicate the order of branch emergence on the main hyphae; white points indicate some of the branches that emerged between developed ones. The graphs display the branching pattern. Bar,10 µm.

mounting for video microscopy. The time-lapse was carried out at room temperature (25°C). Representative frames taken at 2 hours interval show the typical developmental stages as described below.

During the first 6 to 8 hours on full medium wild type needle spores developed into germ bubble. This isotropic growth phase was followed by the first hyphal tube formation. 4 to 6 hours after the first hyphal tube emerged, a second hyphal tube started growing. The formation of bipolar germlings resulted from the initiation of the second germ tube at the opposite site to the first one (91/100) or in less frequent cases at an angle of 90° (9/100). This process was followed by septum formation and branch initiation at the base of the first hyphal tube (Bauer et al, 2004, Knechtle et al. 2003). Every subsequent branch emerged from the hyphae in a rather organized fashion **(Fig. 5A)**.

AgRax1p and AgRax2p are involved in maintenance of polar growth and temporal regulation of branch emergence

Under the same experimental conditions we characterized the development of *Agrax1*∆ and *Agrax2*∆. The developmental pattern of *Agrax1*∆ and *Agrax2*∆ as documented by representative frames in **Fig. 5 B**,**C** was different from the wild type.

Analysis of the video data revealed (i) strong decrease in hyphal growth speed during lateral branches emerge (ii) delay in making new axis of polarity represented by a low number of lateral branches during early mycelium development (iii) irregular order of branching (iv) problems with maintenance of a straight axis of polarity during dichotomous tip branching.

Figures 5B and **5C** document tip extensions of the main hyphae in steps of 2 hours for the *Agrax1*∆ and *Agrax2*∆ based on 2 movies. In both strains the elongation rate was 3.5 to 5 µm/h during two hours after formation of the first germ-tube. During the next 10-12 hours this rate progressively increased up to 35-42 µm /h **(Fig. 6)** and only a few single lateral branches emerged from the hyphae. We did not observe strong reduction in growth speed during development of the first branches, however small fluctuations of the growth speed (up to -5µm/h), described later, typical for the potential septum and branch sites labeling, were seen. In general, mutant hyphae expanded during first 16 hours of growth on average 2 times faster than wild type. Interestingly, shortly before delayed lateral branches emerged on the „branch free hyphae“ the hyphal growth speed reduced markedly from 42µm /h to 30 µm /h for the *Agrax1*∆, and from 40µm /h to 33µm /h for the *Agrax2*∆. Initiations of branches in the compartments separated from the main tip by one or more septa did

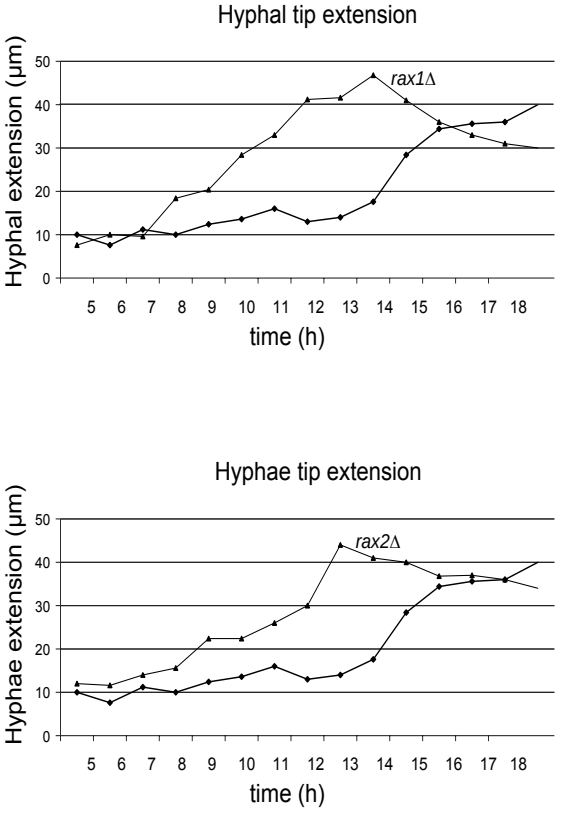

Figure 6
Analysis of the hyphal tip extension of WT *Agrax1*∆ and *Agrax2* ∆. The sources of the measurements are movies presented in Figure 5. The x-axis represents the time in hours, the y-axis the extension of the tip measured in mm. Data obtained were scored with the program “Image J”. Plotted values were obtained by measuring the increase in the hyphal length (extension of the hyphae) every one hour over the entire length of the movie and then multiplied by a pixel factor of 40.

not have an effect on the hyphal tip growth speed of the wild type main tip, however this seemed to have a major effect for the growth speed of mutant main hyphae. Similar fluctuations in the hyphal growth speed were observed for the *Agrax1*∆ and *Agrax2*∆ lateral branches.

However, in the beginning of the development, the mutants growth speed was on average two times faster than the wild type one, the maximal speed determined from radial growth of fungal colonies for the *Agrax1*∆ and *Agrax2*∆ was only 120 to 125 µm/h. The maximal speed determined from radial growth of fungal colonies is close to 200µm/h for the wild type (Bauer et al., 2004), thus, the elongation speed of both mutants hyphae was on average 40% slower. Firstly, a fast development of “branch free” hyphae and secondly, a decrease of growth speed in parallel with emergence of delayed lateral branches suggest problems in control of branching events in the absence of AgRax1p and AgRax2p. Thus, AgRax1p and AgRax2p are involved in the coordination of the branch emergence with the extension of hyphae.

To evaluate the ability to produce a new axis of polarity, quantitative data for total tip numbers were determined based on 4 DIC movies for each investigated strain. For each time point 4 series of measurements were done for the wild type, *Agrax1*Δ *and Agrax2*Δ*,* and the average values in steps of one hour were plotted **(Fig. 7)**.

During the first 8 hours (phase 1) the total number of hyphal tips was constant for all three strains (n=1) and corresponded to the first hyphal tip. During the next 10 hours of measurements (phase 2) the total number of the wild type hyphal tips progressively increased up to 25 whereas the total number of *Agrax1*Δ *and Agrax2*Δ*,*hyphal tips increased only up to 10. During subsequent 4 hours of measurements (beginning of phase 3) the total number of mutant's hyphal tips drastically elevated to reach the value obtained for the wild type. Because of high mycelium density we were not able to continue measurements longer than 22 hours.

Thus, Rax proteins affect the timing of branch development and link branch formation with the rate of hyphal progression.

The presence of some primary lateral branches suggests that at least 2 different pathways control branch emergence.

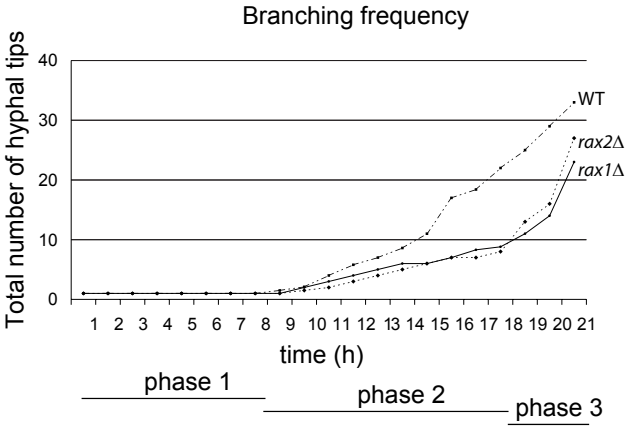

Figure 7
Increase in total number of tips in time for WT, *Agrax1*Δ *and Agrax2* Δ The x-axis represents time in hours, the y-axis the entire number of hyphal/ branch tips. (Phase 1) The value obtained during the first 8 hours of measurements corresponds to the tip of the first hypha. (Phase 2) The complete number of hyphal/ branch tips for the *Agrax1*Δ *and Agrax2* Δ is almost 50% lower than measured for the wild type. (Phase 3). After 20 hours the total number of lateral branches produced by wild type is comparable with those obtained for the *Agrax1*Δ *and Agrax2*Δ. Measurements longer than 21 hours were not possible because the mycelium increased its density and we were not able to identify all new rising tips.

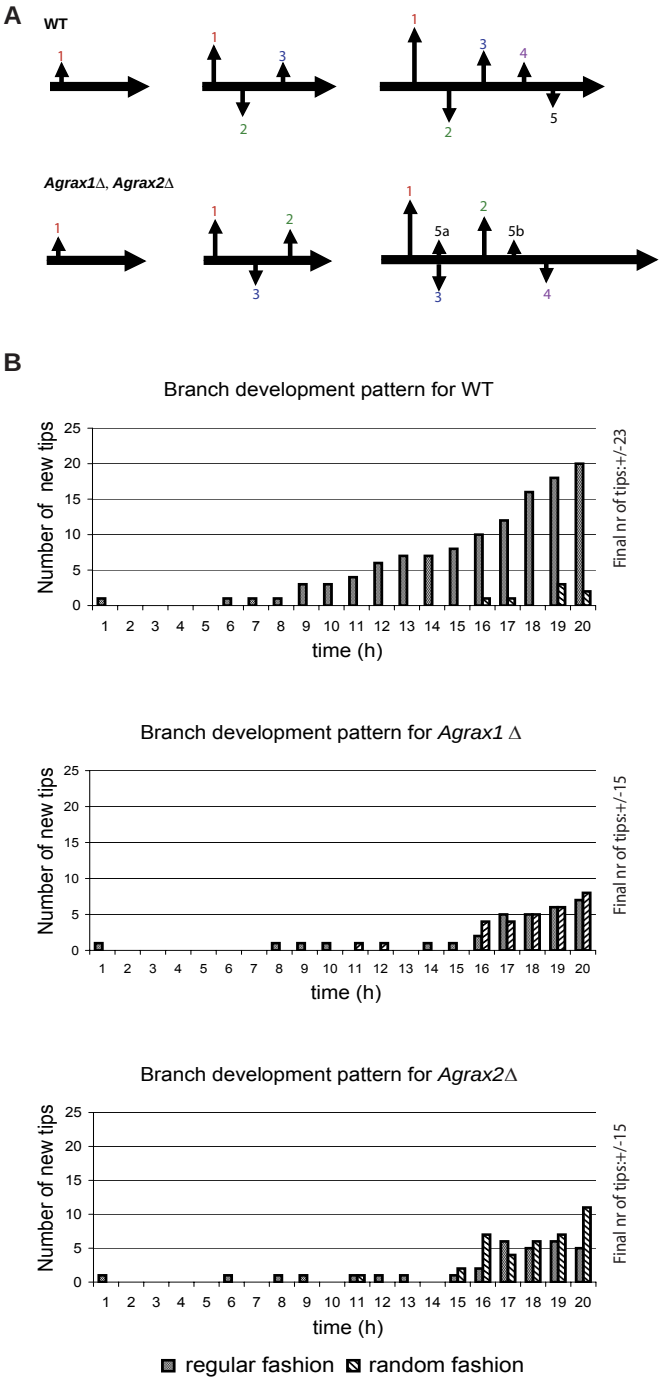

Figure 8
(A) Model of branch development pattern of WT, *Agrax1*Δ and *Agrax2*Δ strains. In the wild-type like pattern every subsequent branch emerged from the hypha in a rather organized fashion (between previous site of emergence and the tip of the hypha). In *Agrax1*Δ and *Agrax2*Δ mutants subsequent branching events often occurred in random fashion. Numbers indicate the order of branch appearance.
(B) Branch development pattern of WT, *Agrax1*Δ and *Agrax2*Δ strains. The x-axis represents time in hours, the y-axis the number of emerging branches and their relative position. The graphs summarize the proportion between the number of branches that emerged in a regular order and those that emerged between old ones. Mutant strains exhibited higher ratio of irregularly emerging branches compared to the WT.

In order to investigate abnormality in branch emergence we compared for the wild type, *Agrax1*∆ *and Agrax2*∆ the number of lateral branches that emerged in an organized fashion (between last developed branch and the tip of the hyphal) with the number of lateral branches that emerged in a random fashion **(Fig. 8)**.

Whereas the wild type produced almost all branches in organized manner, the *Agrax1*∆ *and Agrax2*∆ generated only the first few branches in an organized fashion. The majority of mutant's branches emerged 15 hours after the germination (with about 6 hours delay compared to the wild type) and between already developed ones. Some of them emerged simultaneously with at least one other branch, placed in the same or often neighboring compartment.

In the wild type lateral branching often occurred at sites of previous septation (Wendland et al., 2002). In the *Agrax1*∆ and *Agrax2*∆ 37% of lateral branches emerged in the middle of the compartment **(Fig. 9)**. Interestingly, the majority of lateral branches that appeared during the first hours of development were adjacent to the septum, whereas all "delayed" lateral branches appeared to be distributed more randomly in the compartment.

Randomized position of subsequent branches in respect to already existing ones and to sites of septation suggests that AgRax1p and AgRax2p may be landmark proteins involved in the selection of new polar sites.

Selection of branch and septum sites take place in *Agrax2*∆ but is not always followed by polarity establishment

To verify this hypothesis we measured the hyphal tip growth speed of a wild type and *Agrax2*∆ for 9 hours starting from a single germinating spore. Spores were allowed to germinate on AFM (Ashbya Full Medium) plates at room temperature (25°C) **(Fig 10. A)**.

It was previously reported by Knechtle et. al. that small oscillations (up to -5µm/h) observed during the hyphal extension were related to the potential septum and branch sites labeling.

The average measured hyphal tip growth speed during the first 2h of growth oscillated between 4 and 6 µm/h and was similar for the wild type and *Agrax2*∆. After 9 hours of the growth average measured hyphal tip growth speed increased up to 13 µm/h for the wild type **(Fig 10. Ba)** and 20 µm/h for the *Agrax2*∆ mutant **(Fig 10. Bb)**.

Indeed, after the hyphal tip growth speed dropped either a septum or a lateral branch emerged at this place with a delay of 1-2 hours for the wild type and 6 hours for the mutant.

Additionally, each septation or branching event caused the hyphal tip growth speed to slow down.

After each decrease the main tip growth speed increased to reach the next maximum.

Subsequently we focused on the number of oscillations in hyphal tip growth speed, associated with the selection of new polar sites.

The total number of oscillations observed during growth of the wild type and *Agrax2*∆ hyphae was almost the same (+/-10), thus comparable number of polarization events behind the hyphal tip took place leading to the branch emergence or septum formation.

Although the selection of branch sites and sites of septation took place in the*Agrax2*∆, it presumably was not always followed by a direct polarity establishment. In consequence, AgRax2p itself is not essential for the selection of sites for polar events.

A

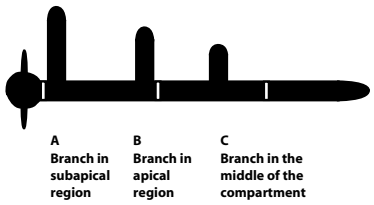

Figure 9
(A) Graph presents position of lateral branches in the compartment. The branch is placed in subapical region when is adjacent behind the actin ring marking potential septation site, in apical region when is adjacent before actin ring and in the middle of compartment, when is place between 2 actin rings, whereas the distances between branch and 2 actin rings are comparable. **(B)** Preferred positions for the lateral branches in the compartment obtained for the wild type, *Agrax1*∆ *and Agrax2* ∆ are presented in the table.

B

		Position of the first branch in the compartment			Position of each subsequent branch in the compartment		
Strain genotype	**Number of investigated compartments**	**A**	**B**	**C**	**A**	**B**	**C**
WT	176	8%	37%	5%	10%	35%	5%
***Agrax1*∆**	197	9%	23%	18%	9%	20%	21%
***Agrax2*∆**	198	12%	20%	15%	8%	23%	22%

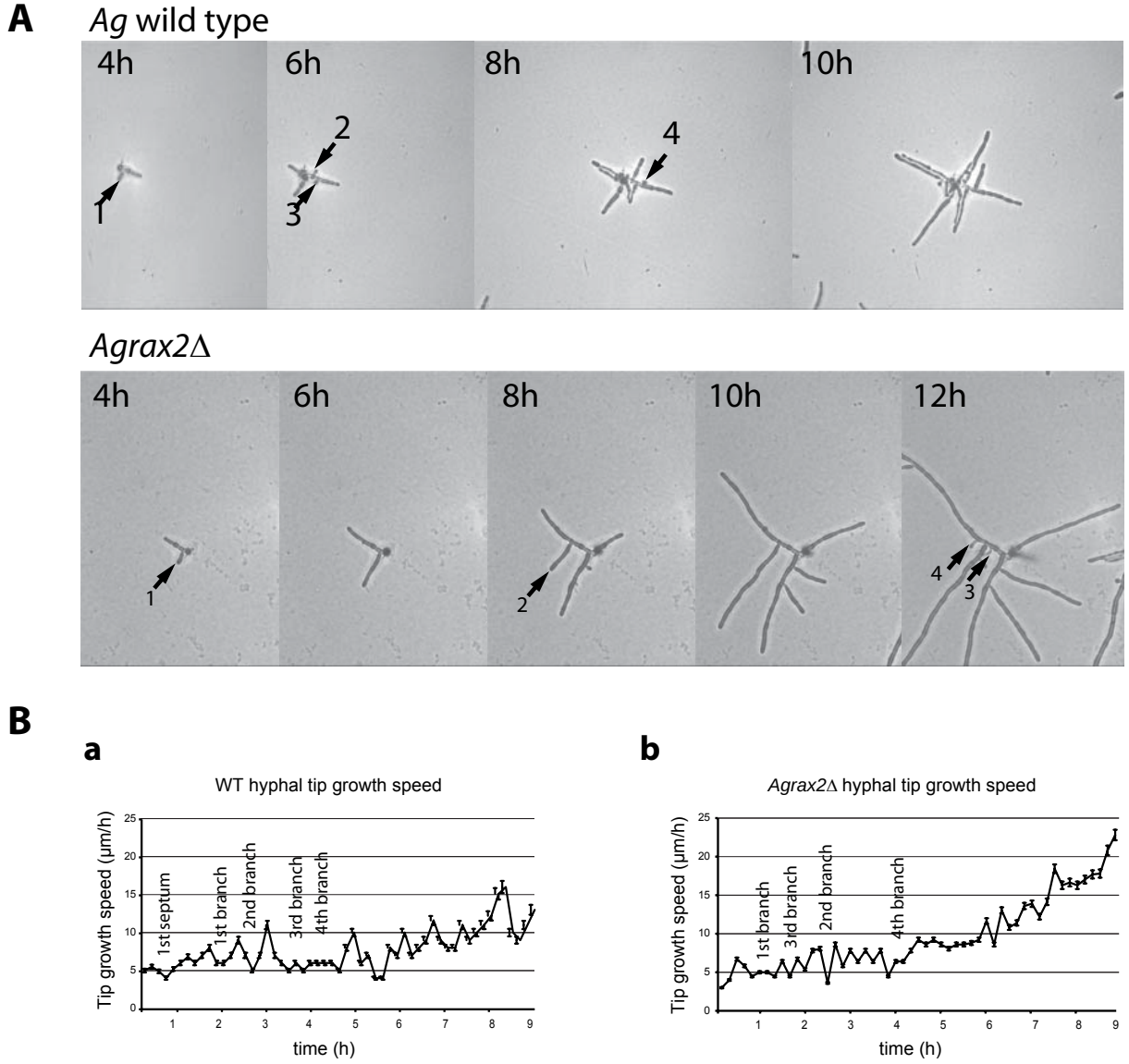

Figure 10
(A) The development of a single spore to a young mycelium was followed in a time-lapse acquisition. Spores from the wild type and *Agrax2*Δ strain were allowed to germinate on AFM plates at room temperature (25˚C). Pictures from a single spore were acquired every 5 min over a time period of 10 h. Representative frames taken 4 hours after germination and at 2 h intervals are presented. **(B)** The hyphal tip growth speed of the first germ tube that emerged (the main tip) was determined for the wild type, and *Agrax2*Δ mutant. Data were collected every 10 min for the time period of 9 hours starting at germination and were plotted against time. The basis for the graphs are movies presented in A. The x-axis represents the elapsed time in min and the y-axis the hyphal tip growth speed in µm/h. Whenever growth speed dropped a septum or a lateral branch emerged with a delay 1-2 hours for wild type and 6 hours for mutant. Numbers (1-4) indicate the order of branch appearence in the places where hyphae reduced its growth speed. Because of the low resolution the beginning of septum formation cannot be seen in phase contrast microscopy. **(a)** Growth speed dropped 30 min after from germination-when the first septum site was labelled. Growth speed dropped after 3 h 00', reached a minimum at 3 h 30' and increased again to reach a maximum at 5 h '. During this time the position for the 3rd and 4th lateral branches were most likely selected (at those places 2 lateral branches initiated after 2 hours). **(b)** Growth speed dropped after 30', reached a minimum at 1h and increased again to reach a maximum at 1 h 30'. During this time the position of the 1st lateral branch was most likely selected.

AgRax1p and AgRax2p are involved in the maintenance of polarity at the tip

To further investigate whether there are some morphology changes that could explain the decrease in radial growth of *Agrax1*Δ and *Agrax2*Δ colonies, we followed the hyphal splitting at fast growing tips into two fast growing branches. Apparently, tip branching occurs in *Agrax1*Δ and *Agrax2*Δ mutants earlier than in wild type and in many cases with quite unusual results **(Fig. 11)**. Approximately 8% (11/138) of the tips of 24h old mycelium formed 3 instead of 2 fast growing tips, another 20 % (28/138) changed the axis of polarity (loops, zig-zag hyphae). The percentage of hyphae that changed the axis of polarity increased with the age of the mycelium. At 48h up to 17% (17/100) of hyphae formed 3 instead of 2 branches and 37% (37/100) exhibited changes in the growth

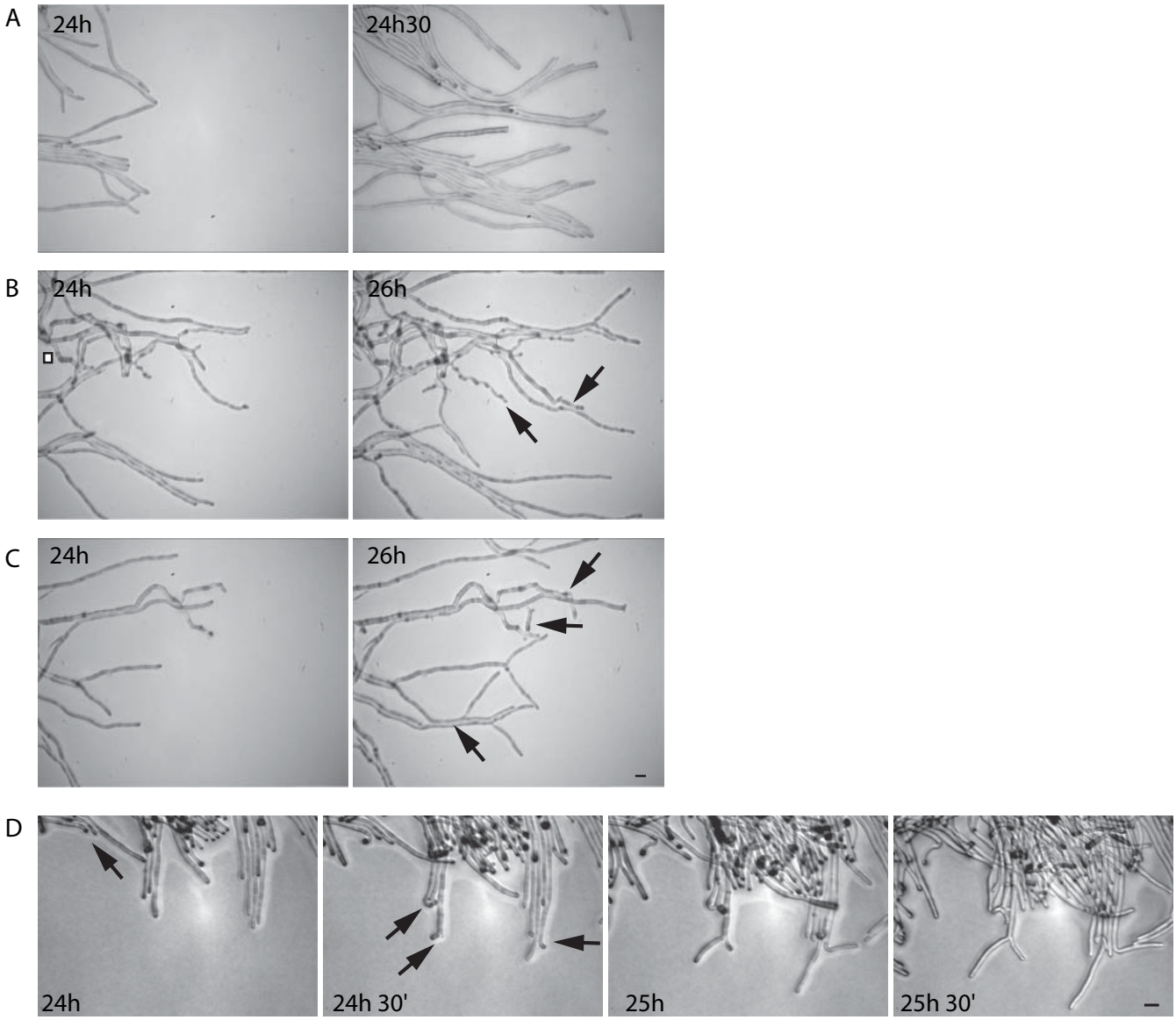

Figure 11
WT, *Agrax1*Δ and *Agrax2*Δ tip branching monitored by in vivo time-lapse microscopy. Mycelia were pregrown for 48 hours on solid medium at 30°C to prior video microscopy. The time-lapse was carried out at room temperature (25°C). **(A)** Representative frames show the development of WT mycelium. **(B)** Representative frames show the development of *Agrax1*Δ mycelium. **(C)** Representative frames show the development of *Agrax2*Δ mycelium. Black arrows indicate substantial changes in growth axis (kincky tip). **(D)** Representative frames show the development of *Agrax2*Δ mycelium. Black arrows indicate substantial changes in growth axis Bar,10 μm.

direction. Additionally, the growth speed of those tips was markedly reduced.

To evaluate the stability of the axis of polarity we measured the length of straight hyphal segments in wild type, *Agrax1*Δ and *Agrax2*Δ. Within the limits of our microscopic setup we observed that 24 hours old wild type hyphae grew straight for up to 200μm, sometimes, minor changes (less than 10°) in growth direction were observed. The maximum angle of deviation from the original axis was 20°, mainly due to tip branching and contact with another hyphae. In 24h *Agrax1*Δ and *Agrax2*Δ hyphae frequent changes in growth direction were observed, in extreme cases up to 85-100°. Diameters at the tip region ranged from 3 to 5 μm for the wild type and remained unchanged in *Agrax1*Δ and *Agrax2*Δ. Frequent changes in growth axis and defective tip branching observed for fast growing tips of *Agrax1*Δ and *Agrax2*Δ explain the overall decrease in tip speeds determined from their radial growth rates.

AgRax1p and AgRax2p play a role in focusing actin patches to the tip region

Since polarization of the cortical actin cytoskeleton is indicative of the axis of cell polarity we examined the organization of the actin cytoskeleton in *A. gossypii* wild type and the *Agrax1*Δ and *Agrax2*Δ deletions. Young and mature mycelia were fixed with

4% formaldehyde and the actin cytoskeleton was stained with Rhodhamine-Phalloidin.
In wild type hyphae we could observe clusters of cortical actin patches in over 95% of the tips, indicative of active growth, as well as actin rings at sites of developing septa **(Fig. 12)** (Wendland and Philippsen, 2000; Knechtle et al., 2003, Bauer et al 2004).
In *Agrax1*Δ and *Agrax2*Δ, 95% of the tips in young mycelium but only 66% of the tips in mature mycelium showed clusters of actin. These data are in agreement with the observed decrease in hyphal tip extension (associated with the disassembly of the actin cup) in *Agrax1*Δ and *Agrax2*Δ during lateral branch development on "branch free" mycelium.
Moreover, the majority of actin clusters present at the tips of (especially) "branch free" mycelium were very dense, suggesting hyper polarisation of actin cytoskeleton **(Fig. 12)**. Presumably, AgRax1p and AgRax2p play a role in focusing actin patches to the tip region. In order to test this hypothesis we analysed the average actin cup area (understood as a surface at the very tip covered with the actin patches) at the hyphal tips of 16 hours WT, *Agrax1*Δ and *Agrax2*Δ mycelium. Spores were pregrown in liquid medium and Rhodamine-Phalloidin staining was performed. 6-8 planes of the Rhodamine-Phalloidin stained mycelium were acquired at z-distances of 0.2 µm. The stacks were compressed in order to visualize majority of the signal present in the cell. Plotted values were obtained by measuring the surface of actin cup at the hyphal tips. For each strain at least 60 actin cup areas at the hyphal tips were measured. The data were scored with program „Image J" and processed in „Excel" **(Fig. 13)**.

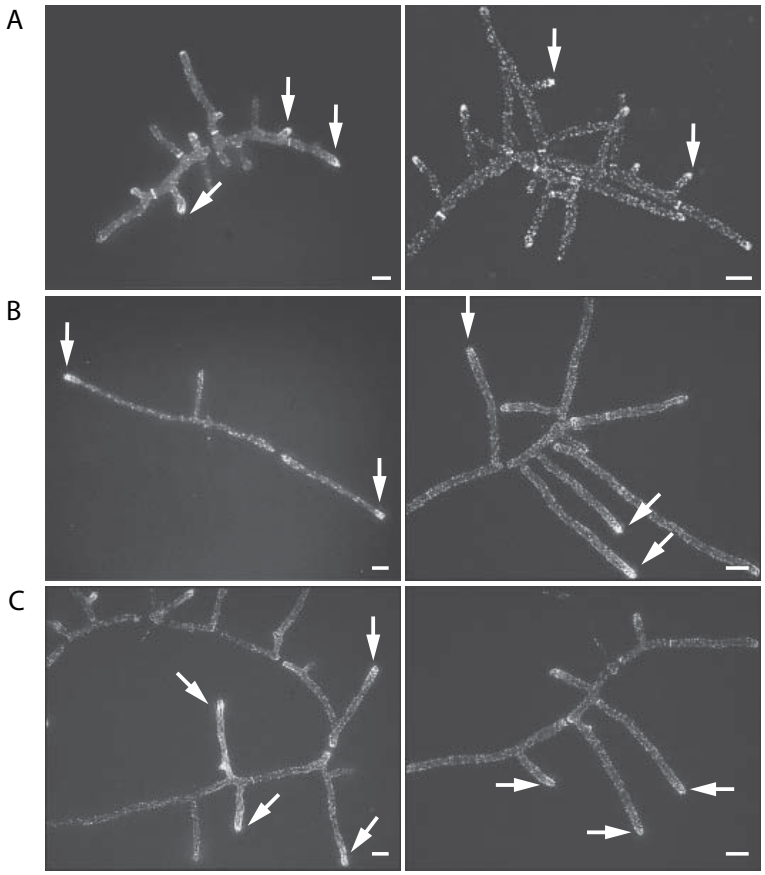

Figure 12
Organization of the actin cytoskeleton in WT, *Agrax1*Δ and in *Agrax2*Δ. Germinated spores of all strains were grown in liquid complete medium for 16 hours at 30°C, fixed with formaldehyde, stained with Rhodamine-Phalloidin and analyzed by fluorescence microscopy. Two representative images are presented for each strain (n=50). (A) WT shows polarized actin at most of the tips (indication for active growth), actin rings at the selected sites for septum formation and regular distribution of branches. (B) Young *Agrax1*Δ shows pronounced, bigger clusters of actin at the hyphal tips and less lateral branches (C) Young *Agrax2*Δ shows pronounced, bigger actin patches at the tips and a decreased number of lateral branches Bar,10 µm.

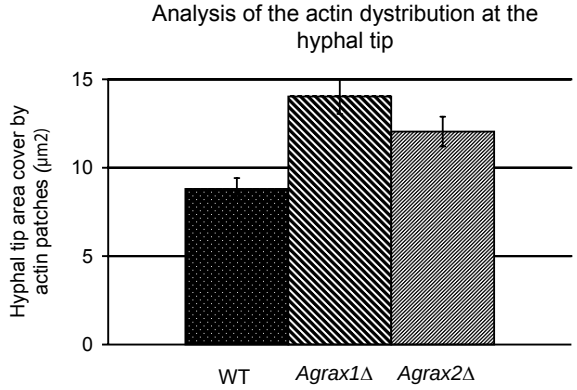

Figure 13
Analysis of the area of accumulated actin patches at hyphal tips for WT, *Agrax1*Δ and *Agrax2*Δ. Spores were pregrown in liquid medium for 16h in 30°C before Rhodamine-Phalloidin staining was performed. Plotted values were obtained by measuring the area of actin patches at the hyphal tips multiplied by the pixel factor. For each strain at least 10 independent pictures were analyzed and for each strain at least 60 actin areas at the hyphal tips were measured. The y-axis represents the average actin area at the hyphal tip measured in µm^2. The data obtained were scored using the program „Image J" and were processed in „Excel".

We found that the average actin cup area for the wild type was 8,8 µm/h², for the *Agrax1*Δ 14µm² and for *Agrax2*Δ 12,1µm/h². Actin cup area for the *Agrax1*Δ was in average 37% bigger than measured for the wild type. The same area for the *Agrax2*Δ was 27% bigger than measured for the wild type. An increase in the average actin cup area suggests less focused actin patches at the tip of *Agrax1*Δ and *Agrax2*Δ mycelium. To summarise, the recruitment of actin patches to the tip is less efficient in *Agrax1*Δ and *Agrax2*Δ.
The polarisation of actin patches is essential for the branch emergance.
The decreased number of lateral branches in young *Agrax1*Δ and *Agrax2*Δ mycelium and the later increase in the number of branches in older *Agrax1*Δ and *Agrax2*Δ mycelium suggest the existence of the "rescue" mechanism that bring all necessary protein complexes to start directed transport of secretory vesicles towards the selected new growth site.

Absence of AgRax1p and AgRax2p do not have an impact for microtubule cytoskeleton organization

Additionally, we compared the distribution of the microtubules in wild type, *Agrax1*Δ and *Agrax2*Δ, as a perturbation of the microtubules leads to a reduction in the linear growth rate of hyphae (That et al., 1988). Cells were grown on solid medium for 48 hours, mycelium was collected, cut into small fragments and the microtubule cytosceleton was visualized with tubulin immunostaining. Wild type microtubules are oriented parallel to the long axis of hyphae and towards the tip. The same length and orientation of microtubules in relation to hyphae was observed for *Agrax1*Δ and *Agrax2*Δ.

Absence of AgRax1p and AgRax2p do not influence chitin deposition

In order to find whether growth speed oscillations and change in the growth direction influence the chitin deposition in *Agrax1*Δ and *Agrax2*Δ we have stained young and mature mycelium of both strains with calcofluor. Calcofluor stains chitin, marks sites of septation and also areas of intense polarized growth such as tips and branching sites. *Agrax1*Δ and *Agrax2*Δ showed correct septation as indicated by accumulation of chitin and also normal staining at tip regions. Although the processes for correct septation were not defective, the size of the compartment in young mycelium was comparible with the size in mature mycelium. This result partially explains the decrease in the colony size observed for the *Agrax1*Δ and *Agrax2*Δ. (Data not shown).

AgRax1p and AgRax2p may function in the same pathway

Examination of deletions showed that *Agrax1*Δ and *Agrax2*Δ produced similar phenotypes. To better understand the relationship between both proteins in *A.gossypii* we constructed a double deletion. To obtain an *Agrax1*Δ*rax2*Δ mutant we deleted the *AgRAX2*Δ ORF from start to stop codon with a cassette coding for resistance against the drug clonNAT in the *Agrax1*Δ strain.

The phenotype of the *Agrax1*Δ*rax2*Δ double mutant was very similar to that of the single mutants. Spores from *Agrax1*Δ*rax2*Δ looked like spores from single deletion. They germinated similar to those of the single mutants and showed changes in the branching pattern like *Agrax1*Δ or *Agrax2*Δ. Hyphae of the double deletion developed as slow as both single deletions. However, often fast growing sectors appeared most likely due to suppressor mutations **(Fig. 14)**. Such sectors were not observed in *Agrax2*Δ, but were sporadically seen in *Agrax1*Δ (1 colony out of 10). Microscopy studies displayed wild type like tip branching and sporulation in the fast growing sectors. Verification PCR proved absence of both genes. These results suggest that AgRax1p and AgRax2p function in the same pathway. Further analyses will show if they are dependent for function.

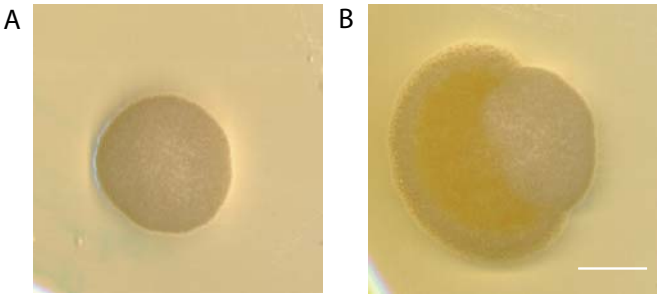

Figure 14
Development of *Agrax1*Δ*rax2*Δ. **(A)** Mycelium of the double deletion grown for 2 days on solid medium at 30°C. **(B)** The same mycelium after 3 days. Microscopy studies displayed correct tip branching and proper sporulation process in the yellow sector. 7 for 10 colonies grown from single double mutant spore exhibited sector formation, probably due to the presence of spontaneous suppresor. Verification PCR proved the absence of both genes. Bar,1 cm.

AgRax1p and AgRax2p act downstream of AgSep7p in the septation process

AgRax2p fused to GFP was shown to localize permanently to the tip and transiently either as a single ring to multiple sites of future septation or as a double ring to newly established septa (see page 28). In order to define whether AgRax2p and AgRax1p act upstream or downstream of AgSep7p

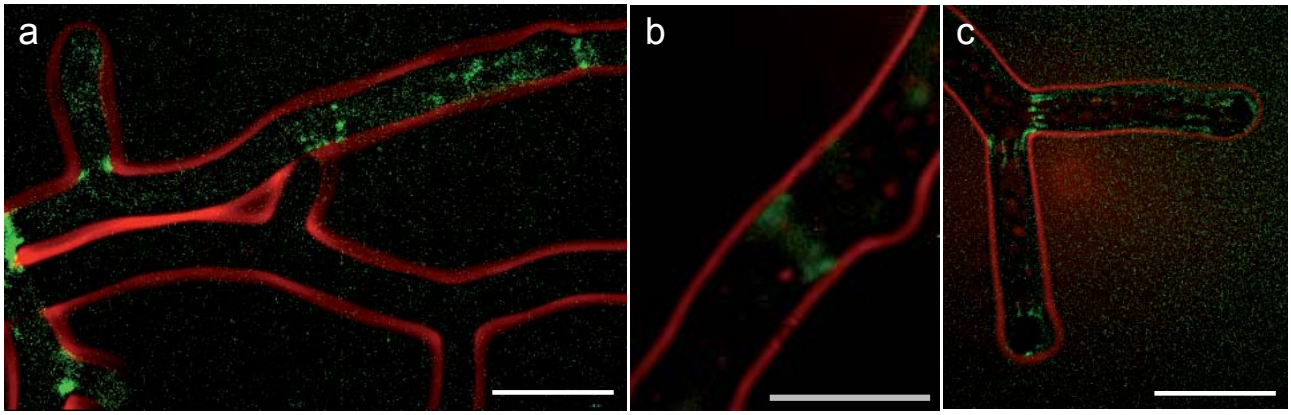

Figure 15
AgSep7-GFP localization in *Agrax1*Δ and *Agrax2*Δ. **(a)** In wild type AgSep7-GFP localizes to septation sites and forms rings close to the hyphal tips (not shown). The lack of the signal in the bottom branch is an artifact caused by not equal plasmid distribution in the mycelium. **(b)** Magnification of a site of lateral branchemergence indicates the presence of a AgSep7-GFP ring in *Agrax1*Δ. **(c)** Magnification of the basis of apical branches indicates presence of AgSep7-GFP rings in *Agrax2*Δ. Two rings mark symmetrically the basis of apical branches. The AgSep7-GFP signal is indicated in green, phase contrast in red. Bar, 10 μm.

septin the plasmid carrying carboxyl-terminal GFP fusion to the endogenous copy of the *AgSEP7* (provided by H-P. Helfer) was introduced into the *Agrax1*Δ and *Agrax2*Δ strains. The *A.gossypii* homologue of ScSep7p assembles as a ring that marks the septation sites during hyphal development (H-P. Helfer *et al.*, unpublished). In both mutants the AgSep7-GFP localization remained wild type like **(Fig. 15)**. These observations clearly show that both investigated proteins act downstream of AgSep7p in the septation process. Additionally these findings are in agreement with the above described proper chitin deposition at the septum in *Agrax1*Δ and *Agrax2*Δ mutants.

AgRax1p and AgRax2p do not have an impact on the localization of the polarisome marker AgSpa2p at the tip but may have an impact on the protein abundance at the septum

Because changes in the growth axis were previously reported to be the effect of destabilization of the polarity marker AgSpa2p at the tip we employed in vivo time-lapse microscopy and monitored AgSpa2-GFP in the absence of AgRax1p and AgRax2p.
Previous studies showed that AgSpa2p controls the area of surface extension at the hyphal tip and the growth speed.
AgSpa2p was shown by fusion to GFP to be permanently localized at the tips of growing hyphae, as soon and as long as hyphae grow polar, to appear as small patches at initiation sites for lateral branches and to be present transiently at the septum (Knechtle *et al.*, 2003, Bauer *et al*. 2004).
We have shown herein that the tip growth speeds of *Agrax1*Δ and *Agrax2*Δ mutants displayed small oscillations associated either with the selection or establishment of polarity. Pausing induced by polar events behind the tip observed for the extending hyphal tip of *Agrax1*Δ (not shown) and *Agrax2*Δ was not associated with the disappearance of AgSpa2-GFP patches from the hyphal tips **(Fig. 16A).**
As well the localization of AgSpa2p-GFP as small patches at initiation sites for lateral branches was not changed **(Fig. 16B)**.
Additionally AgSpa2-GFP signal was seen at the septum in the *Agrax1*Δ and *Agrax2*Δ. AgSpa2-GFP used to split into two rings/ discs labelling two neighbouring compartments. Moreover, the AgSpa2p-GFP signal was more pronounced at the septum in both mutant strains than it was reported for the wild type **(Fig. 17A)**.
Actin staining revealed for the *Agrax1*Δ and *Agrax2*Δ co-localization of AgSpa2p with the actin rings in the early septum formation phase. In the late phase AgSpa2p seemed to accumulate as a cloud/ or disc at the septum site.
The protein abundance at the septum was likely greater than reported by Knechtle for the wild type **(Fig. 17B)**.
Interestingly, whenever a branch emerged in the neighbourhood of the septum labeled with AgSpa2p-GFP, the signal at the septum was less than at the wild type. Whereas in wild type the AgSpa2-GFP signal remained visible up to 2 hours after the septa fully separated two compartments, in *Agrax1*Δ *(*not shown) and *Agrax2*Δ the signal was gone after 30 min.
We suppose that in the absence of AgRax1p and AgRax2p AgSpa2p from the septum may be relocalized to support the branching event.

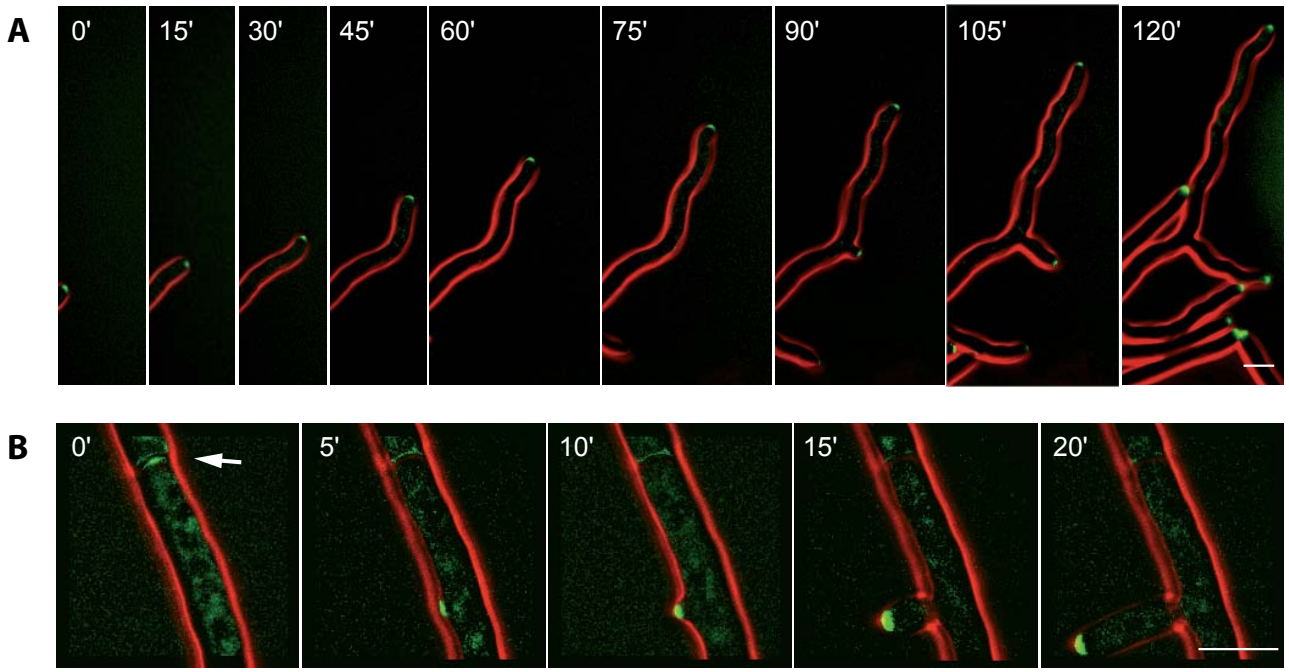

Figure 16
Localization of the polarisome component AgSpa2-GFP in *Agrax2*Δ. AgSpa2p-GFP distribution in growing hyphal tips as well as during lateral branch initiation was monitored by in vivo time-lapse microscopy. The series of images represents selected frames of movies (see supplementary materials). **(A)** Permanent localization of AgSpa2p-GFP in a growing tip. Although hyphae have changed the direction of growth we did not observe disappearance of AgSpa2-GFP in *Agrax2*Δ. **(B)** Polarized AgSpa2-GFP at branching site in *Agrax2*Δ. Bar, 10 μm.

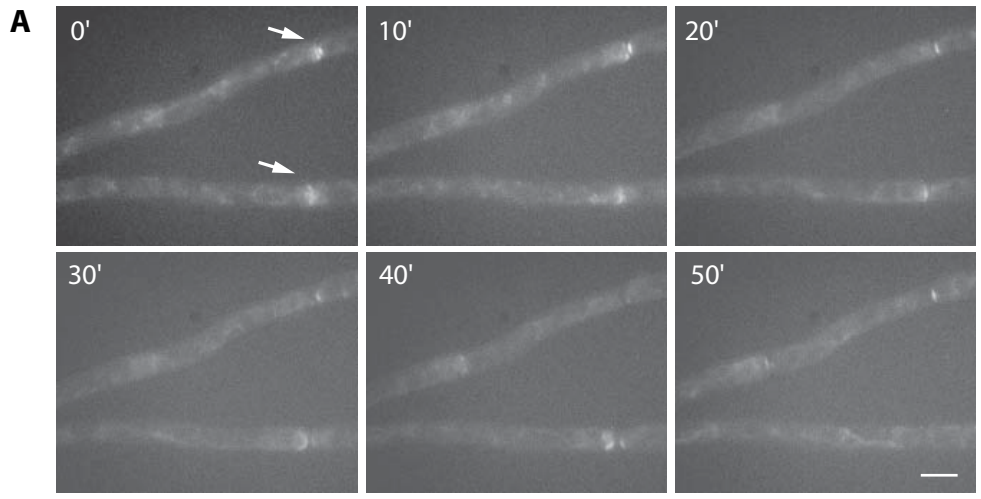

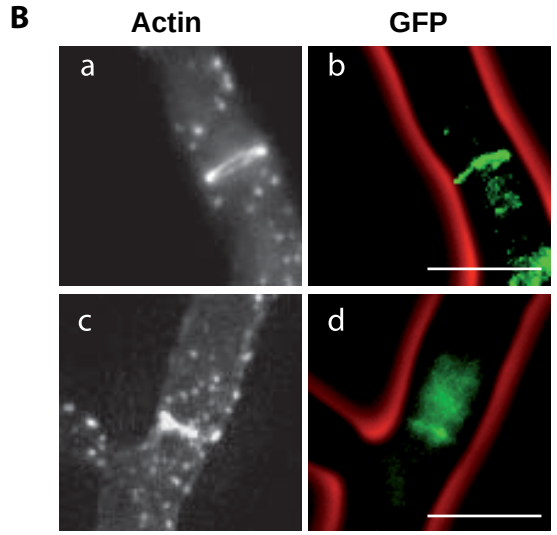

Figure 17
Localization of the polarisome component AgSpa2-GFP during septum formation in *Agrax2*Δ. AgSpa2p-GFP distribution during septation was monitored by in vivo time-lapse microscopy in *Agrax2*Δ. The series of images represents selected frames of the movie. **(A)** Dynamics of AgSpa2-GFP at the septum in *Agrax2*Δ. (see supplementary materials). **(B)** Co-localization of AgSpa2p-GFP with actin ring. **(a,c)** Rhodamine-Phalloidine actin staining; **(b,d)** Overlay of AgSpa2-GFP (green) and outline of the hyphae (red). Bar, 10 μm.

AgSpa2p acts independently on AgRax1p and AgRax2p to maintain a new axis of polarity

To investigate the relation between AgSpa2p, AgRax1p and AgRax2p proteins we deleted both *AgRAX1* and *AgRAX2* genes in an *Agspa2*Δ strain with the cassette coding for resistance against the drug cloNAT. Dissection on selective medium, more than 100 spores originating from a heterokaryotic mycelium for each *Agspa2*Δ*rax1*Δ and *Agspa2*Δ*rax2*Δ never gave rise to mature mycelium. Some of the colonies reached the size of wild type mycelium, but further investigation, particularly phenotypic studies and verification PCR, confirmed the presence of *AgRAX1* or *AgRAX2* genes.

The majority of the dissected spores were able to

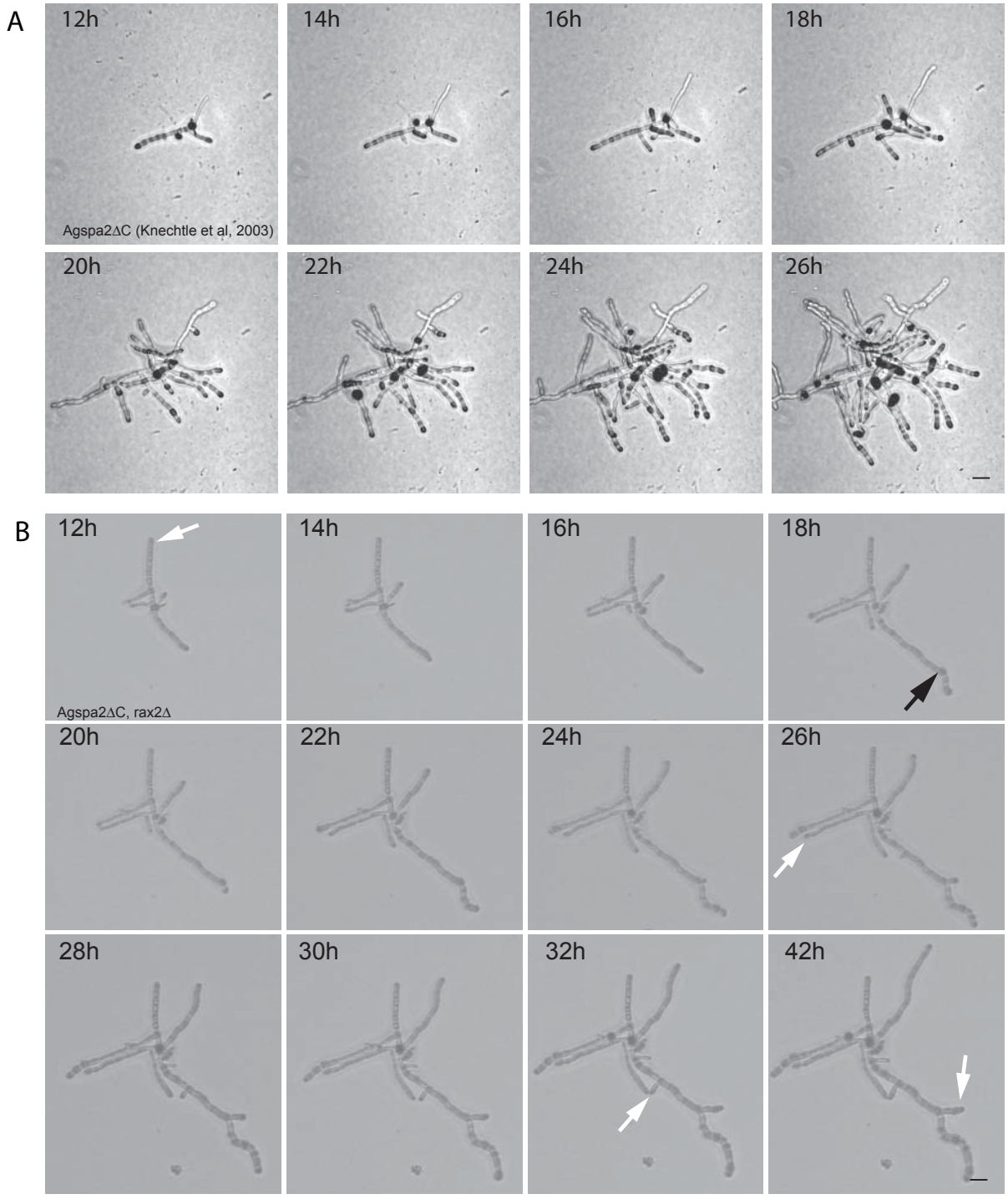

Figure 18
Development of *Agspa2*Δ and *Agspa2*Δ*rax2*Δ young mycelium monitored by in vivo time-lapse microscopy. Spores were pregrown for 10h in complete liquid medium at 30°C prior to mounting for video microscopy. Digital images were collected at 5 min intervals for the first movie and at 2h intervals for the second movie. The time-lapse was carried out at room temperature (25°C).**(A)** Representative frames show the development of *Agspa2*Δ. **(B)** Representative frames show the development of *Agspa2*Δ*rax2*Δ mycelium. Black arrow point to changes in growth direction, the white arrows mark a complete growth arrest of a lateral branch. Bar, 10µm.

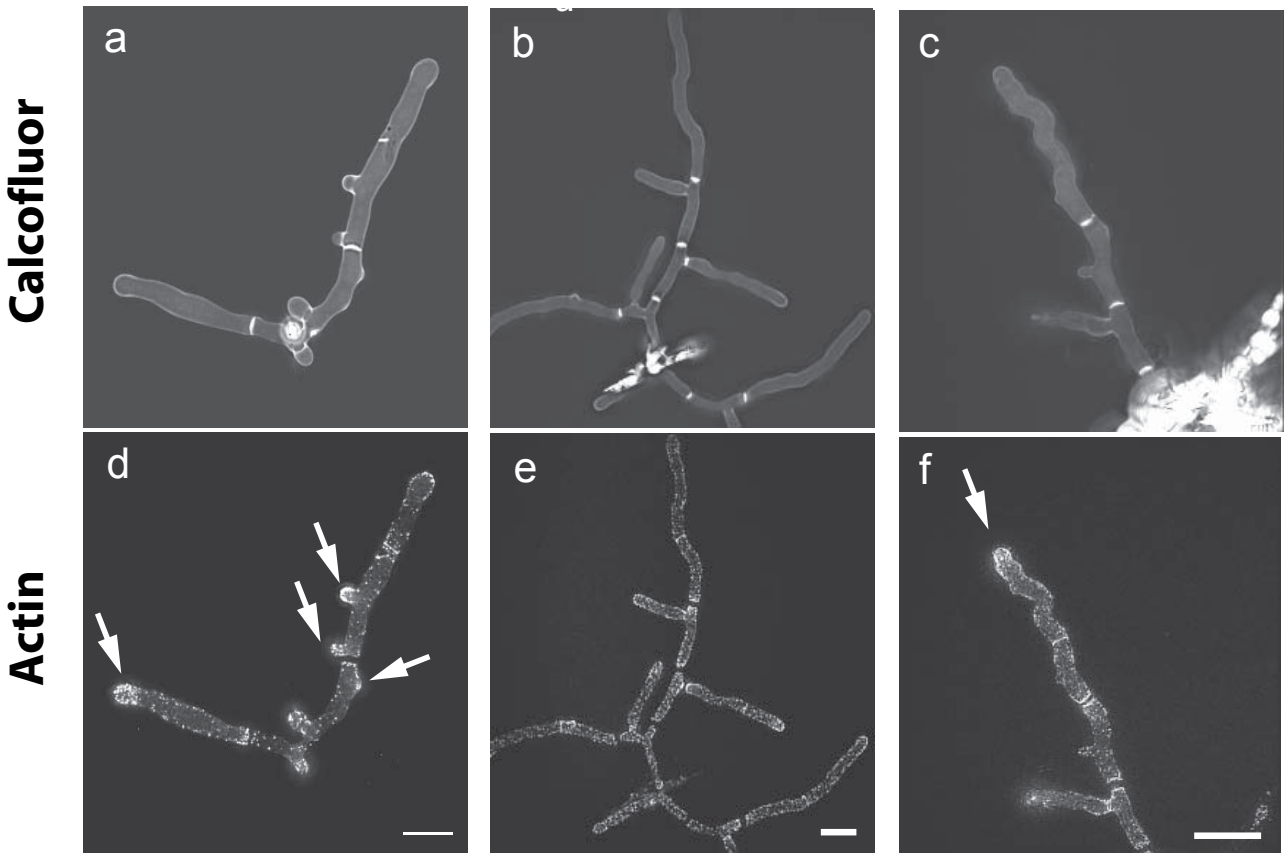

Figure 19
Calcofluor distribution **(a,b,c)** and organization of the actin cytoskeleton **(d,e,f)** in *Agspa2*Δ*rax2*Δ during different development stages. **(d)** Polarized actin cytoskeleton indicates active growth (white arrows). **(e)** Lack of polarized actin at the tips indicates growth arrest. **(f)** Polarized actin at the tip of 30h old mycelium Bar,10 µm.

form small mycelium (10-20 tips). In those cases, 12-16 hours after germination, hyphae and branches reduced growth speed up to a complete stop. 25% of hyphal tips frequently changed the axis of polarity before their growth ceased **(Fig. 18)**.
Additionally, proportionally to the age of the mycelium the number of the tips showing polarized actin decreased **(Fig. 19)**. In many cases we could not see properly formed, symmetric chitin rings, as well as correctly shaped septa. Those results indicate problems in the maintenance of polarity at the hyphal tip and at the septum in the absence of AgRax1p/ AgSpa2p and AgRax2p/ AgSpa2p. Further they support the hypothesis that AgRax1p and AgRax2p are part of different pathway than AgSpa2p.

AgRax2p acts independently of AgBud10p to maintain a new axis of polarity

Although *A.gossypii* shows a completely different morphological development than *S.cerevisiae,* it has the homologue of the *S.cerevisiae* ScBud10p/ Axl2p. In the *S.cerevisiae* ScBud10p/Axl2p functions as a cortical cue necessary for the axial localization pattern of ScRax1p that was shown to be required for localization of ScRax2p at the division sites. Additionally, it promotes local activations of ScBud1p followed by ScCdc24p, which induces cytoskeletal polarity. (Lord et al, 2002). Considering the *S.cerevisiae* model we decided to investigate the role of AgBud10p and its relation to AgRax2p in *A.gossypii.*

To investigate the functions of AgBud10p we deleted the whole ORF´s from start to stop codon using standard PCR-based gene targeting. For the single deletions we used the cassette coding for the resistance against the drug G418. To obtain *Agrax1*Δ*rax2*Δ mutants we deleted the entire *AgRAX2* ORF with a cassette coding for resistance against the drug clonNAT in the *Agrax1*Δ strain. Examination of the deletion showed that the maximal speed of *Agbud10*Δ determined from radial growth of fungal colonies was wild type like (198 µm/h). The characteristic bipolar branching pattern found in wild-type germ cells, which produce two hyphae at an angle of 180° (n = 90) or in less frequent cases at the angle of 90° (n=10), was not disturbed in germinating *Agbud10*Δ spores. Deletion of AgBud10p revealed slightly changed branching patterns. Although lateral branching

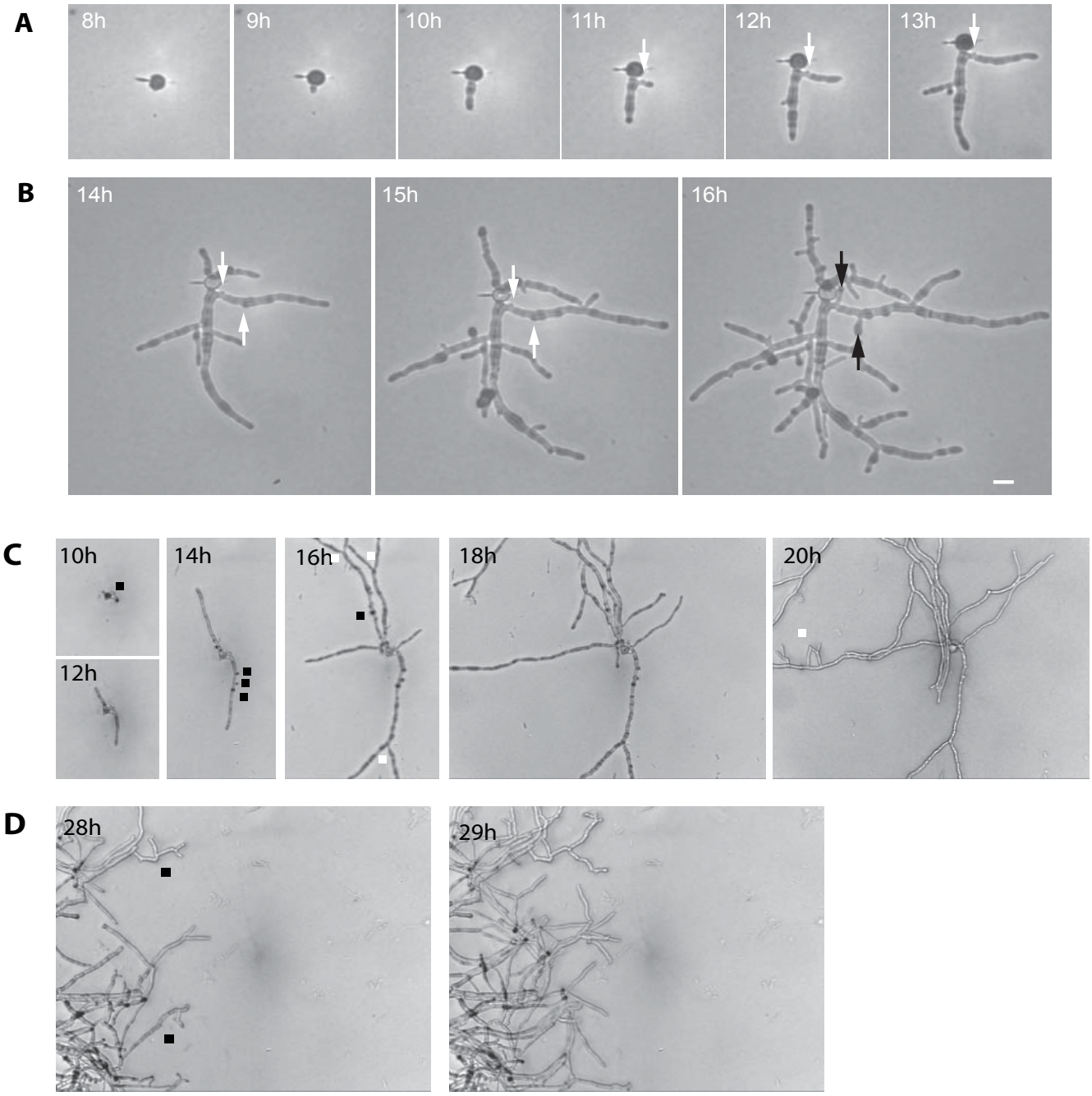

Figure 20
(A) Representative frames show the development of *Agbud10*Δ young mycelium. Spores were pregrown for 8h on AFM medium at 30°C prior to mounting for video microscopy. The time-lapse was carried out at room temperature (25°C). White arrows indicate lateral branches that showed extended growth arrest shortly after they emerged; Black arrows mark the same branches after resumption of growth. **(B)** Development of, *Agbud10*Δ*rax2*Δ mycelium monitored by time-lapse microscopy. Spores were pregrowngrown grown for 8 h on solid medium at 30°C prior to mounting for video microscopy. The time-lapse was carried out at room temperature (25°C). **(C)** Representative frames display lower number of lateral branches, frequent attempts of lateral branch formation (black points) and premature apical branching (white points). **(D)** Representative frames show the development of *Agbud10*Δ*rax2*Δ 28h old mycelium. Fast growing tips display frequent deviations from the axis of polarity resulting in zig-zag-shaped hyphae. Bar,10 µm.

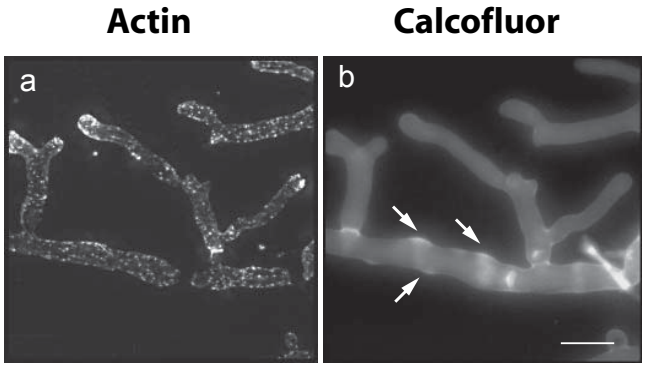

Figure 21
Organization of the actin cytoskeleton in *Agrax2*Δ*bud10*Δ. Spores were grown in liquid complete medium for 16 hours at 30°C, fixed with formaldehyde, stained with Rhodamine-Phalloidine and calcofluor and analyzed by fluorescence microscopy. **(a)** Picture displays polarized actin at most of the tips (indication for active growth). **(b)** Picture shows premature apical branching and attempts of lateral branch formation, which only lead to irregular thickening of originally evenly shaped hyphae (indicated with white arrows). Bar,10 µm.

occurred predominantly in wild type like manner in *Agbud10*∆, single lateral branches emerging with a delay between already developed ones, could be observed. Interestingly, some of the lateral branches revealed temporarily a growth arrest. In all these cases we observed resumption of growth after 1-4 hours from arrest (12 branches were investigated) **(Fig. 20A)**. The dichotomous branching of hyphal tips occurred as regular as in the wild type (not shown).
To summarise, AgBud10p is important, however not essential to maintain polarity at the tip.

As both AgRax2p and AgBud10p appeared to be part of the polar machinery we decided to investigate the relation between them. Thus, we deleted the *AgRAX2* gene from start to stop codon with a cassette coding for resistance against the drug clonNAT in an Ag*bud10*∆ strain **(Fig. 20B)**.
Analysis of the video data displayed (i) lower number of lateral branches, (ii) frequent attempts of lateral branch formation, which only lead to irregular thickening of originally evenly shaped hyphae, (iii) and premature apical branching **(Fig. 21)**. As the observed phenotype was stronger than those described for the single deletions we propose that AgRax2p and AgBud10p act independently in order to regulate branching pattern and frequency. Further studies have to be performed to verify whether AgBud10p is important for the localization of AgRax2p.

A functional GFP fusion to AgRax2p locates to the tip and the septum region

AgRax2p seems to control the time and the homogeneity of tip branching in young mycelium. Further, it maintains the capacity of mature hyphae to grow straight and form apical branches.

In order to investigate whether AgRax2p localizes to sites of polar growth as seen for ScRax2p in S.cerevisiae (Chen et al., 2000) we constructed a carboxy-terminal GFP fusion to the endogenous copy of the AgRAX2 ORF in the A.gossypii wild type strain. The radial colony growth rate and the morphology did not differ in the AgRax2-GFP strain compared with the wild type (Fig. 2). This result indicates that the GFP-tag did not affect the function of AgRax2p.

GFP fluorescence of the AgRax2-GFP transformant was highly enriched in tip regions with a sharp zone at the very tip. Additionally, we could observe enriched zones of GFP fluorescence at presumptive septa, which will be discussed later.

Furthermore, plasmids *pRS415RAX2* with carboxyl-terminal GFP fusion under control of the *A.gossypii RAX2* promoter transformed into *Agrax2*Δ strain showed the signal at the tip and at the septum site. Moreover, we were able to localize an episomal copy of the AgRax2-GFP in the AgΔ*lt* strain that still a wild type copy of the *AgRAX2* gene.

AgRax2p localises permanently to sites of polarised growth

To determine whether AgRax2-GFP locates permanently or transiently to the sites of polar growth (emergence of the first hyphae from germ bubble, initiation of lateral branches and dichotomous tip branching) we monitored the development of *A.gossypii* GFP labelled strain by *in vivo* fluorescence video microscopy.

First, we followed the appearance of the GFP signal during spore germination. Pictures were taken every 3 min over a time period of 1hour. Representative frames are shown below **(Fig. 22)**. Already in the germling the GFP signal formed a cloud at the site where later the first hyphae emmerged. This observation may reflect the cytoplasmic localization of AgRax2-GFP in the early stage of development. Over time the cloud of protein became denser to form finally an arc at the site of polar growth which may reflect cortical localization of the AgRax2-GFP at that stage. Parallel with the GFP signal accumulation we observed deformation of a germling **(Fig. 22A)** Furthermore, AgRax2-GFP remained localized to the original tip without delocalisation when a new portion of the protein was deposited at the opposite side of the germ bubble to form a second, bipolar germling **(Fig.22 B)**. To better visualize the position of the GFP signal at the tip acquired images were three dimensionally reconstructed and 90° rotated **(Fig.22 C)**.

Second, we investigated the localization of AgRax2-GFP during lateral branch formation. The emergence of a novel branch was always preceded by a concentration of AgRax2p-GFP at the cell cortex, as it was seen during germination. The newly initiated branches permanently maintained a signal at the tip. We have not seen the disappearance of AgRax2-GFP from the hyphal tip when a new branch was formed in the neighbourhood. **(Fig. 23 A,B)**.

Than we followed the division of an existing AgRax2-GFP during apical branching. When the tip speed reaches 80µm/h or more wild type switches to tip branching (Knechtle, 2003 et al, Bauer et al., 2004). Pictures of a tip splitting in 22h old mycelium were taken every 30 sec over a time period of 5 min. the first eight representative frames show the protein localization during tip branching **(Fig. 23 C,D)**. Shortly before the hyphal tip split generating two branches, AgRax2-GFP signal intensity increased and after remained permanently localized at the tips of the two independently formed branches.

The establishment of polarization sites does not occur randomly in *A.gossypii* but most likely at preformed landmarks (see above and Knechtle et al., 2003). Sites of polarization determine where the first hypha emerges from the germ bubble, where lateral branches initiate and also when a hyphal tip splits into two branches.

AgRax2p was present shortly before polar growth occurred and later was permanently maintained at the tip, thus, although AgRax2p is not essential for polar events it may be one of the polarity landmarks involved in this process.

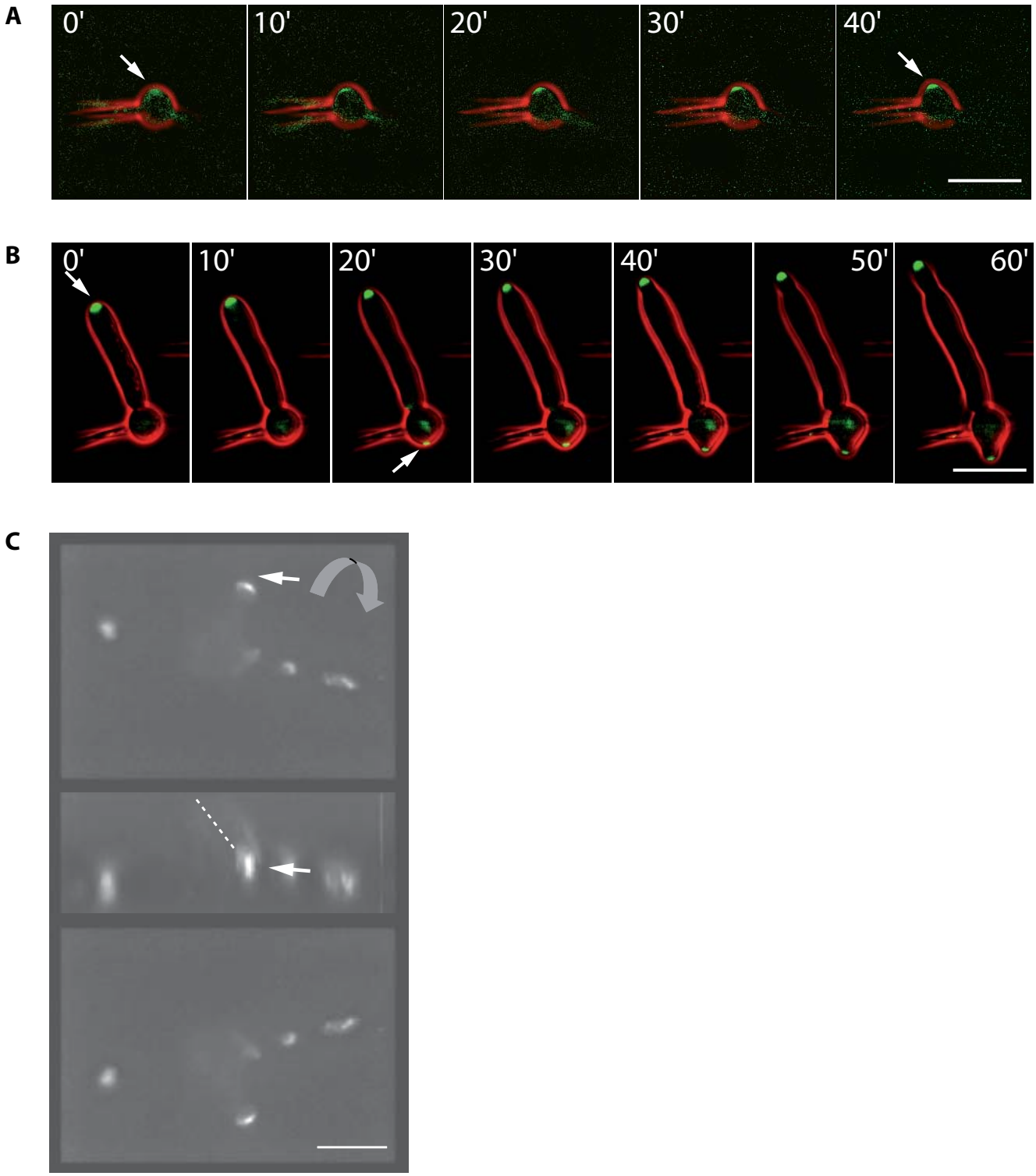

Figure 22
Distribution of AgRax2p-GFP during germination and sustained polar growth. **(A)** GFP signal localizes as a spot at a polar site just before emergence of first germ tube (white arrow). The GFP signal is indicated in green, the phase contrast in red. **(B)** The GFP signal remains at the tip during hyphal elongation. Also seen is the AgRax2-GFP polarisation at the site where second germ tube emerges (white arrow). The GFP signal is indicated in green, the phase contrast in red. **(C)** 3-D reconstruction of the AgRax2-GFP tip localization. 46 planes of the AgRax2GFP signal were acquired at z-distances of 0.3 µm. The stack was three dimensionally reconstructed and 2x90° rotated at the x-axis. The dashed lines are at constant positions in each image to allow monitoring of the rotation. The „double needles“ visible in picture A and B are an artifact caused by compression of different focal planes in order to visualize all GFP signals present in the cell. Auto-fluorescence of the spore needle is observed in picture C. Bar, 10 µm.

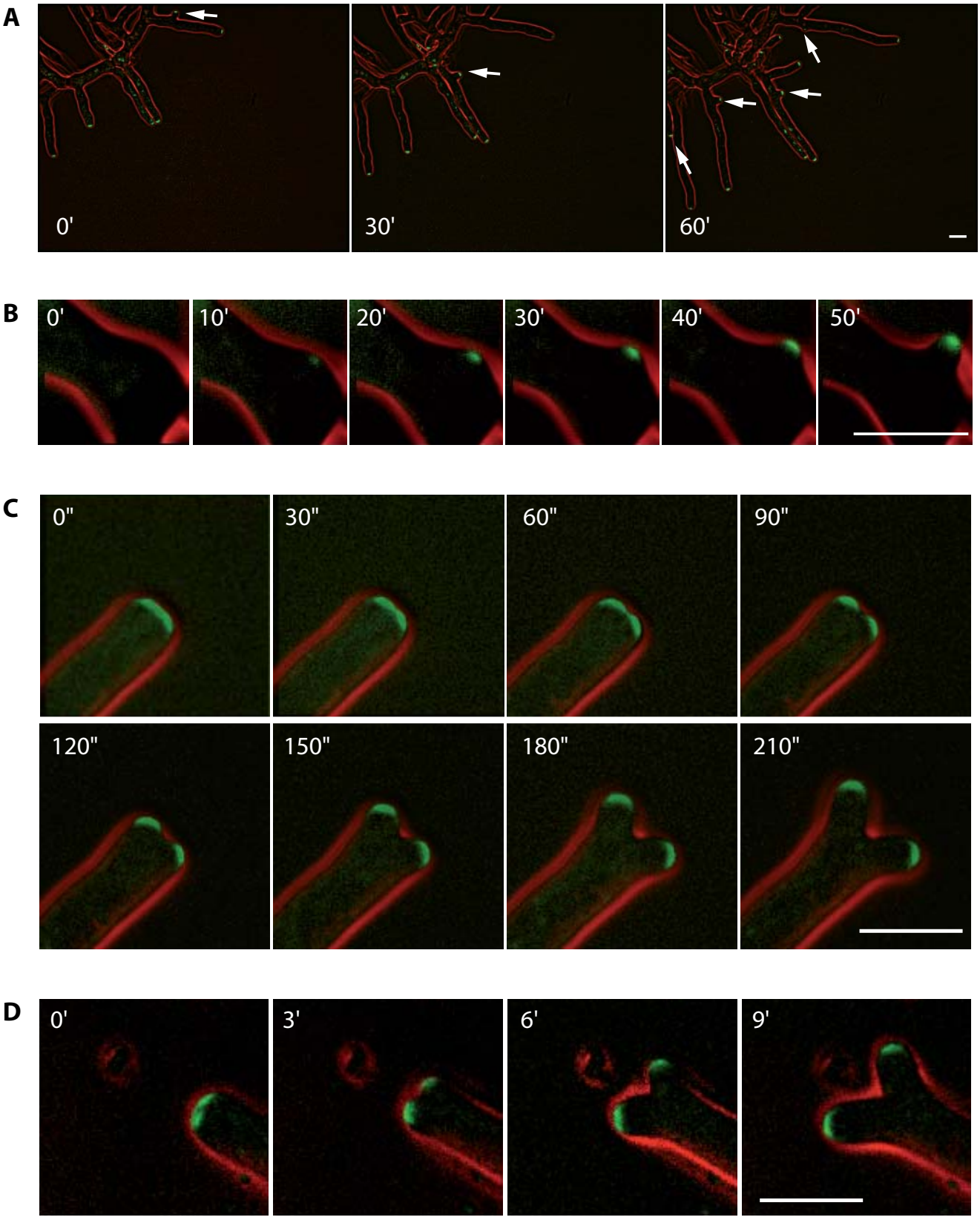

Figure 23
Temporal organization of AgRax2p-GFP. **(A)** During sustained polar growth the GFP signal remains at the hyphal tip even during lateral branch formation. **(B)** AgRax2-GFP appears at the hyphal cortex prior to lateral branch emergence. **(C)** The GFP signal remains at the hyphal tip during apical tip branching. The GFP signal is indicated in green, phase contrast in red. The GFP signal sometimes appears slightly dislocalized from the tip. This is caused by a microscopy artifact, when the focal planes of the phase contrast and the GFP fluorescence are not completly adjusted. Bar, 10 µm.

AgRax2p is continuously delivered to the tip

We have shown herein that AgRax2-GFP was present already in a very early stage of the development marking polar sites during spore germination and that it later localized permanently to the tip of hyphae and lateral branches. Almost all tips displayed AgRax2-GFP. In order to investigate the dynamics of the protein at the tip we bleached the GFP with fluorescence light for 5 min and we followed the reappearance of its signal at the tip with video microscopy. Pictures were taken every 5 min for a 40 min period **(Fig. 24)**. The recovery of AgRax2-GFP signal was taken as an evidence for continuous delivery of the protein to the tip.

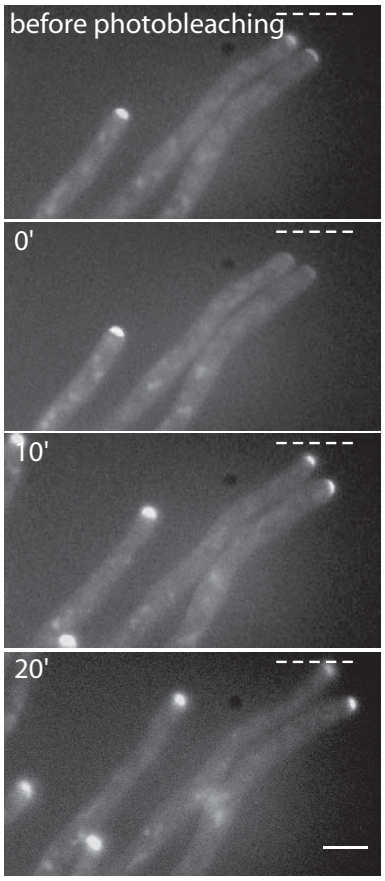

Figure 24
Fluorescence Recovery of AgRax2-GFP signal after the photobleaching. Signal at two tips in the upper right corner (top panel) was bleached with fluorescence light (second panel). After 5 min recovery time the signal at both tips reappeared and hyphae continued to grow (last two panels). The dashed lines are at constant positions in each image to allow monitoring of growth. Bar, 10 μm.

AgRax2p delivery to the tip is actin dependent

Because the actin cytoskeleton serves as the structural basis for cell polarity (Hall, 1998; Johnson, 1999) we tested whether the recovery of the bleached AgRax2p-GFP signal was actin dependent. To investigate the role of actin in AgRax2-GFP signal distribution we applied Latrunculin A (LatA). Addition of LatA disrupts actin structures, abolishes vesicular movement and apical localization, giving rise to a uniform fluorescence within hyphae. First, we followed the AgRax2-GFP signal with video microscopy for about 15 min. Next, we applied 3 μl of 2mM LatA directly under the cover slide, and followed the disappearance of the AgRax2-GFP signal from the tip.

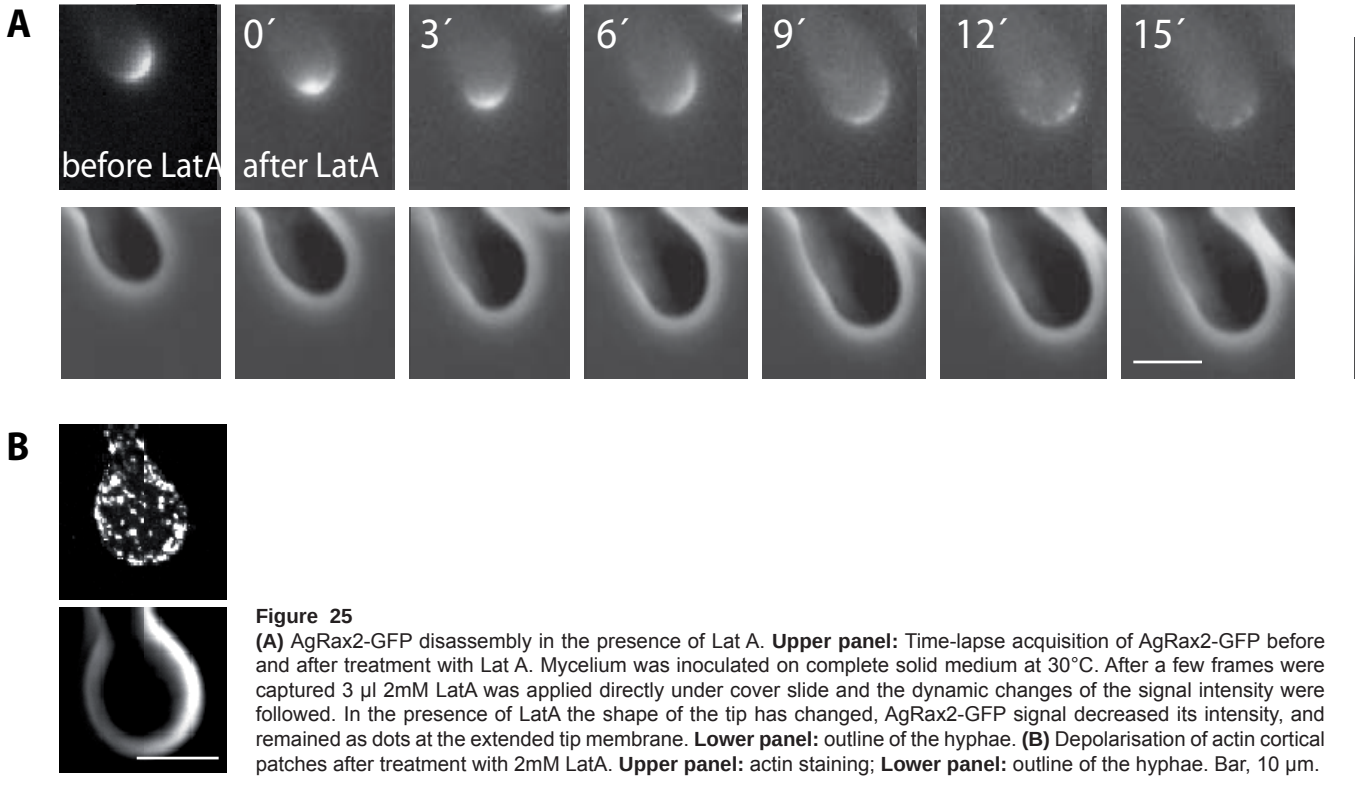

Figure 25
(A) AgRax2-GFP disassembly in the presence of Lat A. **Upper panel:** Time-lapse acquisition of AgRax2-GFP before and after treatment with Lat A. Mycelium was inoculated on complete solid medium at 30°C. After a few frames were captured 3 μl 2mM LatA was applied directly under cover slide and the dynamic changes of the signal intensity were followed. In the presence of LatA the shape of the tip has changed, AgRax2-GFP signal decreased its intensity, and remained as dots at the extended tip membrane. **Lower panel:** outline of the hyphae. **(B)** Depolarisation of actin cortical patches after treatment with 2mM LatA. **Upper panel:** actin staining; **Lower panel:** outline of the hyphae. Bar, 10 μm.

Pictures were taken every 3 minutes for a time period of 30 min **(Fig. 25)**. Upon the 2mM LatA treatment AgRax2-GFP signal extended over the tip surface, and remained as little dots fused into the membrane. During the next 20 min its intensity decreased, however the signal did not disappear. These observations support the model that AgRax2p transport to the tip is likely to be actin-dependent.

A functional GFP fusion to AgRax2p only partially colocalizes with Spitzenkörper

GFP fluorescence of the AgRax2-GFP transformant was highly enriched in tip regions with a sharp zone at the very tip. This observation suggested two possible localizations for AgRax2-GFP. First, typically membrane, fused to the very tip, and secondly localization, as a part of the Spitzenkörper (apical body), an apical cluster of vesicles, cytoskeletal elements, and other proteins, which play a crucial role in hyphal extension.

In order to decide which localization pattern is correct we applied FM464 “life staining” to visualize Spitzenkörper, further we analyzed the position of AgRax2-GFP signal in respect to the apical body (in co-operation with M. Köhli). AgRax2-GFP only partially co-localized with Spitzenkörper. The GFP signal was present at the very tip, most likely fused to the cell cortex, whereas Spitzenkörper covered an approximately three times bigger area **(Fig. 26)**.

Another three lines of evidence support our findings. First, during protein analysis we identified one potential transmembrane domain at the amino-terminal end of AgRax2p. Secondly, the Spitzenkörper consisting of microvesicles disassembles upon Lat A treatment whereas part of the AgRax2-GFP signal remains visible fused to the membrane after Lat A treatment. And finally, co-staining with Rhodamine-Phalloidine exhibited no complete co-localization of AgRax2-GFP signal with actin patches at the tip **(Fig. 27)**. The GFP fluorescence was fused to the very tip, whereas the actin patches were dispersed over a wider tip region. AgRax2-GFP was not seen to co-localize with actin cables.

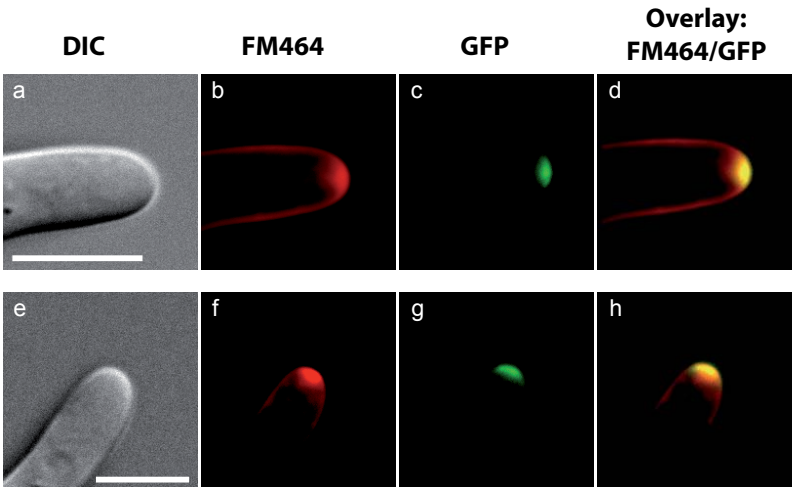

Figure 26
During sustained polar growth AgRax2p-GFP is present at the hyphal cortex where it partially co-localizes with Spitzenkörper. **(a,e)** DIC image of hyphal tip; **(b,f)** FM464-staining; **(c,g)** AgRax2-GFP; **(d,h)** overlay of b and c images . Bar, 10 µm.

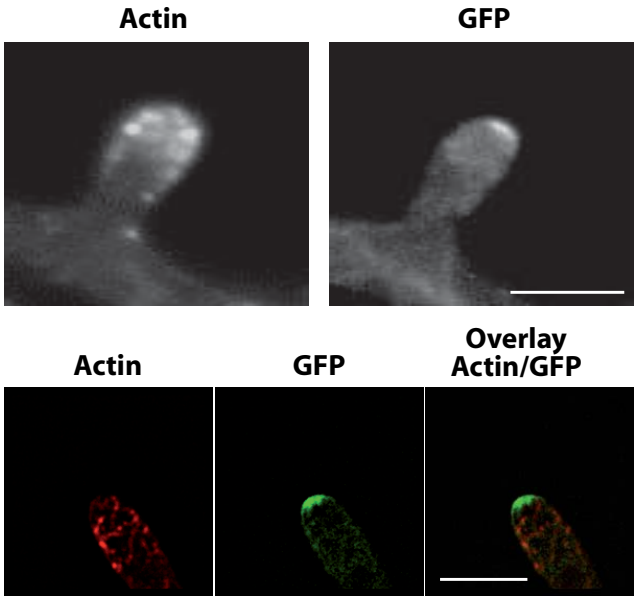

Figure 27
Localisation of AgRax2p-GFP and actin at hyphal tips. Rhodamine-Phalloidin / AgRax2p-GFP double staining. AgRaxp-GFP cdoes not co-localize with actin at the tip. Bar, 10 µm.

A signal sequence is essential for the localization of AgRax2p

To further investigate the mechanism that directs the protein to the tip we tested if the 21 amino acid hydrophobic region behind the first codon at the N-terminus may be a putative signal sequence important for secretion of the protein to the growing hyphal tips.

Therefore, we constructed plasmid *pRS415RAX2_DSP* with carboxy-terminal GFP fusion under the control of the *A.gossypii RAX2* promoter.

The vector was able to replicate in *A gossypii* using an *S.cerevisiae* ARS element and it could be selected in an *Ag*D*lt* strain due to the *S.cerevisiae LEU2* gene. It could also be selected on plates containing the drug G418 due to the presence of the GFP cassette carrying resistance against the G418.

As a control we tested the localization of *pRS-415RAX2-GFP* in *Ag*D*lt* strain.

The transformants expressing the GFP fusion from the *pRS415RAX2GFP* vector displayed the signal at the tip and at the septum, where it was seen in carboxy-terminal GFP fusion to endogenous copy of the *AgRAX2* **(Fig. 28A)**. When the plasmid carried a signal sequence deletion after the first codon of the *AgRAX2 ORF (pRS415RAX2-GFP_DSP)* all transformants failed to localize AgRax2-GFP properly **(Fig. 28B)**. Considering the general role of signal peptides, the AgRax2-GFP expressed from the vector most likely could not pass through the secretory pathway. Thus, the putative signal peptide is essential for the proper localization of AgRax2p in order to direct polarity to the tip.

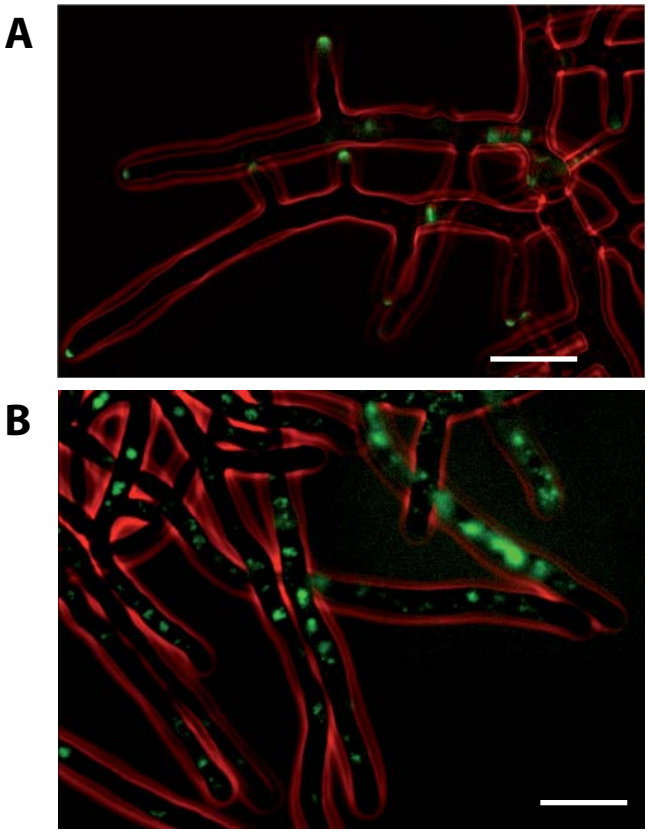

Figure 28
Localization of AgRax2p depends on its signal peptide. **(A)** Δ*leu2,thr4* cells carrying pRS415_RAX2GFP plasmid were grown in media containing G418 to select for the plasmid and were then examined for the localization of GFP fluorescence (positive control). GFP signals were present at tips and septa. **(B)** Δ*leu2,thr4* cells carrying plasmid pRS415_RAX-2GFP_deltaSP were grown in presence of G418 and examined for the localization of GFP fluorescence. The signals could not be associated with any known cellular structure. Bar, 10 μm.

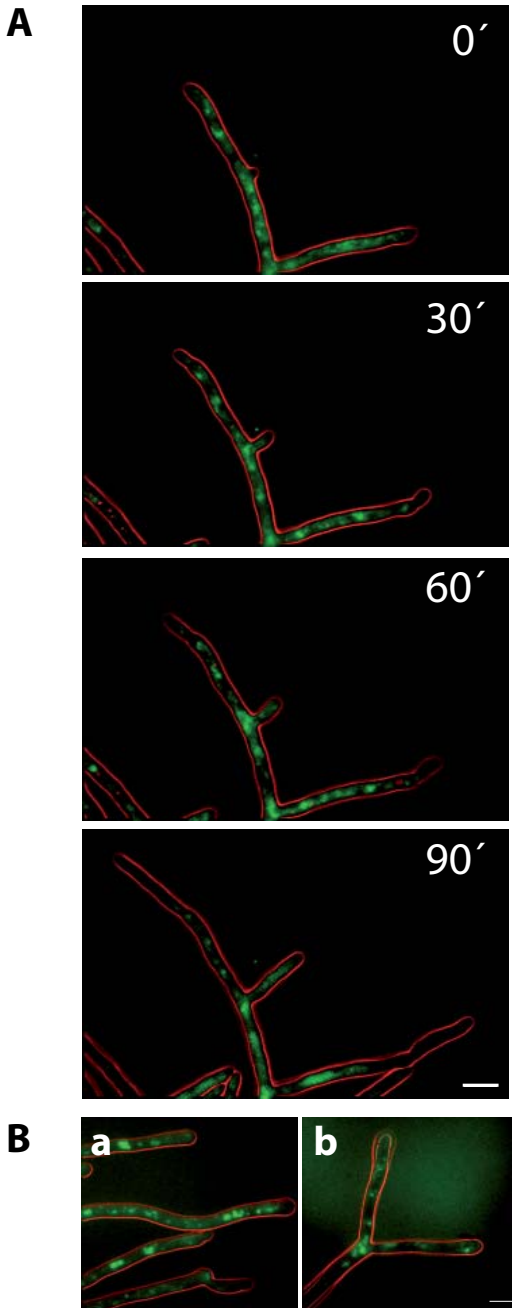

Figure 29
Localization of AgRax2p depends on AgRax1p. (A) AgRax2-GFP cells lacking the *AgRAX1* were examined for the localization of GFP fluorescence. The signals observed could not be associated with any known cellular structures. (B) **(a-b)** shows the localization of GFP signal in 30h old mycelium. Bar, 10 μm.

AgRax1p is essential for the proper AgRax2p deposition at the tip and septum

The phenotype of the *Agrax1*Δ*rax2*Δ double mutant was very similar to those of the single mutants suggesting that AgRax1p and AgRax2p may function in the same pathway and perhaps depend on each other. A point of particular interest was to determine the relationship between both proteins.

For this purpose we deleted *AgRAX1* ORF from start to stop codon with the cassette coding for resistance against the drug clonNAT in a strain expressing GFP-labelled *Ag*Rax2p. AgRax2-GFP failed to localize normally in the *Agrax1*Δ mutant strain. The GFP signal was observed in small patches or vesicles or in structures that appeared to be the vacuoles (DIC image). We could not see the signal at the tip or at the septum **(Fig. 29)**. This observation suggests that AgRax1p may be important for the positioning of AgRax2p and therefore may function upstream of AgRax2p.

AgBud10p stabilizes AgRax2p at the tip

Considering the fact that both AgRax2p and AgBud10p act independently on each other in order to regulate the branching pattern and frequency and

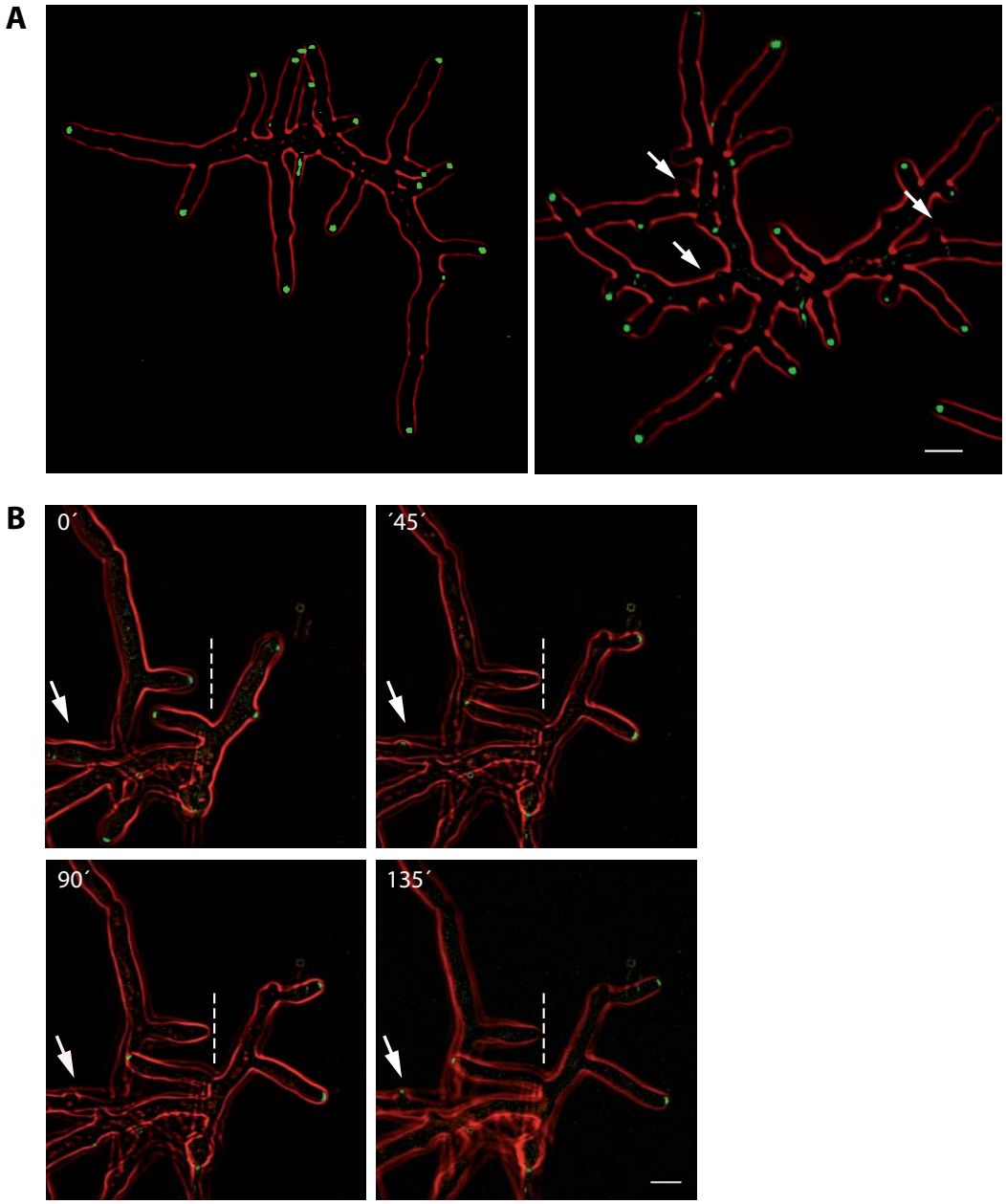

Figure 30
Loss of localization of AgRax2p-GFP during tip growth arrest in *Agbud10*Δ. **(A)** Left image: WT; right image: *Agbud10*Δ. In absence of AgBud10p AgRax2p-GFP was not seen in association with all tips. **(B)** Disappearance of AgRax2-GFP in *Agbud10*Δ was monitored by in vivo microscopy. The dashed lines are at constant position in each image to allow monitoring of growth arrest. We have seen resumption of tip growth and reappearance of the GFP signal at the tips. GFP signals are indicated in green and the phase contrast in red. Bar, 10 µm.

that some of the *Agbud10*Δ lateral branches revealed temporary growth arrest we decided to verified wheather AgRax2p still localizes correctly in *Agbud10*Δ.

We deleted AgBud10p with a cassette coding for resistance against the drug cloNAT in a strain expressing GFP-labelled *Ag*Rax2p. In absence of AgBud10p AgRax2-GFP was only seen in a sub fraction of tips **(Fig. 30A)**. Disappearance of the GFP signal in *Agbud10*Δ was monitored by in vivo time-lapse microscopy **(Fig. 30B)**. Dashed lines present at constant positions in each image allow monitoring of growth arrest that in this case took 1 hour. During this time the AgRax2-GFP signal was not present at the tip. The time between arrest and resumption of growth was comparable with those estimated based on DIC movies (1-4 hours). After one hour we have observed reappearance of the GFP signal at the tip and resumption of the tip growth. We suggest that loss of localization of AgRax2-GFP during tip growth in *Agbud10*Δ leads to a temporal growth arrest. This observation strongly argues that AgBud10p is important, however not essential, for the maintenance of AgRax2-GFP during tip growth.

AgCdc24p is essential for the cortical localization of AgRax2p at new growth sites

To further investigate the role of the actin cytoskeleton in AgRax2p positioning the essential GEF-*AgCDC24*, required for the establishment of actin polarization in *A.gossypii* germ cells (Wendland et al. 2000,) was deleted with the cassette coding for resistance against the drug cloNAT in *Ag*Rax2-GFP. An *Agcdc24*Δ mutant continued to grow isotropically, became large and round. In the absence of AgCdc24p we could not see polar distribution of actin patches, moreover, we did not see polarized AgRax2p neither as a cloud nor at the cell cortex. AgRax2-GFP was seen in dot-like structures whose number increased with the age of the cell **(Fig. 31)**.
Therefore, AgCdc24p is essential for the correct localization of AgRax2p at new growth sites. Further, those results support the hypothesis already mentioned in respect to AgRax1p that the delivery of AgRax2p to the membrane goes throughout the actin dependent secretory pathway. When the transport of secretory vesicles was abolished, AgRax2p could not be delivered towards the polar sites.
If AgRax2p would be involved in the selection of new polar sites we would expect the signal to be present at the cortex independently on AgCdc24p.

*Ag*Bni1p is not essential for the AgRax2p initial polarization

To define other proteins required to position AgRax2p we deleted using a cassette coding for resistance against the drug cloNAT *AgBNI1* in a *Ag*Rax2-GFP. *Agbni1*Δ shows irregular isotropic growth that leads to potato–like cells. *Ag*Bni1p is essential for hyphal emergence and elongation, as well as for organization of actin cables and thus tip-directed transport of secretory vesicles. (Schmitz et al., 2005 (in preparation)). In 58% (n=70) of *Agbni*Δ*1* germlings

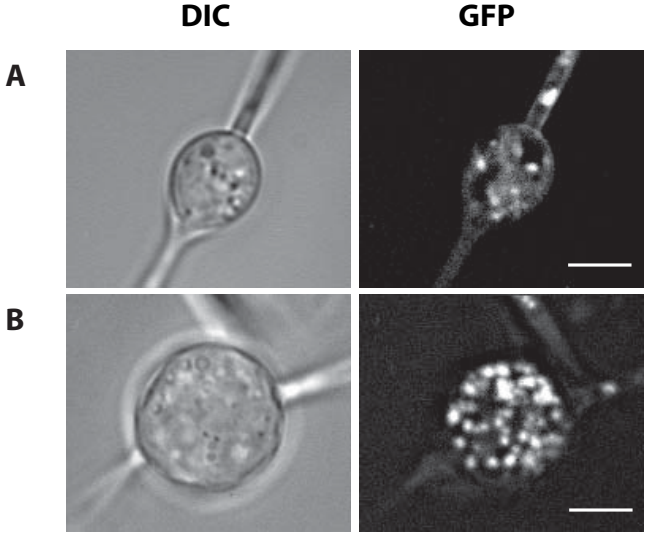

Figure 31
AgRax2-GFP distribution as vesicles in *Agcdc24*Δ. **(A)** A germinating spore shows depolarised AgRax2-GFP spots. **(B)** The number of vesicle-like structures carrying GFP increases with time in swollen germling of the non-polarizing Agcdc24 deletion strain. Left panels are brightfield and right images are fluorescence images. Bar, 10 µm.

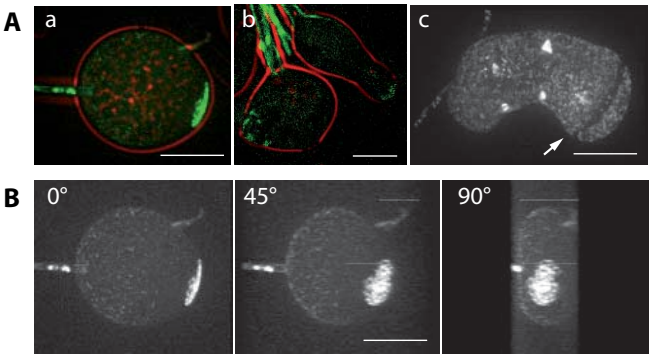

Figure 32
AgRax2-GFP distribution in *Agbni1*Δ which forms swollen, round, potato-like germlings. **(A)** The germinating spore shows a polarized AgRax2-GFP signal **(a)**. The signal intensity seems to decrease when the germling changes its shape. The signal is visible as dots closely associated with the tip cortex **(b).** The GFP signal sometimes disappears from the tip of the cells that formed septum (white arrow) **(c)**. The unspecific signals are probably fluorescence background. An AgRax2-GFP signal was not seen in association with a closed septum. **(B)** The AgRax2-GFP signal in *Agbni1*Δ mutant is present at the cell cortex. 50 planes of the AgRax2-GFP signal at the tip were acquired at a z-distance of 0.3 µm. The stack was three dimensionally reconstructed and 2x45° rotated at the y-axis. Bar, 10 µm.

an AgRax2-GFP signal was found at the end opposite to the spore needle **(Fig. 32A)**. The signal intensity decreased when hyphae extended; only part of the signal remained visible as dot-like structure fused to the membrane **(Fig. 32B)**. 42% (n=70) of the *Agbni1*Δ cells, apparently round ones, showed *Ag*Rax2-GFP signal as dot-like structures of approximate size present all over the cell periphery resembling the localization of AgRax2p in *Agcdc24*Δ. The high percentage of potato-like cells exhibiting polarized GFP signal suggest that *Ag*Bni1p is not essential for the AgRax2p initial polarization, however it seems to be important for the delivery of the protein to the tip of very elongated cells.The presence of the AgRax2p at the tip of *Agbni1*Δ elongated cells indicates the role of AgRax2p in the maintenance of polar growth.

A functional GFP fusion of AgRax2p locates to the septum region

Additionally to the earlier described localization of AgRax2p at the tip, the AgRax2-GFP was seen transiently in association with the septum either as a single ring to multiple sites of future septation or as a double ring to newly established septa **(Fig. 33A)**. During septum formation AgRax2-GFP signal encircled hyphae and split into two rings marking two neighbouring compartments, the signal remained visible up to 2 hours after the septum fully separated two compartments **(Fig. 33B)**.

Representative frames taken at 15 min intervals show the typical developmental stages of septum formation. Between two contracting GFP rings we could observe in DIC images the appearance of septum structures **(Fig. 34)**.

Relatively little is known about the mechanisms leading to septum formation. The septation process was previously shown as not to be essential for the polar growth of *A.gossypii*, however to be essential for its sporulation (Wendland et. al 2001). Considering the localization of AgRax2p at the septum and the sporulation defect observed in *Agrax2*Δ it was of particular interest to investigate this process.

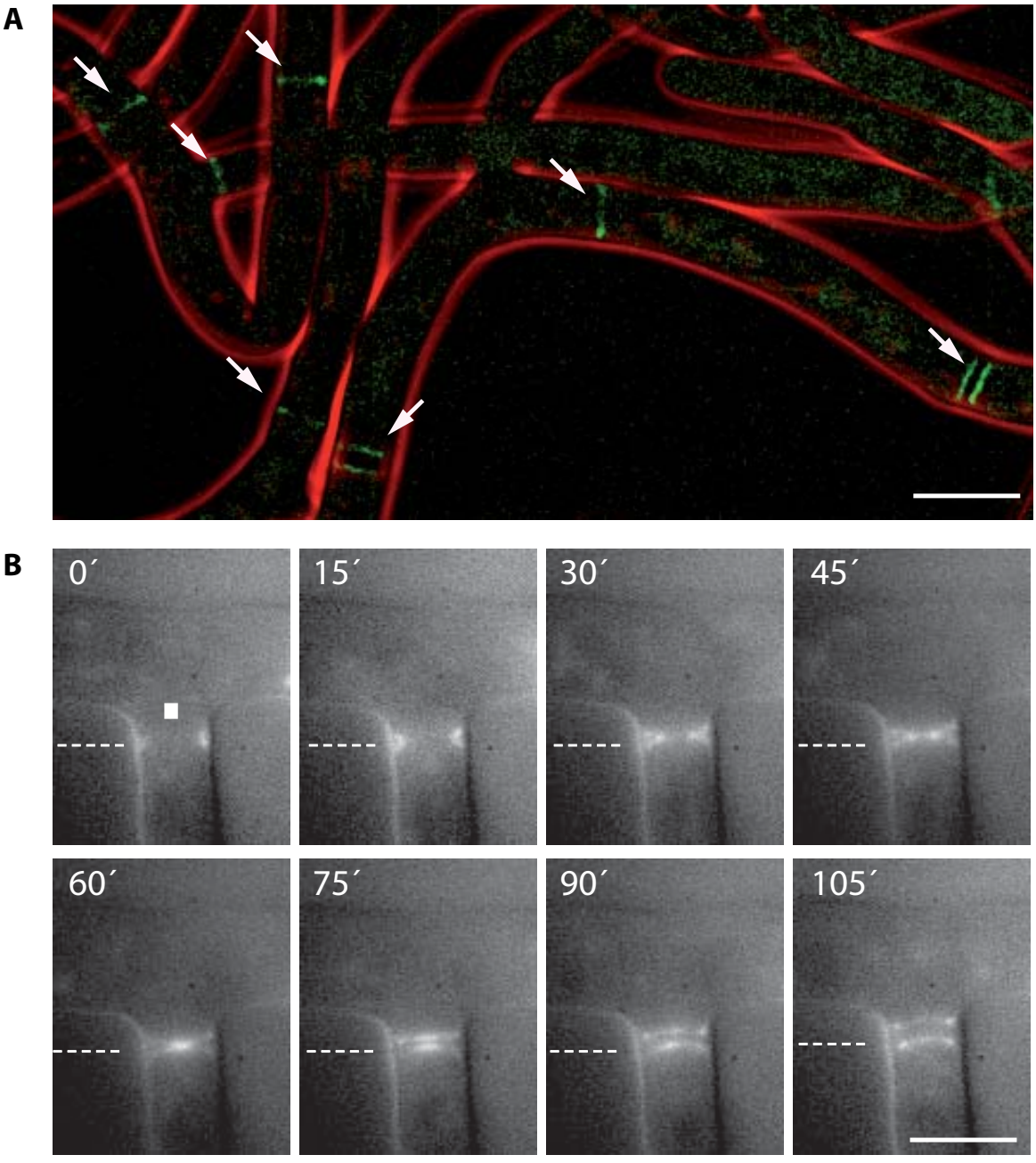

Figure 33
(A) AgRax2-GFP localizes to sites of septum formation. The GFP fluorescence is indicated in green and phase contrast in red. **(B)** Organization of AgRax2p-GFP during septum formation. The GFP signal is indicated in white, the outline of the hypha is represented in gray. The dashed lines are at constant positions in each image to allow monitoring of septum formation. The white square indicates the subapical (older) compartment. AgRax2-GFP contracts during septum formation. Bar, 10 µm.

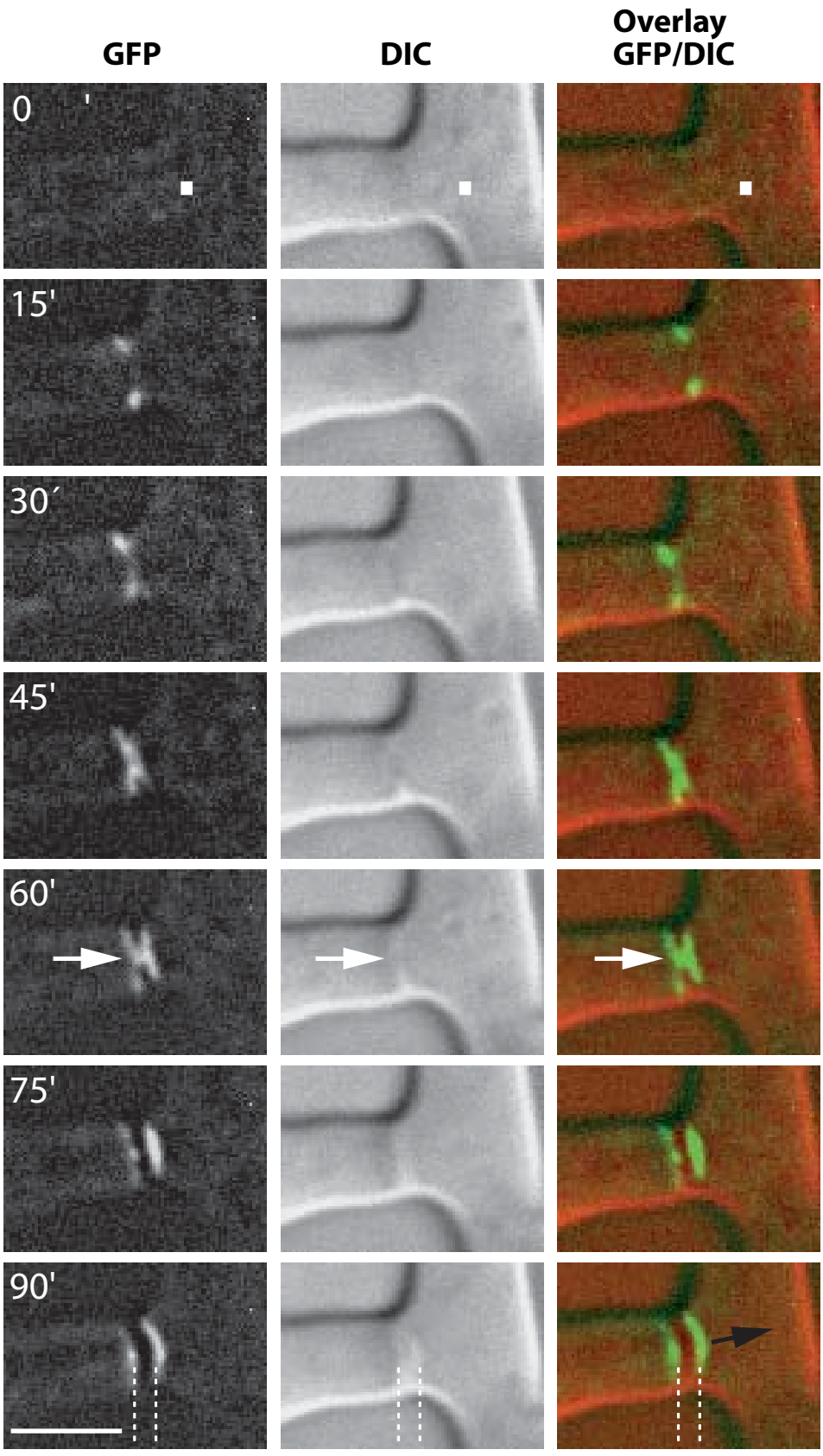

Figure 34
Organization of AgRax2p-GFP during septum formation. The left column shows GFP signals, the middle column the DIC outline of the hyphae with a septum ring; the right column shows overlays of DIC and GFP images. White points indicate old compartment. Arrows indicate position of GFP signal shortly before septum visible in DIC form the ring. The dashed lines are at constant positions in each image to allow monitoring of GFP in respect to septum visible in DIC. GFP signal does not overlap with septum structure visible in DIC images. AgRax2-GFP stays up to 2 hours after septum was formed. The white square marks the hypha from which the branch emerged. Bar, 10 µm.

AgRax2p co-localizes only with the single actin ring and its localization to the septum region depends on actin

AgRax2p fused to GFP was shown to localize permanently to the tip and transiently, as a single ring, to multiple sites of future septation or as a double ring to newly established septa.

To investigate transient localization of AgRax2-GFP at the septum we performed co-staining with rhodamine-phalloidine and calcofluor. In an early septum formation phase the AgRax2-GFP signal always co-localized with transiently appearing, as a precursor for septation, actin rings **(Fig. 35A)**. After the AgRax2-GFP split labelling each compartment with an AgRax2p ring we could not see a clear co-localization of AgRax2-GFP with actin patches. The space between two GFP rings was filled with chitin, visualized by calcofluor staining **(Fig. 35B)**.

In order to examine the role of actin in the primary deposition of AgRax2-GFP at the septum, we applied Latrunculin A that disrupts actin structures and abolishes vesicular movement. First, we followed the AgRax2-GFP signal with *in vivo* video microscopy for about 15 min, than we applied 2mM LatA directly under the cover slide.

In the presence of LatA, new AgRax2-GFP rings were not formed, and existing ones did not split.

Furthermore we investigated AgRax2-GFP dynamics at the septum. From two discs marking two compartments, the one attached to the older compartment (indicated by a white arrow on the side opposite to

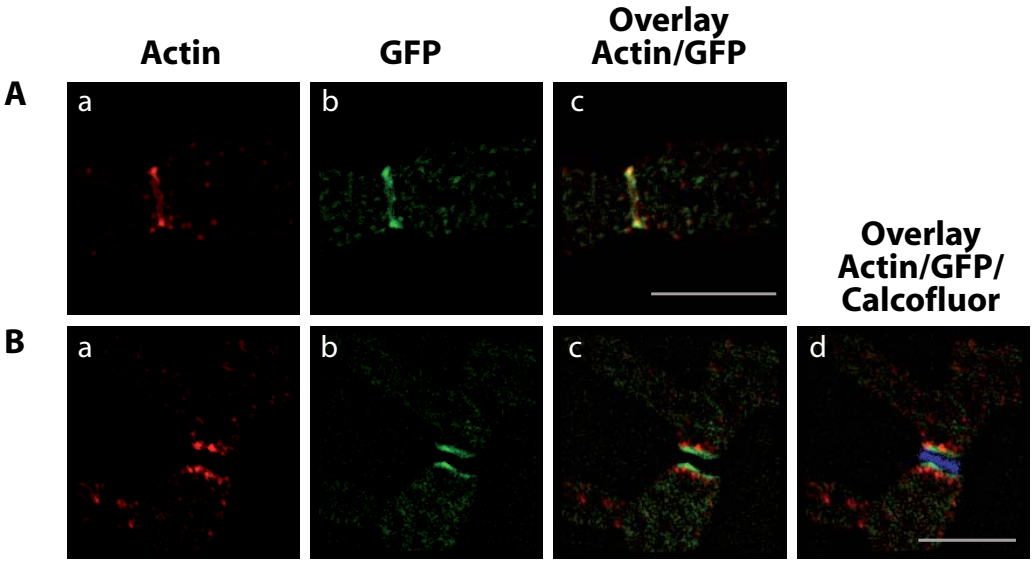

Figure 35
Actin Rhodamine-Phalloidin/AgRax2p-GFP colocalization at the septum. **(A)** Colocalisation of AgRax2p-GFP and actin at sites of septation. AgRaxp-GFP co-localises perfectly with the actin ring **(B)** Lack of colocalization at developed septum, where a chitin ring is already visible. Bar, 10 μm.

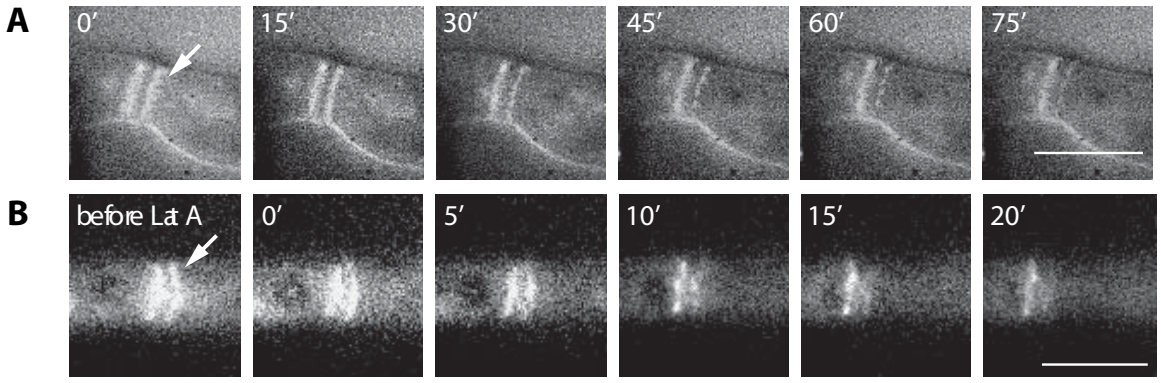

Figure 36
Stability of AgRax2-GFP rings in presence or absence of Lat A. **(A)** Time-lapse acquisition of AgRax2-GFP in the absence of Lat A. The mycelium was inoculated on complete solid medium at 30°C. During 75 min one of the two AgRax2-GFP rings decreased its intensity faster than the other one and disappeared. The remaining ring marked the compartment on the side of the extending hypha. **(B)** Time-lapse acquisition of AgRax2-GFP after treatment with Lat A. The mycelium was inoculated on complete solid medium at 30°C. After a few frames were captured LatA was applied directly under the cover slide and the dynamic changes of signal intensity were followed. 20 min after LatA has been applied one ring of AgRax2-GFP was gone. The other ring remained marking the compartment on the side of the extending hypha. In the presence of LatA the less stable AgRax2-GFP ring (white arrow) disappeared 4x faster than in WT. Bar, 10 μm.

growth direction) changed its intensity after Lat A treatment. The other being attached to the new compartment showed delay in intensity changes **(Fig. 36B)**. This is consistent with the signal behaviour at the septum under normal condition, where observed changes were less dynamic **(Fig 36A)**. In the presence of LatA one of the two AgRax2-GFP rings, adjacent to the older compartment, disappeared four times faster than in the WT.
Thus, the initial AgRax2p deposition at the septum, as well as the AgRax2p transport to the established septum are likely to be actin dependent.

AgBni1p is not essential for the AgRax2p initial localization at the septum

To further investigate the role of actin polarization in *Ag*Rax2-GFP deposition at the septum we deleted *AgBNI1* in a *Ag*Rax2-GFP strain. *Ag*Bni1p is essential for organization of actin cables and thus, transport of secretory vesicles, however, *Ag*Bni1p is not essential for the initial polarisation of *Ag*Rax2p at the tip of potato-like cells and for actin ring and septum formation (Schmitz et al., 2005 (in preparation)). In the absence of AgBni1p a remnant of the AgRax2-GFP signal was found at the ongoing septum, but we were not able to find AgRax2-GFP signal in association with fully closed septum, visible as a dark bar in DIC images.
Interestingly, we could not see tip polarized AgRax2-GFP signal in the cells with established septum **(Fig. 37)**. Therefore AgBni1p is not essential for the AgRax2p initial localization at the septum.

AgCyk1p dependent actin ring formation is essential for the initial deposition of AgRax2p at the septum

To define other proteins required upstream of AgRax2p at the septum we deleted *AgCYK1* in a strain expressing GFP-labelled AgRax2p. The *AgCYK1* gene is required for actin ring formation and septation without interfering with polarized hyphal tip growth. In the *Agcyk1*Δ hyphae are totally devoid of actin rings at presumptive septal sites. *Agcyk1*Δ hyphae are aseptate and do not accumulate chitin in their cell walls. (Wendland and Philippsen, 2002.) We have investigated over 100 dichotomously branching tips for presence of AgRax2p ring at the bottom of two branches. Loss of the AgCyk1p results in the absence of the AgRax2p rings at the septum site, however, this gene loss does not influence the localization of the AgRax2-GFP signal at the tip of hyphae **(Fig. 38)**.This observation leads us to the conclusion that AgCyk1p dependent actin ring formation is essential for the initial deposition of AgRax2p at the septum.

These results strongly argue for a mechanistic distinction between the placement of AgRax2p at the tip and at the septum.

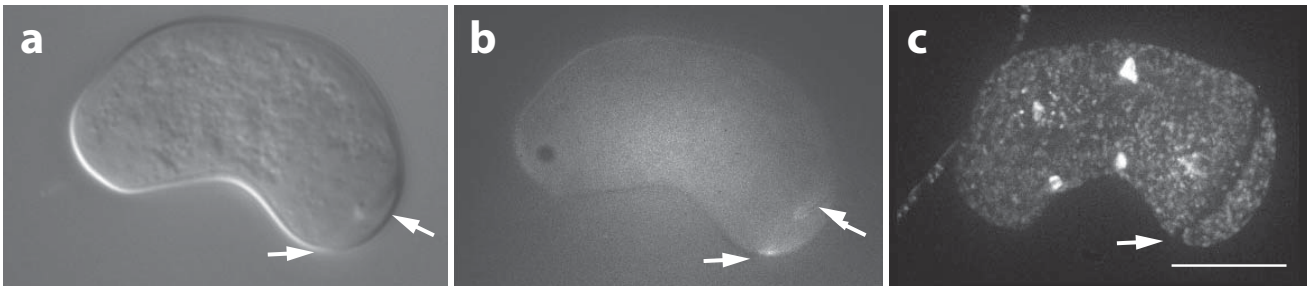

Figure 37
AgRax2-GFP at the septum of *Agbni1*Δ. GFP signal is gone from the tip of the cells that form septum (indicated with white arrows). **(a)** DIC image of *Agbni1*Δ with visible septum ring. **(b)** Remnant of AgRax2-GFP signal at the ongoing septum is indicated. AgRax2-GFP was not seen in association with fully closed septum. Unspecific signal is probably fluorescence background. Bar, 10 µm.

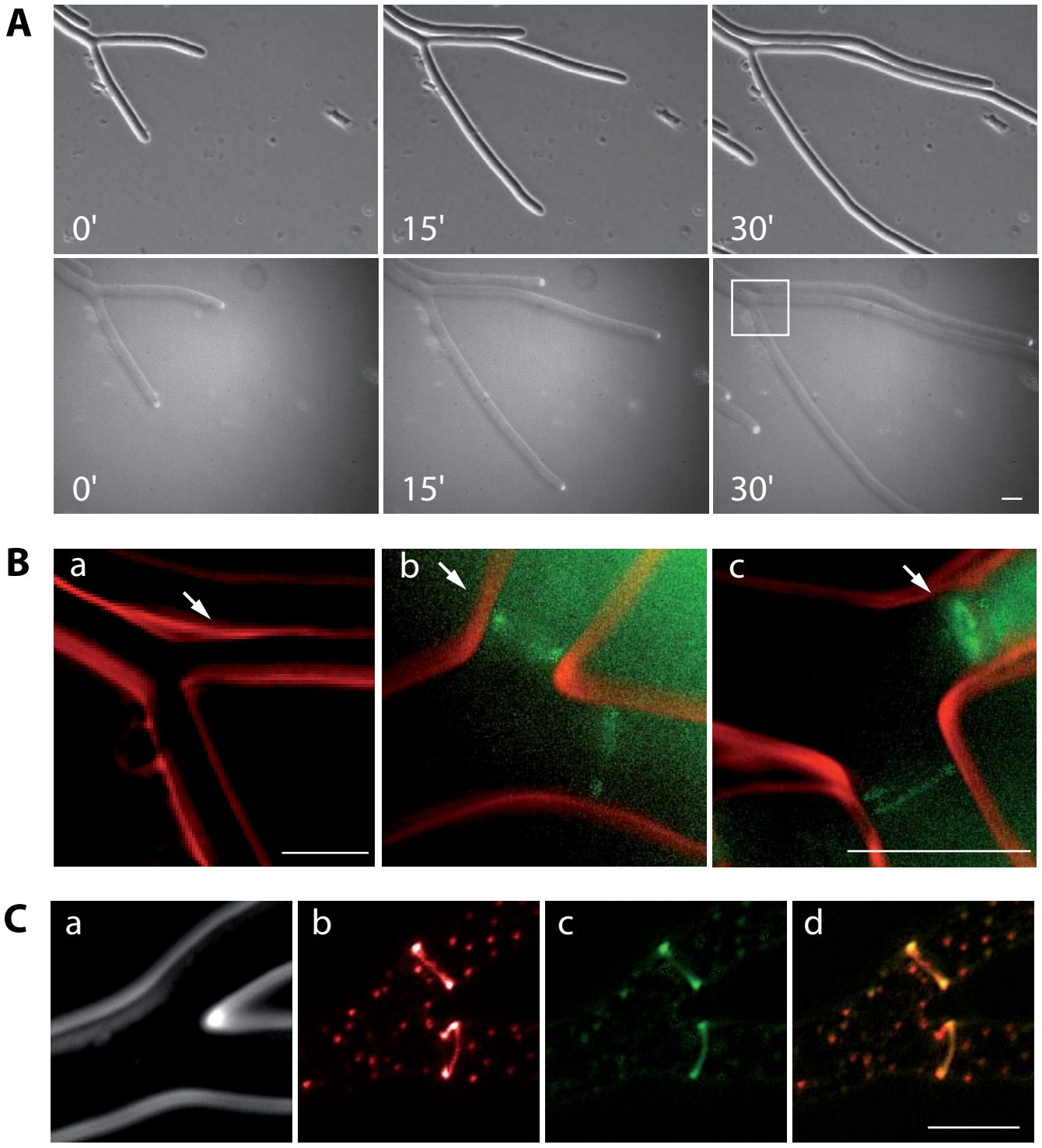

Figure 38
(A) AgRax2-GFP distribution in *Agcyk1*Δ. The series of images represent selected frames of movie (see supplementary material). The upper panel shows the outline of the hyphae and the bottom panel the localization of AgRax2-GFP at the tip of growing hyphae. **(B) (a)** Magnification of the basis of apical branches indicates lack of AgRax2-GFP rings. **(b-c)** AgRax2-GFP in WT localizes to the septation sites at the bottom of the apical branches. Two rings mark symmetrically the basis of apical branches. **(C)** AgRax2-GFP distribution in wild type: **(a)** Outline of the hyphae, **(b)** Rhodamine-Phalloidine actin staining, **(c)** AgRax2-GFP, **(d)** Overlay of b and c images. AgRax2-GFP co- localizes perfectly with the actin ring. Bar, 10 μm.

Discussion

Regulation of cell polarity

The filamentous fungi *A.gossypii* and the budding yeast *S.cerevisiae* have different life styles despite very similar gene contents and conserved domain compositions of gene products (Dietrich et al., 2004). Both organisms can establish polar growth but in *S.cerevisiae* periods of growth alternate with cell divisions whereas *A.gossypii* cells (hyphae) grow for unlimited periods without undergoing divisions.
Yeast cells have a tightly regulated budding pattern where emergence of a new bud is spatially determined. In the light of recent studies *A.gossypii* branching or septation does not occur at random sites, however it is still not clear how cells establish polarity and control stability of growth axis.
Different than *S.cerevisiae* cell morphology and development but very similar polarity gene content makes the filamentous ascomycete *A.gossypii* a promising model organism for studying the molecular network allowing constitutive polarized growth of fungal hyphae, formation of lateral branches and apical branching.
Analysis of the regulation of the polar growth process is difficult because it depends on the integrated workings of intact cells.
The studies reported here have now clarified several questions considering the regulation of the polar growth process.

AgRax1p and AgRax2p are potential candidates for control of polarity in *A.gossypii*

The genetic and molecular analysis of polarity has been carried out mainly with *S.cerevisiae* (Durbin 1996, Madden and Snyder 1998, Chant 1999, Pruyne 2004). Only limited data are available from well known filamentous ascomytes like N. crassa (Virag and Griffiths, 2003, Riquelme and Bartnicki-Garcia, 2004) and A. nidulans (Guest and Momany, 2004).

In *S.cerevisiae* more than 200 genes were shown to be involved in polar growth control. Over 20 genes were described to control budding patterns (axis of polarity). For these *S.cerevisiae* genes syntenic homologues were detected in *A.gossypii* and for some of them the function has already been proposed. However, up to now relatively little was known about potential landmark proteins.

Previous studies have identified many proteins that are involved in determining the cell-type-specific budding patterns in *S.cerevisiae*. It has been shown that the position of bud emergence, and thus the position of the cleavage plane, is determined by landmark proteins. The specific set of genes called „BUD“ genes seems to be required for either the haploid-specific axial budding pattern (Bud3p, Bud4p, Axl1p and Axl2p/Bud10p/Sro4p) or the diploid-specific bipolar bud site selection (including: Bud8p, Bud9p, Rax1p and Rax2p) (Chant and Herskowitz, 1991; Fujita et al., 1994; Adames et al., 1995; Chant and Pringle, 1995; Halme et al., 1996; Roemer et al., 1996; Sanders and Herskowitz, 1996; Zahner et al., 1996; Park et al., 1993, 1999, 2002; Lord et al., 2000, 2002; Kang et al., 2001; Marston et al., 2001; Harkins et al., 2001; Schenkman et al., 2002). Mentioned proteins are thought to encode landmark proteins that act upstream of a GTPase module consisting of the Ras-like GTPase ScRsr1p/Bud1p, its guanine-nucleotide exchange factor ScBud5p and its GTPase-activating protein ScBud2p.

ScRax1p and ScRax2p, the homologues of AgRax1p and AgRax2p are also implicated in bipolar budding in diploid *S.cerevisiae* cells. The genes encoding these proteins were originally identified by mutations that appeared to suppress the loss of axial budding in a Scaxl1 mutant (Fujita et al., 1994; Chen et al., 2000). A deletion of any of these genes caused similar phenotypes. Analysis of S*crax1*Δ and *Scrax2*Δ budding patterns indicated that both proteins were involved in selecting bud sites at both the distal and proximal poles of daughter cells, as well as near previously used division sites on mother cells. ScRax1p and ScRax2p both appeard to be integral membrane proteins, where ScRax2p resembled the other putative landmark proteins in having a long glycosylated N-terminal domain in the extracytoplasmic space and C-terminal domain in the cytoplasm (Kang et al, 2004). In *S.cerevisiae* ScRax1p and ScRax2p were both observed at the distal pole as well as at the division site on both mother and daughter cells; localization to the division sites was persistent through multiple cell cycles.

Previous studies have been done on BUD-gene homologues present in *A.gossypii*. *A.gossypii* Ras-like GTPase AgRsr1p/AgBud1p localized to the tip region and was involved in apical polarization of the actin cytoskeleton thus was a key regulator of hyphal growth guidance (Bauer, 2004). AgBud3p showed landmark protein features as it localized to the sites of future septation in order to recruit AgCyk1p, the homologue of a *S.cerevisiae* protein controlling cytokinesis (Wendland, 2003). It was also proposed to play a role in lateral branch formation that in *A. gossypii* often takes place adjacent to sites of previous septation.
This model would resemble axial budding in yeast (Wendland, 2003). However, hyphal growth in *A.gossypii* can mostly be compared to the bipolar budding pattern in yeast diploids, therefore proximal or distal budding in mother cells resembles the formation of lateral branches in *A.gossypii.*

In this work we have focused on the *A.gossypii* homologues of *S.cerevisiae* genes involved in bipolar budding pattern and we presented evidence that AgRax2p is a landmark for filamentous growth.
Several observations based on synteny and sequence comparisons suggested that *A.gossypii* contains homologues of ScRax1p and ScRax2p. Additionally, syntenic homologues of both proteins were detected in S. pombe (SPAC23G3.05c and SPAC6f6.06c), but none so far in higher cells.

During germination cell selects polar growth sites. Although AgRax2p was found in the germling during its isotropic growth phase, which would suggest its role in the selection of previous polar sites, in absence of AgRax2p cell was still able to form correctly germ tube. Furthermore, if AgRax2p would be involved in the selection of new polar sites we would expect the signal to be present at the cell cortex independently on AgCdc24p. Interestingly, the *Agrax2*Δ mutant was not able to correctly select sites for the subsequent germ tubes. Currently we do not have an explanation for this observation.

Young mycelia lacking AgRax1p and AgRax2p revealed a 50% decrease in the growth speed compared to the wild type. Analysis of the video data revealed (i) strong decrease in hyphal growth speed when lateral branches emerge (ii) delay in making new axis of polarity represented by a low number of lateral branches during early mycelium development (iii) irregular order of branching (iv) problems with maintenance of a straight axis of polarity during dichotomous tip branching.

The phenotypes in the *Agrax1*Δ and *Agrax2*Δ deletions were very similar and pronounced, both strains exhibited similar growth defects to those described for single mutants. Most likely changes in the branching frequency, tip morphology and the hyphal tip growth speed in *Agrax1*Δ and *Agrax2*Δ strains were the result of alterations in the same pathway.

A decrease of the hyphal tip growth speed during lateral or apical branching has already been described in the filamentous ascomycetes Aspergillus nidulans (Trinci, 1970) and Aspergillus oryzae (Spohr et al., 1998, Christiansen et al., 1999) and also in *A.gossypii* (Knechtle et al., 2003). In the latter work the decrease was associated with the selection of sites for polar growth and later formation of new lateral branches or septum.
*Agrax1*Δ and *Agrax2*Δ strains show delay in making new axis of polarity represented by a low number of lateral branches during the first 20 hours of development. We have shown herein that in wild type and mutant, at the sites where growth speed of the main hyphae reduced new branches or septa were seen later. Thus, although selection of subsequent polar sites occurred, was not followed by an immediate polarity establishment at those very sites.
Consequently, alterations in hyphal tip growth speeds observed for *Agrax1*Δ and *Agrax2*Δ mutants were most likely direct consequences of the emergence of many delayed lateral branches after 20 hours of development. Thus Rax proteins are dispensable for the selection of polar sites but seem to be important to coordinate the time of branch emergence with the extension of the hyphae.

In the wild type, at early stages of growth, the branching frequency increases, whereas later it decreases to reach a constant value. Majority of lateral branches emerges adjacent to the septum “one after the other”.
The presence of some lateral branches adjacent to the septum and emerging in wild type like fashion during the first hours of development could be explained by the existence of yet not identified factors that most likely sit at the septum to help trigger the establishment or maintenance of polarity in the absence of AgRax proteins.
Occurrence of many subsequent lateral branches in the middle of the compartment suggests that although AgRaxp are not required for the selection they may be necessary to localize the cortical landmarks for branching.
Since lack of AgRax1p and AgRax2p did not eliminate hyphal growth but lead only to the delay in the establishment/ maintenance of polarity some other proteins seem to be able to initiate growth independently of both proteins.
Some of those proteins were already described by Y.Bauer (AgBud1p), J.Wendland (AgCdc24p) or A.Kaufmann (AgBni1p), however, no detailed studies were done on the role of putative landmark proteins in polar growth control of *A.gossypii* resembling those discussed for *S.cerevisiae*.
It was proposed that normal localization of ScBud8p in *S.cerevisiae* was partially dependent on ScRax1p and AgRax2p and normal localization of Bud9p appeared largely or entirely dependent on ScRax1p and ScRax2p. (Kang el al, Chen,). Further, in response to a cell cycle cue, GTP-bound Rsr1p/Bud1p recruits ScCdc24p to the membrane. This local enrichment triggers activation of ScCdc42p at sites of bud formation. Downstream *S. cerevisiae* targets of ScCdc42p-GTP are then activated (Dong et al., 2003; Kawasaki et al., 2003).

When A. gossypii wild type hyphae reach a growth speed of about 80 µm/h tip branching is initiated (Ayad-Durieux et al., 2000; Knechtle et al., 2003). Previously reported *Agbud2*Δ and *Agrsr1*Δ showed deviations from the axis of polarity resulting in zigzag shaped hyphae (Bauer et al., 2004). Other mutants like *Agbnr1*Δ (H-P. Schmitz, personal communication) and *Agcla4*Δ showed premature branching events. In *Agcla4*Δ premature tip splitting was observed at all tips after normal development of a young mycelium including lateral branching (Ayad-Durieux

et al., 2000).
Our studies of *Agrax1*Δ and *Agrax2*Δ mutants revealed frequent changes in the growth axis and defective tip branching, though both mutants were still able to form some correct apical branches.
Although primary localization of AgRax2-GFP at the tip of the wild-type cells supports the role of AgRax2p in tip division, only a partial abolishment of apical branching suggests a nonessential role of AgRax proteins for this process.
On the other hand, the different morphology of the incorrectly formed tips resembling those described for various mutants suggests that the absence of AgRax proteins may be rescued on different levels of the cell polarity machinery.

ScSpa2p belongs to a group of proteins that localize to sites of growth in a cell cycle dependent manner (Sheu et al., 2000). AgSpa2p-GFP signal was observed as a stable marker of growing hyphal tips (Knechtle et al., 2003). In the Agbud1Δ mutant AgSpa2p delocalized temporarily from the hyphal tip, and thus growth arrested. Only upon the reoccurrence of AgSpa2p-GFP in the hyphal apex, growth resumed.
In *Agrax1*Δ (data not shown) and *Agrax2*Δ the AgSpa2p-GFP signal was continuously fused to the tip, even when the hyphae changed growth axis.
Thus, AgRax1p together with AgRax2p are not essential to coordinate polarized hyphal growth with polarisome functions and likely they act independent on the polarisome component AgSpa2p in maintenance of a sustained polar growth. Our findings are in agreement with the phenotypes of double deletions of AgRax1p and AgSpa2p, and AgRax2p and AgSpa2p. Although single deletions were viable, the double deletion mutants developed very slowly only for a restricted period of time. The late lethal effect was probably due to the presence of remaining protein in the needle-shaped spore.
Consequently, both AgRax proteins are part of 2 different than AgSpa2p pathways operating at hyphal tips allowing a permanent hyphal tip extension.
Previously, AgSpa2p was shown to have a regulatory function on the actin cytoskeleton and to play a role in balancing the branching time and position versus the hyphal tip growth speed (Evangelista et al., 2002; Sagot et al., 2002, Knechtle et al., 2003).
Our studies of *Agrax1*Δ and *Agrax2*Δ mutants revealed some changes in the actin cytoskeleton organization.
Pronounced polarized actin, indicative of active growth, at the tip of main hyphae and of some of the lateral branches is in agreement with the increase in hyphal tip growth speed caused by a decreased number of polarization events observed behind the tip.
Additionally, we observed depolarized actin cytoskeleton at the tip of some, mainly delayed lateral branches that clearly indicated lack of active growth.
We suppose that in the absence of AgRax1p and AgRax2p the recruitment of actin patches to the selected sites was presumably less efficient which caused the delay in the lateral branch formation.
However, the localization of AgRax2p at the tip fits well with its function in regulating the actin distribution at the polar sites, the fact that AgRax2p delivery to the tip was shown to be actin dependent exclude this option.
We propose that AgRax2p may have a regulatory function on cell polarity parallel with AgSpa2p and actin.

Organization of polarization at the tip in *A.gossypii*

An implication of AgRax2p in cell polarity is supported by its localization to sites of polarized growth.
AgRax2p was found to be permanently present at the hyphal tips and transiently at the septum. In A. gossypii polarization at the tip was not lost during seputation, the initiation of a new lateral branches or apical branching.
In general, AgRax2p localized permanently to all sites thought to possess landmark of polar growth. Thus, it is considered to be a part of the landmark complex that controls the branching pattern.
Further, this localization resembles those described for *S.cerevisiae*.
Interestingly, AgRax2-GFP expressed from the A. gossypii promoter was detected in yeast cells at the neck and at the tip. Moreover, it complemented the defect in bud site selection which additionally supports the role of this protein in the maintenance of polarity.
Examination of AgRax2-GFP localization in absence of *Agrax1*Δ revealed severe problems in positioning of AgRax2p at the tip. AgRax1p appeared to be able to provide a spatial signal without which AgRax2-GFP was not able to localize correctly. This suggests that the functions of both proteins depend on each other, though is not yet clear whether the AgRax1p-AgRax2p interaction is direct or mediated by other proteins. Additional studies will be required to clarify this point.
Moreover, abolished AgRax2-GFP placement in absence of a potential signal peptide provides evidence that this domain is essential for proper AgRax2-GFP localization. Taking into account that signal peptides are a hallmark of transport all over the secretory pathway we assumed that AgRax2p may be delivered to the tip and likely to the septum via the secretory pathway and its transport may depend on the function of AgRax1p.
Our findings are in agreement with *S.cerevisiae* studies, where ScRax1p was shown to be essential for the delivery of ScRax2p (Chen et al., 2000), the localization of ScRax1p and ScRax2p was interde-

pendent and both proteins could be co-purified from yeast (Kang et al 2005).
Additional two lines of evidence support our statement.
First, in synthetic lethal screen AgRax1p was shown to be part of the same pathway and thus likely to be important for the AgRax2p delivery.
Secondly, although the AgRax2-GFP localization pattern was similar to polarized actin its transport to the tip seemed to rely on the actin cytosceleton. The deletion of AgCdc24p, essential for actin polarization and thus essential for building up the network allowing cells the proper localization of proteins, abolished localization of AgRax2p. To explore the role of the actin cables in AgRax2-GFP distribution, the localization of AgRax2p was investigated in the Agbni1D mutant essential for actin cable formation and hyphal morphology (H-P Schmitz et. al, manuscript in preparation).
In the Agbni1D mutant lacking polarized actin cables, the AgRax2-GFP protein remained fused to the cortex of the elongated cells. Presumably the same mechanism that led to the formation of the “potato-like “ structures in the Agbni1Δ mutant was involved in the placement of the AgRax2p.
To answer the question what provides the spatial signal for AgRax2p we investigated the localization of this protein in Agbud10Δ and Agbud8Δ (ongoing studies)
We showed herein that AgBud10p, the homologue of ScBud10p that acts as the key proximal landmark in axial budding, and transduces the signal between axial landmarks and downstream factors (Fijuta 2004, Marston, 2001 P.J. Kang, 2001, Lord, M.C., 2000) is involved in the maintenance of AgRax2-GFP at the tips of *A.gossypii* hyphae.
Further, the deletion of both proteins displayed a stronger polar growth defect than those described for the single gene deletions and thus, AgRax2p and AgBud10p are expected to be involved in two different pathways. Observed genetic interaction is similar to yeast where in the absence of both ScBUD10 and *ScRAX2*, stronger budding defect than obtained for the single deletion was observed. We propose that AgBud10p may transduce a signal between AgRax2p and members of landmark complex.
Furthermore, an implication of ScBud8p in ScRax2p localization was suggested in *S.cerevisiae.* When ScRax2-GFP was expressed in cells lacking Bud8p, localization to the bud tips and the distal poles of daughter cells was largely or entirely lost, while localization to the mother-bud neck, proximal poles, and previous division sites seemed unaffected. Thus ScBud8 was essential for the localization of ScRax2p to the bud tip and distal pole (Kang et al 2005).
Despite high gene homology we could not observe the changes in the localization of AgRax2-GFP in the absence of AgBud8p likely due to different set of proteins serving as a landmarks for the AgRax2p.

The studies reported here have shown that AgRax2p acts downstream or parallel of AgCdc24p, AgBni1p and AgBud10p in polar growth which strongly argues the role of AgRax2p in the maintenance of polarity rather than in its establishment.
AgRax2-GFP localizes to the hyphal tip, indicating that its localization is one of the early events in growth. Thus *Agrax2*Δ could function as a part of a landmark complex upon which an array of subsequent proteins could be assembled.

Organization of polarization at the septum in *A. gossypii*

AgRax2p formed a single ring at the site of a future septum that completely separated during septum formation into two rings marking two compartments, however, *A.gossypii* does not exhibit cytokinesis.
Consistent with our findings is the localization of an orthologue of AgRax2p in *S.cerevisiae*. Observations of a ScRax2-GFP fusion protein showed that it localized to the mother-bud neck of large-budded cells and hence to the division site on both mother and daughter cells, where it persisted through multiple cell generations. (Chen et al., 2000 , Fujita et al., 2003).
Although AgRax2p localized to sites of septation we could not detect a defect in septation in *Agrax2*Δ. Therefore AgRax2p is not essential for septum formation, moreover, it plays a rather structural than functional role in the septation process. The observed phenotype was in agreement with *S.cerevisiae* data.

Our studies revealed that AgRax2p co-localizes with a single actin ring and its deposition at the septum strongly depends on AgCyk1p, that provide a spatial signal for the incorporation of secretory vesicles at sites of septum construction, which potentially lead to closed septa (Wendland, 2002).
Because the formation of new AgRax2-GFP rings was abolished in the presence of LatA the primary deposition of AgRax2p seems to depend on actin.
Interestingly, after treatment with LatA only one of the two AgRax2p rings labeling both sites of fully formed septa decreased its intensity. The remaining ring marked the compartment on the side of the extending hypha. Similar behavior exhibited one of the two AgRax2p rings in LatA free condition, however, the dynamics of the changes were different.
A.gossypii displays compartmentalization by formation of septum separating the incoming segment from the tip of the hyphae. Our observations suggest that the dynamics of the cellular structures decrease with the age of the segment, which may lead to the less efficient transport of new portions of protein to the septum. Newer segments display a more dynamic

cytoskeleton, thus more efficient transport of proteins even in the presence of LatA that abolishes vesicular movements.
Thus the AgRax2-GFP intensity decreased on the site of older segment.
The long life of AgRax2p rings in presence of LatA could be explained by the presence of one potential transmembrane domain in AgRax2p, that may lock the protein at the septation sites.
Weak intensity of the AgRax2-GFP signal in Agbni1Δ was most likely due to the abolished transport of new portions of protein to the septum. Consequently only pre-deposited AgRax2p gave rise to AgRax2-GFP rings.
Otherwise, in the absence of AgBni1p many other proteins may still function in order to produce septa and likely one of them may recruit AgRax2p to those sites. This and the other results provided evidence that actin dependent transport is important for AgRax2p efficient deposition at the septum.
Based on our microscopy studies we are in favor of the hypothesis that AgRax2p appears at the septum after the actin ring is formed. To verify this statement the localization of AgRax2p should be tested in the Agbud3Δ that shows linear actin filaments attached to the cell cortex, instead of actin rings.

We showed by light microscopy that 40% of spores carrying a complete deletion of *Agrax1*Δ and *Agrax2*Δ displayed different morphology. Considering the fact that the septation process, as previously reported in the PhD thesis of S. Brachat, is part of the spore formation process, AgRax1p or AgRax2p may be involved in sporulation. Further, the presence of the AgRax2p at the septum supports the engagement of this protein in this process and thus presumably in the spore development.

The characterization of the AgRax2p deletion phenotype favours the hypothesis that it has a structural role in the septum construction rather than in septum positioning.

AgRax proteins are likely part of a landmark complex- Model

Polar growth requires selection of specific sites, establishment of polarity at those sites and, finally, it requires mechanisms that maintain the stability of the growth axis. The goal of this work was to find the potential landmarks that control polarity.
Sites of polarization determine where the first hypha emerges from the germ bubble, where lateral branches initiate and probably also when a hyphal tip splits into two branches.
We report for the first time on the identification and characterization of fungal genes important for the temporal control of polar events like branch emergence, dichotomous tip branching and maintenance of sustained polar growth. These novel *A. gossypii* genes have closest homologues in the *S. cerevisiae* ScRax1 and ScRax2; the *A. gossypii* protein is therefore called AgRax2p.

Regarding the delay in making a new axis of polarity, the irregular order of branches and localization studies we propose that AgRax1p and AgRax2p are implicated in the temporal control of late polarity events (branch emergence, dichotomous tip branching).
Presumably, AgRax2p recruited by other landmarks to the polar sites remains at the tip where it serves as a scaffold for other factors in order to preserve polar growth. AgRax2p fused to the cell cortex is constantly delivered to the tip membrane via a secretory pathway with the help of AgRax1p to maintain branch emergence and later sustained polar growth in a time dependent manner. It seems that AgBud10p interacts with AgRax2p in order to keep it permanently at the tip of newly formed branches.
In the absence of AgRax2p or AgRax1p, polar sites were still selected though not all of them were used at the right time. Probably, when both AgRaxp are lost their potential effectors/s are recruited to the new polar sites however with a delay leading to the formation of postponed lateral branches.
Presence of some „primary“ lateral branches emerging adjacent to the septum in a wild-type like pattern suggests the existence of a factor that has an affinity to the septum site and is able to maintain polar growth independently on both AgRaxp. This factor could potentially be employed by AgRax1p or, if absent, by AgRax2p.
The function of AgRax2p is probably tightly regulated by a number of other proteins and actin dependent transport.
Further, septum formation likely does not depend on AgRax proteins and proteins associated with the septum sites are able to trigger branch emergence independently on AgRax proteins. Our evidence strongly suggests that AgRax2p at the septum follows actin ring contraction and acts downstream of AgCyk1p.

Table below summarizes all interactions described in this manuscript. Figure 1 **(Fig. 1)** proposes the place of AgRax proteins in the polarization machinery.

Studied factors	Localization of AgRax2-GFP at the tip depends on	Localization of AgRax2-GFP at the selected sites for septum formation depends on
AgRax1p	+	+
AgRax2 ΔSignal Peptide	+	+
AgCdc24p	+	No septation event
AgBni1p	-	-
AgBud10p	-	-
AgCyk1p	-	+
Actin cytoskeleton	Only transport to the tip	Only transport to the septum
Co-localization with actin	no	Yes - with actin ring only

	Localization of AgSpa2-GFP at the tip depends on	Localization of AgSpa2-GFP at the selected sites for septum formation shows
AgRax1p	-	Increased affinity of AgSpa2p to septation sites
AgRax2p	-	Increased affinity of AgSpa2p to septation sites

	Localization of AgSep7-GFP at the selected sites for septum formation depends on
AgRax1p	-
AgRax2p	-

Double mutants-survival ratio	*Agrax1* Δ	*Agrax2*Δ
Agspa2 Δ	-	-
*Agbud10*Δ	+	+
Agrax1 Δ		+

Table1
Summary of the results from the Chapter1

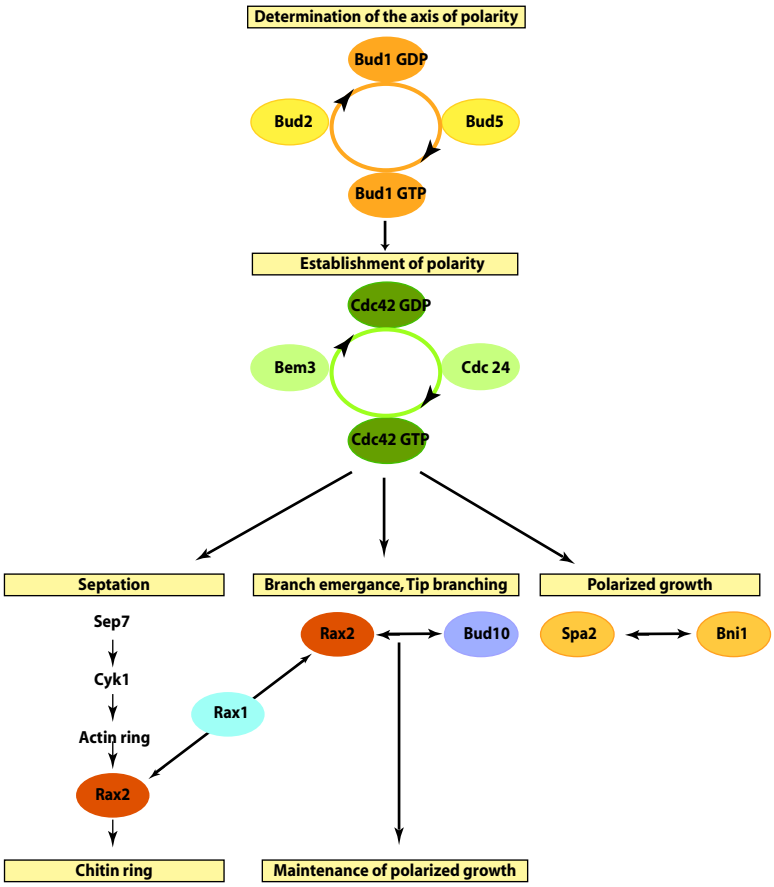

Figure 1
Working model of a protein network that involves AgRax proteins. AgRax2p recruited to the polar sites triggers polarity establishment in time dependent manner.

AgBud7p helps to maintain sustained polar growth

Introduction

Many *S.cerevisiae* genes were shown to be involved in the determination of the the budding pattern in diploid cells. In order to find landmark proteins implicated in cell polarity of the filamentous fungus *A.gossypii* which shows a completely different morphological development than unicellular yeasts, we have performed a comparison of the recently annotated genome of *A.gossypii* with the already well known genome of *S.cerevisiae.* Consequently, we detected only one homologue of *ScBUD7* and its twin ORF *ScBCH1* in A.gossypii named *AgBUD7*.
Since relatively little was known about the function of ScBud7p and ScBch1p when we started this study we have decided to investigate the phenotypes of a the *ScBUD7* and *ScBCH1* double deletion in a haploid and in diploid *S.cerevisiae* strains. For our *S.cerevisiae* studies we have used strains provided by L. Schenkman (Please see Table 4 in Chapter "Materials and Methods").

To explore the functions of ScBud7p and its twin ORF ScBch1p, we deleted the complete ORFs from start to stop codon. The PCR method (Wach, et al 1994, Wach, et al 1997) was used to replace one wild-type ScBud7p *and* one wild-type ScBch1p allele in YEF473A (a and alpha; *trp*-Δ*3*, *leu2*-Δ*1*, *ura3-52*, *his3*-Δ*200*, *lys2-801*). For the deletions in *S.cerevisiae* strains we have used two cassettes coding for resistance against the drug G418 and carrying HISMX for complementation of the strain carrying the auxotrophic marker his3Δ. The presence of the deletions was confirmed by PCR. Appropriate haploid strains were mated to obtain the homozygous mutant strains, carrying a deletion of both alleles of *ScBUD7* and *ScBCH1*. Interestingly, both created diploid strains showed a decreased sensitivity to calcofluor, which caused some difficulties for our further analysis.

Parallel with the analysis of *S.cerevisiae* gene deletions we focused on the *A.gossypii* homologue of those genes, AgBud7p. To explore the function of AgBud7p we also deleted the complete *AgBUD7* open reading frame from start to stop codon (according to materials and methods) using the cassette *GEN3* coding for resistance against the drug G418 (Wendland et al. 2000).

The *A. gossypii* homologue of the *S. cerevisiae* twin genes *ScBUD7* and *ScBCH1*

Based on amino acid comparisons of *A. gossypii* sequences with *S.cerevisiae* proteins we identified one *A.gossypii* homologue of both ScBud7p and its twin open reading frame ScBch1p. The predicted sequences of ScBud7p and ScBch1p and AgBud7p revealed that these three proteins are very similar in overall structure. Interestingly, although *A.gossypii* is a haploid, these *S.cerevisiae* genes are known as diploid specific. Additionally, homologues of all three proteins were detected in *S.pombe* (SPBC31F10.16), *C.albicans* (IPF6332), and in higher cells.

AgBud7p shares 54% identity on the amino acid level with ScBch1p and 55% identity on the amino acid level with ScBud7p. AgBud7p encodes a 76,9 kDa, ScBud7 a 84,8 kDa, and ScBch1 a 82 kDa-polypeptide.
Commonly used programs predict different topologies for these three proteins. Program TMHMM did not predict any transmembrane domains, whereas applications available at EMBOSS predicted one TM domain for ScBud7p (325-342) and one signal peptide cleavage site at the C-terminus end (706). The same program predicted three TM domains for ScBch1p (190-207; 294-317; 662-685) and one signal peptide cleavage site (50) **(Fig.1)**. Apparently, AgBud7p appears not to be an integral membrane protein, for the reason that most of the screening programs did not detect any TM domain.

ScBud7p and ScBch1p may be involved in the final step of cell wall synthesis at the septum

Both haploid *Scbud7*Δ and *Scbch1*Δ had no detectable effects on axial budding. Although *Scbud7*Δ and *Scbch1*Δ cells produced a few buds at their distal poles **(Table 1)**, both mutants budded almost exclusively at their proximal poles during their first and third cell cycles.
The newly made deletions of genes *ScBUD7* and *ScBCH1* genes in the haploid background strain resembled, however only partially, the original phenotypes described for *Scbud7*Δ and *Scbch1*Δ mutants (Ni and Snyder, 2001, Schenkman, Caruso et al., 2002, Harkins, Page, et. al, 2001).

The double deletion *Scbud7*Δ*,bch1*Δ budded almost exclusively from the proximal poles during the first cell cycle, but formed 40% of the buds in the equatorial region during the third cell cycle. It should also be noted that the morphology of the double mutant was slightly changed compared to the wild type cell morphology of single *Scbud7*Δ and *Scbch1*Δ*.* The *Scbud7*Δ*,bch1*Δ double mutant showed a more elongated cell shape, moreover, although rarely, we could observe defects in cytokinesis manifested by the presence of elongated mother-daughter necks **(Table 2)**. This observation suggested that ScBud7p and ScBch1p may be involved in the final step of cell wall synthesis at the septum.

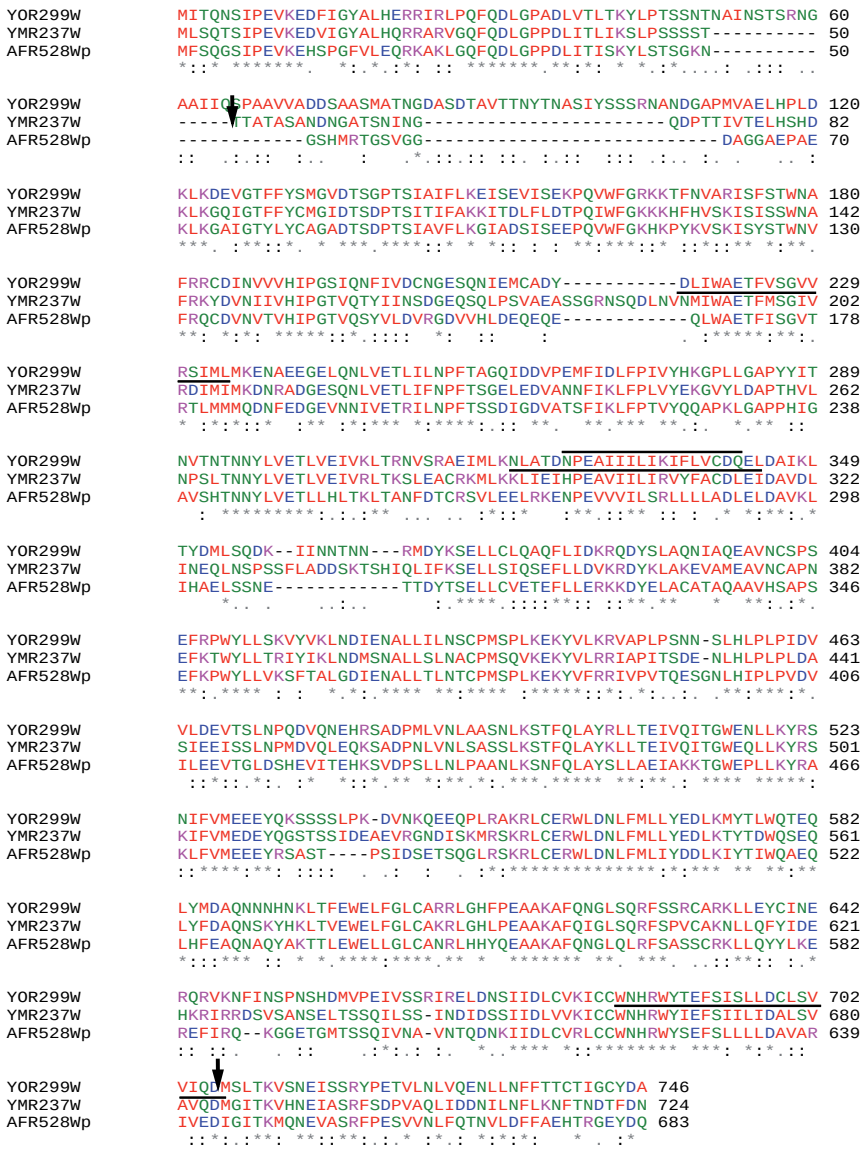

Figure 1
Analysis of the ScBud7p (YOR299W), ScBch1p (YMR237W) and AgBud7p (AFR528W) sequences. Sequences of ScBud7p, ScBch1p and AgBud7p were aligned with the use of the „Clustlaw" Program. Grey dots indicate identical amino acids; double dots- similar amino acids (I, L, V; D, E; N, Q; K, R; S, T); dashed lines- gaps introduced to maximize sequence alignment; long black overlines- putative transmembrane domains; arows- possible signal peptide cleavage sites.

			Position of the 1st bud			Position of the 3rd bud		
Homozygous strains	Genotype	Marker used for the deletion	Proximal	Equatorial	Distal	Proximal	Equatorial	Distal
a/alpha YEF 473	*his3-Δ200/his3-Δ200, leu2-Δ1/leu2-Δ1, lys2-801/ lys2-801, trp1-Δ63/trp1-Δ63, ura3-52/ura3-52*		6%	1%	93%	19%	3%	78%
a or alpha YEF 473A	*his3-Δ200, leu2-Δ1, lys2-801, trp1-Δ63, ura3-52*		92%	1%	7%	81%	4%	15%
KB003	YEF473 except *bud7/bud7*	HIS3	69%	1%	30%	64%	8%	28%
KB006	YEF473 except *bch1/bch1*	kanMX	59%	6%	35%	68%	11%	21%
KB009	YEF473 except *bud7/bud7, bch1/bch1*	HIS3, kanMX	63%	10%	37%	28%	58%	14%
KB001	YEF473A except *bud7*	HIS3	88%	3%	9%	81%	4%	15%
KB004	YEF473A except *bch1*	kanMX	90%	3%	7%	79%	6%	15%
KB007	YEF473A except *bud7, bch1*	HIS3, kanMX	78%	8%	14%	46%	40%	14%

Table 1.
Quantitative evaluation of bud position in wild-type and mutant strains. Cells of the indicated strains were grown and stained with 0.1–1 mg/ml Calcofluor as described by Pringle *et al.* (1989). For each strain, the positions of all bud scars were determined for 100 cells with one bud scar, and 100 cells with three bud scars. The positions of bud scars were scored as distal pole (the third of the cell most distal to the birth scar), equatorial (the middle third of the cell), or proximal pole (the third of the cell centered on the birth scar). The table presents obtained values.

Homozygous deletion strains/ Genotype	**Morphological phenotype**
a/alpha YEF 473 *his3-Δ200/his3-Δ200, leu2-Δ1/leu2-Δ1, lys2-801/lys2-801, trp1-Δ63/trp1-Δ63, ura3-52/ura3-52*	
a or alpha YEF 473A *his3-Δ200, leu2-Δ1, lys2-801, trp1-Δ63, ura3-52*	
KB003 *YEF473 except bud7/bud7*	
KB006 *YEF473 except bch1/bch1*	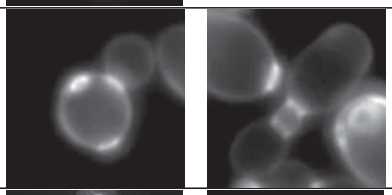
KB009 *YEF473 except bud7/bud7, bch1/bch1*	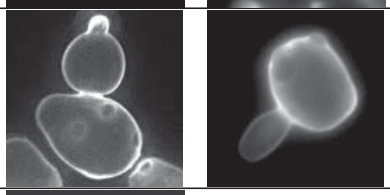
KB001 *YEF473A except bud7*	
KB004 *YEF473A except bch1*	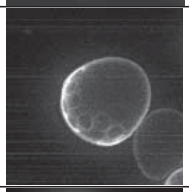
KB007 *YEF473A except bud7, bch1*	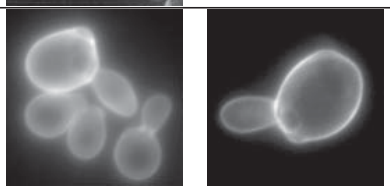

Table 2
Examples of budding pattern and cell morphology for obtained homozygous strains.

ScBud7p and ScBch1p are involved in budding of diploid *S. cerevisiae*

Single deletions of ScBud7p and ScBch1p in a diploid background led to very similar budding defects, whereas double deletion showed a more pronounced phenotype.

Scbud7Δ/bud7Δ and *Scbch1Δ/bch1Δ* cells produced almost 30 % of buds at their distal poles **(Table 1)**. Both mutants budded at their proximal poles during their first and third cell cycles.

Budding of the homozygous double mutant *Scbud7Δ/bud7Δ, bch1Δ/bch1Δ* resembled that of the single deletion only during the first cell cycle. During the third cell cycle the majority of buds appeared in the equatorial region, however, the bud scars neither formed chains nor clusters but rather resembled a random budding pattern. In subsequent cell cycles *Scbud7Δ/bud7Δ bch1Δ/bch1Δ* diploid strain showed predominantly randomised budding. The occurrence of some apparent chains of bud scars and a tendency to bud at the proximal pole suggested that under these conditions (i.e., the putative absence of two bipolar-budding markers), a diploid strain might show some ability to use axial cues for bud-site selection.

Some significant differences were found when we compared single *Scbud7Δ/bud7Δ* and *Scbch1Δ/bch1Δ* mutants with *Scbud7Δ/bud7Δ bch1Δ/bch1Δ*. The homozygous double mutant showed a more elongated cell shape, moreover, although rarely, we could observe defects in cytokinesis, similar to those described for the deletion in haploid background strains, and manifested by the presence of the elongated mother-daughter necks **(Table 2)**. This observation supported our previous hypothesis, that ScBud7p and ScBch1p may play a role in the cell wall synthesis during cytokinesis.

To summarize, partial loss of proximal-pole budding in *Scbud7Δbch1Δ* and Scbud7Δ/bud7Δbch1Δ/bch1Δ mutants during third cell cycle suggests that function of other proteins at proximal pole could be affected in subsequent cell cycles by deletion of both *ScBUD7* and *ScBCH1* genes.

Agbud7Δ deletion influenced the average growth speed of the mycelium

In order to explore the function of *Agbud7Δ,* we analysed the maximal speed determined from radial growth of fungal colonies. For the wild type the maximal speed is close to 200µm/h.

For *Agbud7Δ* the maximal speed determined from radial growth colonies is 40% slower **(Fig. 2)**. Interestingly, this difference was observed only during the first three to four days of measurements, after, the colony increased its growth speed about 20%.

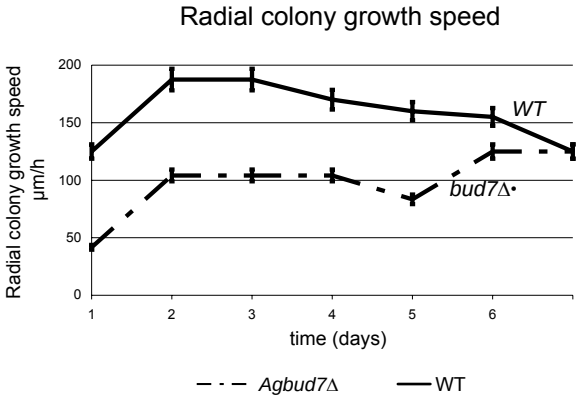

Figure 2
(A) Radial growth speed of WT, and *Agbud7Δ* strains. The x-axis represents the time in days, the y-axis the radial growth speed in µm/h. The value measured after the first day was the difference between the inoculums (1 mm in diameter) and the radial growth distance after 1 day divided by 24 h. The inoculums were taken from plates that had already been growing for 3 days and should have reached the maximal radial growth speed. Bar, SEM.

This may hint to a spontaneous change to mediated hyphal growth control, as this result was reproducible, although the observed hyphal speed fluctuations occurred 24h earlier or later. As the effect of *Agbud7Δ* deletion influenced the average growth speed of the mycelium we hypothesized that *Agbud7Δ* may play an important role in growth maintenance.

Agbud7Δ plays a role in the selection of sites for germ tube formation at the cortex of germinating spores

To further investigate the role of AgBud7p we analysed the growth pattern of a mutant strain. Because the *Agbud7Δ* strain exhibited a sporulation defect, all our studies on the function of AgBud7p were performed using heterokaryotic spore preparations. Isolated single spores were grown selectively on solid AFM plates containing G418 which blocks growth of non-transformed spores.

The characteristic bipolar branching pattern found in wild type germ cells, which produces two hyphae at an angle of 180° (Wendland and Philippsen, 2002), was disturbed in germinating *Agbud7Δ* spores. Additionally, we observed a decrease in the radial colony growth speed, although the dichotomous branching pattern of hyphal tips occurred as regularly as in the wild type. Lateral branching occurred predominantly in a wild type manner (89% of *Agbud7Δ* branches were adjacent to a septum), however some of the branches showed changes in growth direction.

In order to investigate the altered hyphal number and distribution in the *Agbud7Δ* mutant we studied a number of young mycelia pregrown at 30°C for 16h.

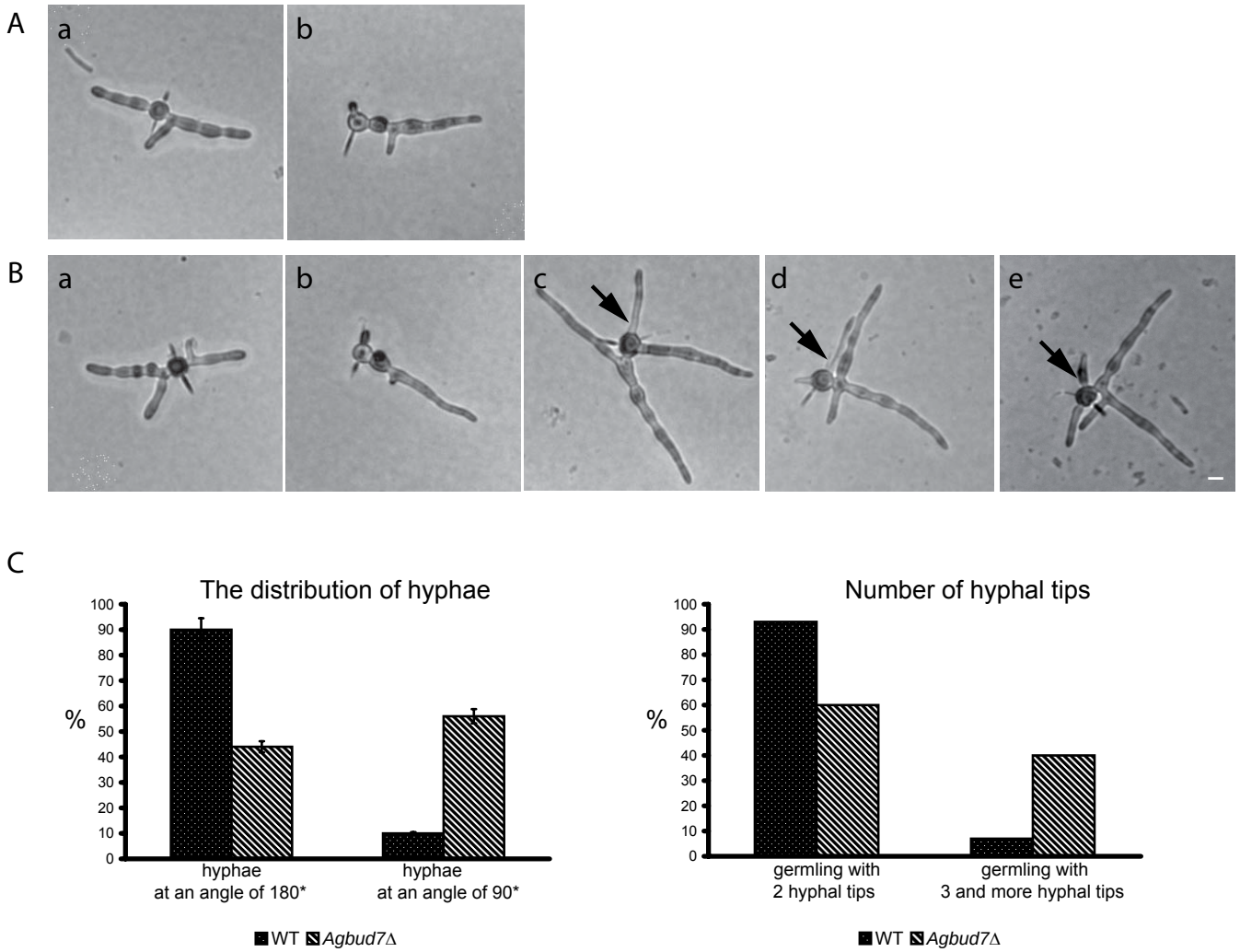

Figure 3
Altered numbers of hyphae and distribution in *Agbud7*Δ mutant. Spores were grown at 30 °C for 16h before pictures of wild type and *Agbud7*Δ germlings were acquired. **(A)** 90% of wild type cells produce two hyphae at an angle of 180 **(a)** or in 10% cases at the angle of 90 **(b)**. **(B)** 44% of *Agbud7*Δ cells produce two hyphae at an angle of 180 **(a)** or 56% at an angle of 90 **(b)**. After 16 hours 7% of wild type cells (n=100) produce third hyphae at random position versus 40% of *Agbud7*Δ cells that produce between 1-3 additional hyphae (n=100) **(c-e)**. In *Agbud7*Δ mutant the third, forth and every subsequent hyphae appear at random position with respect to the first two hyphae. **(C)** The distribution and the number of hyphae are given in %. Bar, 10 µm.

We found out that 90% of the wild type cells produce two hyphae at an angle of 180° and in 10% of the cases at an angle of 90°. After 16 hours 7% of the wild type cells (n=100) produced a third hypha at a random position. This observation was in agreement with studies done on the wild type by Wendland (Wendland, review 2005, Knechtle PhD thesis).

Furthermore, we investigated the number of small mycelia carrying an *Agbud7*Δ deletion. Results differed significantly from wild type cells. 44% of *Agbud7*Δ produced two hyphae at an angle of 180° and 56% at an angle of 90°. 40% of *Agbud7*Δ cells produce between 1-3 additional hyphae (n=100). The third, forth and every subsequent hyphae usually appeared at random positions with respect to the first two hyphae **(Fig. 3).** Thus, we conclude that *Agbud7*Δ plays a role in selection of sites for germ tube formation at the cortex of germinating spores.

AgBud7p could be required for the maintenance of hyphal tip shape

To examine the phenotypic changes underlying the decrease of the growth speed we focused on the branching frequency and branching positions in *Agbud7*Δ. The lateral branch positions did not differ from wild type excluding the possibility that AgBud7p might play a role in the selection of branch sites. Apparently, some of the lateral branches exhibited changes in the growth direction, which points to a possible role of AgBud7p in growth guidance **(Fig. 4)**. The growth speed of tips decreased only shortly before they changed their direction of growth.
To evaluate the maximal alteration from the axis of polarity we measured the maximum angle of deviation from the original axis. For the wild type this value was between 0-20° **(Fig. 4A)**. In *Agbud7*Δ strain up

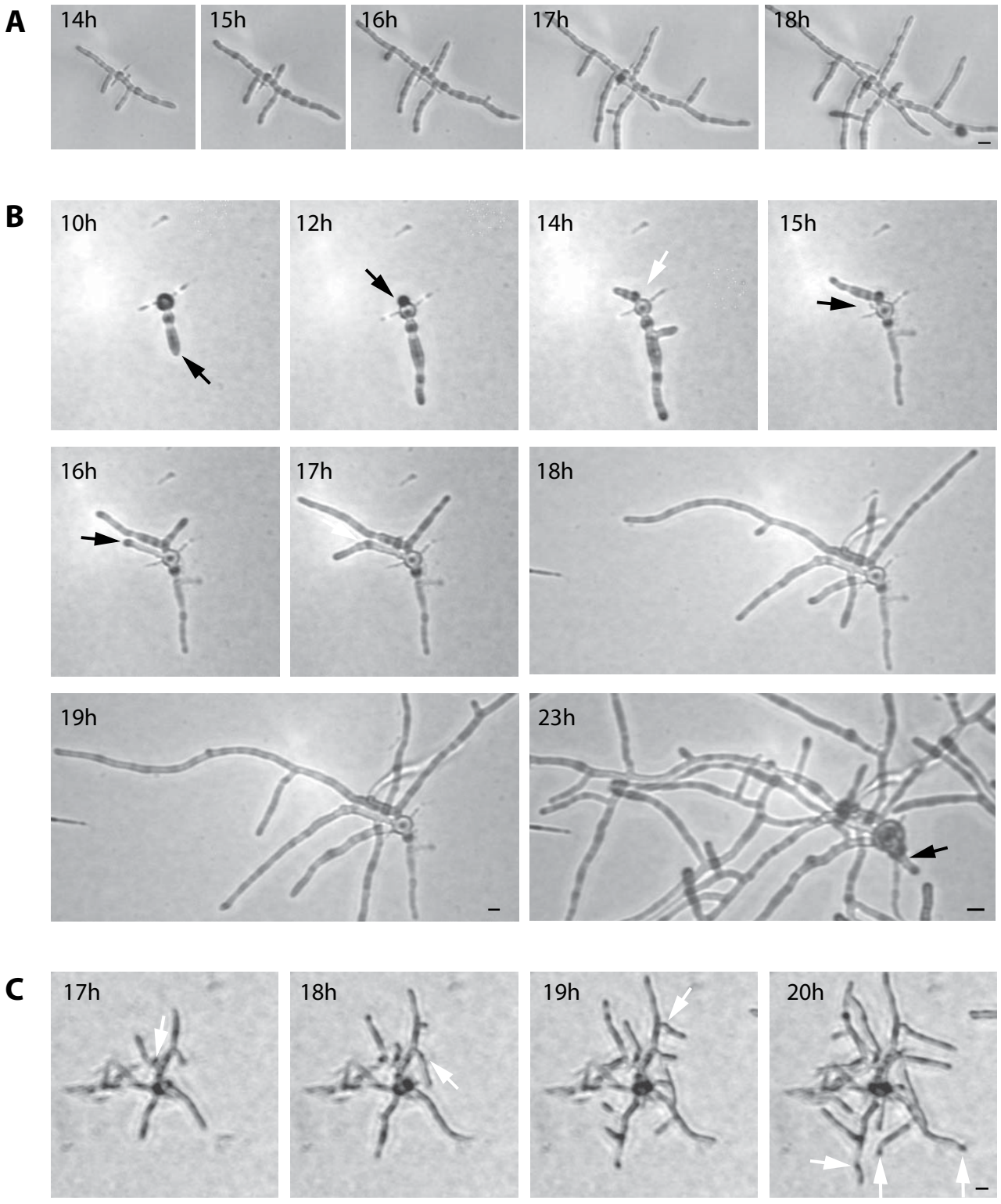

Figure 4
Development of WT and *Agbud7*Δ mycelium monitored by in time-lapse microscopy. Spores were pregrown for 12 h on AFM medium (Ashbya Full Medium) at 30°C prior to mounting for video microscopy. Digital images were collected at 5 min intervals. The time-lapse was carried out at 30° °C. **(A)** Representative frames show the development of wild type. **(B-C)** Representative frames show the development of *Agbud7*Δ. Black arrows point to all hyphae that emerged from germ cell. White arrows point to all hyphae that changed the direction of growth. Bar, 10 µm.

to 45° deviations from the growth axis was observed. Diameters at tip regions ranged from 3 to 5,5 µm for wild type, whereas they were reduced to 2-4 µm in the *Agbud7*Δ mutant. Thus, we hypothesized that AgBud7p could be required for the maintenance of the hyphal tip shape by delivering certain substances into the cell membrane. Consequently, in the absence of AgBud7p an insufficient amount of building materials is transported to the growing tips, leading to a decrease in hyphal diameter and to changes in growth direction that may later influence the radial colony growth speed. Moreover, at the place where a lateral branch changed its growth axis in 22 cases (n=93) a new lateral branch emerged shortly afterwards as if tip branching was attempted but was not successful, or the weaker structure of the cell wall would give a rise to the new branch emergance. **(Fig. 4B-C)**. A similar growth pattern of branches was not observed for the wild type.

Actin rings are formed with a delay in *Agbud7*Δ

To further investigate the defects underlying the polar growth deficiency we have tested the localization of actin patches and rings. From wild type and mutant strains young and mature mycelia were fixed with 4% formaldehyde and the actin cytoskeleton was stained with Rhodhamine-Phalloidine. In wild type as well as in *Agbud7*Δ hyphae we could observe clusters of cortical actin patches in over 95% of the tips, indicative of active growth, and also actin rings were visible at sites of developing septa **(Fig. 5)** as described earlier (Wendland and Philippsen, 2000; Knechtle et al., 2003, Bauer et al. 2003). Furthermore, actin rings were present in mature mycelium, not far from the tips of the hyphae.

In contrast to wild type mature *Agbud7*Δ displayed less actin rings placed close to the hyphal tip.

Thus, additionally to previously described AgBud7p possible role in the transport of cell wall components to the cell membrane, AgBud7p may be involved in incorporation of the actin patches at sites of septum construction. Since in absence of AgBud7p new actin rings marking potential sites of septation were formed with a delay AgBud7p is not essential for this process.

Furthermore, the delay in actin ring formation did not abolish septation and sporangia formation process, described previously by Brachat. Sporangia formation is an indication for successful chitin depo-

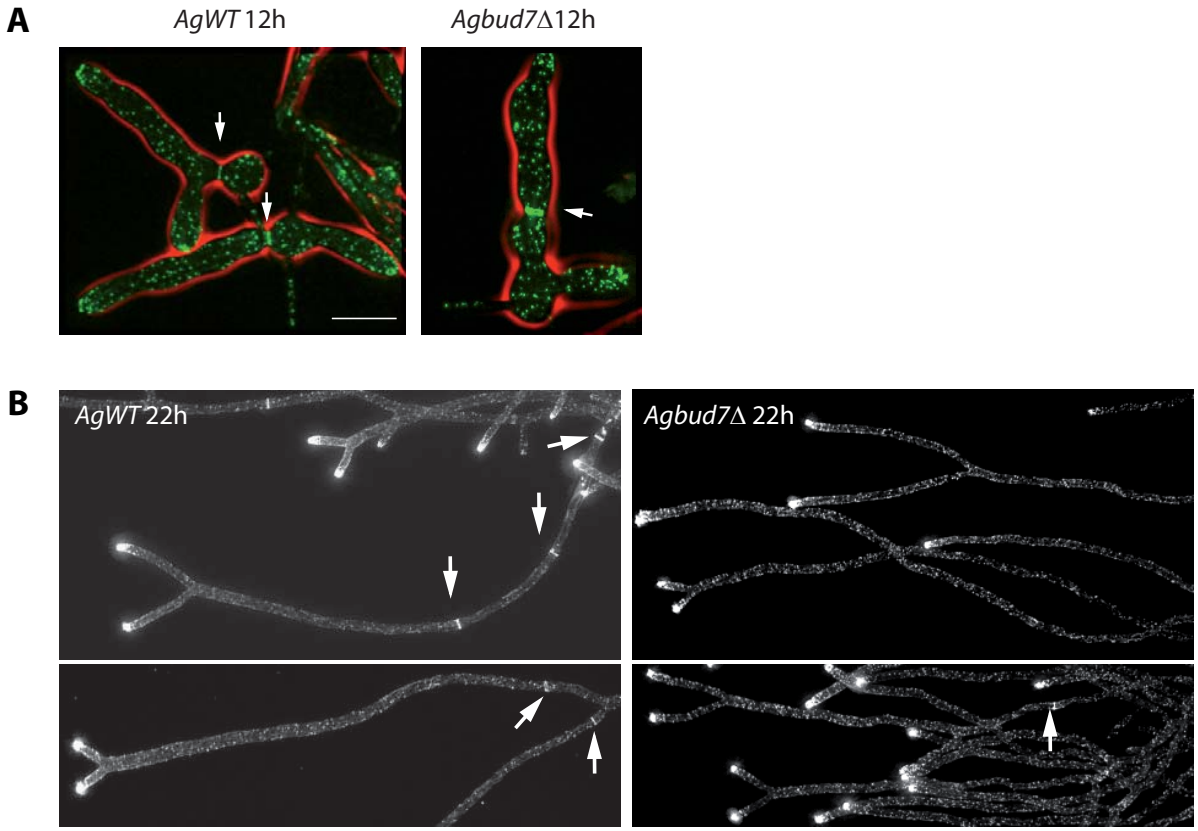

Figure 5
Organization of the actin cytoskeleton in WT and *Agbud7*Δ. Germinated spores of both strains were grown in liquid complete medium for 12 and 22 hours at 30°C, fixed with formaldehyde, stained with Rhodamine-Phalloidine and analyzed by fluorescence microscopy. Representative images are presented. **(A)** Young WT and *Agbud7*Δ show polarized actin at the tip (indication for active growth) and actin rings at the potential septum sites. **(B)** Mature WT and *Agbud7*Δ show clusters of actin at the hyphal tips, however mature *Agbud7*Δ mutant displays much less actin rings than the wild type at potential sites of septation. Bar,10 µm.

sition at the sites of septation. Indeed, we observed calcofluor rings in the subapical region of *Agbud7*Δ hyphae (not shown).
To summarize, frequent changes in the growth axis together with the decrease in the growth speed and delayed actin ring formation in apical parts of *Agbud7*Δ leading to the delayed compartmentalization explain the observed decrease in tip speed determined from radial growth of fungal colonies.

AgBud7p is involved in sporulation

Although the sporangia formation process was not disturbed, *Agbud7*Δ did not produce spores. To determine the reason for this defect we performed a nuclei staining of the wild type and the *Agbud7*Δ mutant.
In wild-type spore formation consist of a few steps. First, when the mycelium reaches the age of three days sporangia containing from one to a few nuclei are formed (Brachat, PhD thesis). Before nuclei are packed in needle shaped spores they first divide forming eight nuclei. Next, all of them align. Afterwards, the spore wall is formed around those nuclei. Eight newly formed spores divide into two groups each consisting of four spores connected with flagellum **(Fig. 6A)**.
In *Agbud7*Δ nuclei never align and the spore wall is never formed **(Fig. 6B)** which is an evidence for the role of AgBud7p in sporulation process. Co-localization experiments presented in next part of this work provide further data supporting this theory.

A functional GFP fusion to AgBud7p locates to vesicle-like structures

To better understand the mechanisms underlying the defects in the development of *Agbud7*Δ described above we constructed a functional GFP fusion to the wild type copy of *AgBUD7* gene.
The radial colony growth rate and the morphology did not differ in the AgBud7-GFP strain compared to the wild type. This result indicates that the GFP-tag did not affect the function of AgBud7p. Fluorescence of the AgBud7-GFP transformants was highly enriched in small organelles constantly oscillating with about the same amplitude in young and old mycelium.

In order to describe the dynamic of AgBud7p, we first focused on the GFP localization during the spore germination. In the very early stage of development, we could observe the GFP signal in spherical structures **(Fig. 7)**. This may reflect the vesicular localization of AgBud7-GFP during early stages of polar growth. The number of these AgBud7p vesicles in germlings ranged from 3-7 (for a total n=50). Interestingly, we could not observe any directed movements of these organelles towards the growing tip. However, we could observe divisions and fusions of these structures.

Secondarily, we investigated the localization of AgBud7-GFP in young mycelium where as well AgBud7-GFP signal was present in the spherical structures **(Fig. 8)**. As it was observed before, these structures oscillated, but did not show any directed movements towards the hyphal tip or septum. To estimate the number of spherical organelles in the cell

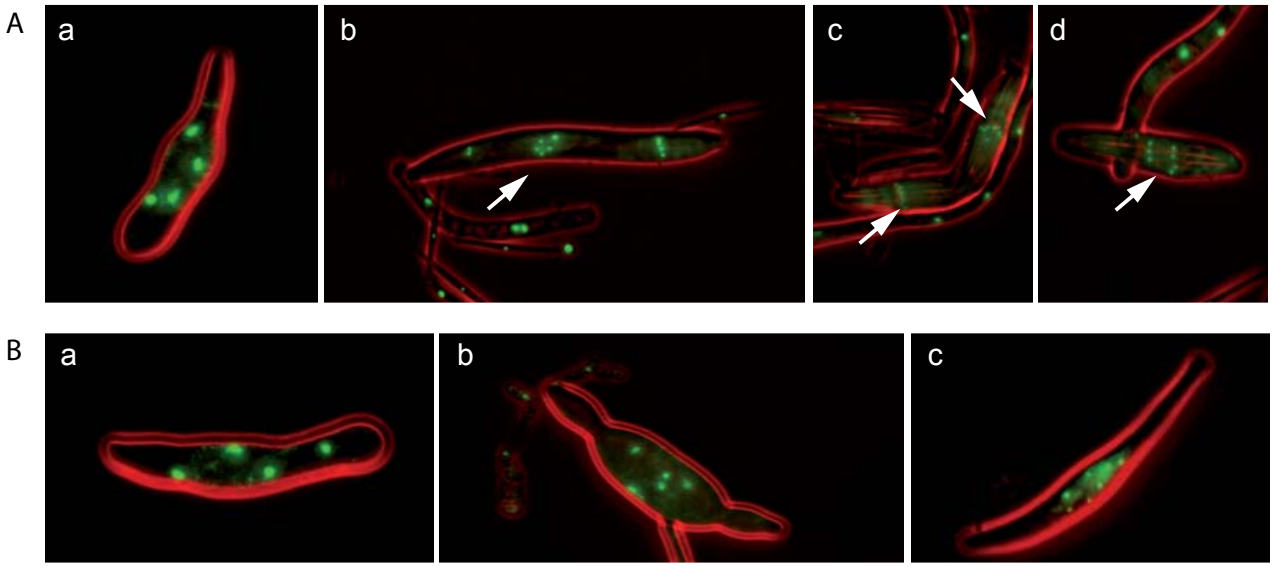

Figure 6
Homokaryotic *Agbud7*Δ mycelium does not produce spores. Wild type and mutant spores were grown for 4 days in liquid AMM medium (Ashbya Minimal Medium) at 30°C. After, cells were fixed with ethanol and DAPI staining was performed. **(A)** Representative pictures show different stages of wild type spore formation. (a) Wild type sporangium containing 4 nuclei (prior division). **(b,c)** Wild type sporangium containing 8 nuclei (before and after aligment). **(d)** 8 wild type nuclei separate prior closing into needle shape spores. White arrows point to all nuclei that aligned or separated. In some cases we could observe more then 8 spores in one sporangium **(b,c)**. **(B)** Representative pictures show different stages of *Agbud7*Δ spore formation. We could observe up to 8 nuclei although they never aligned and separated **(b,c)**. We did not see needle shape spores inside the sporangia.

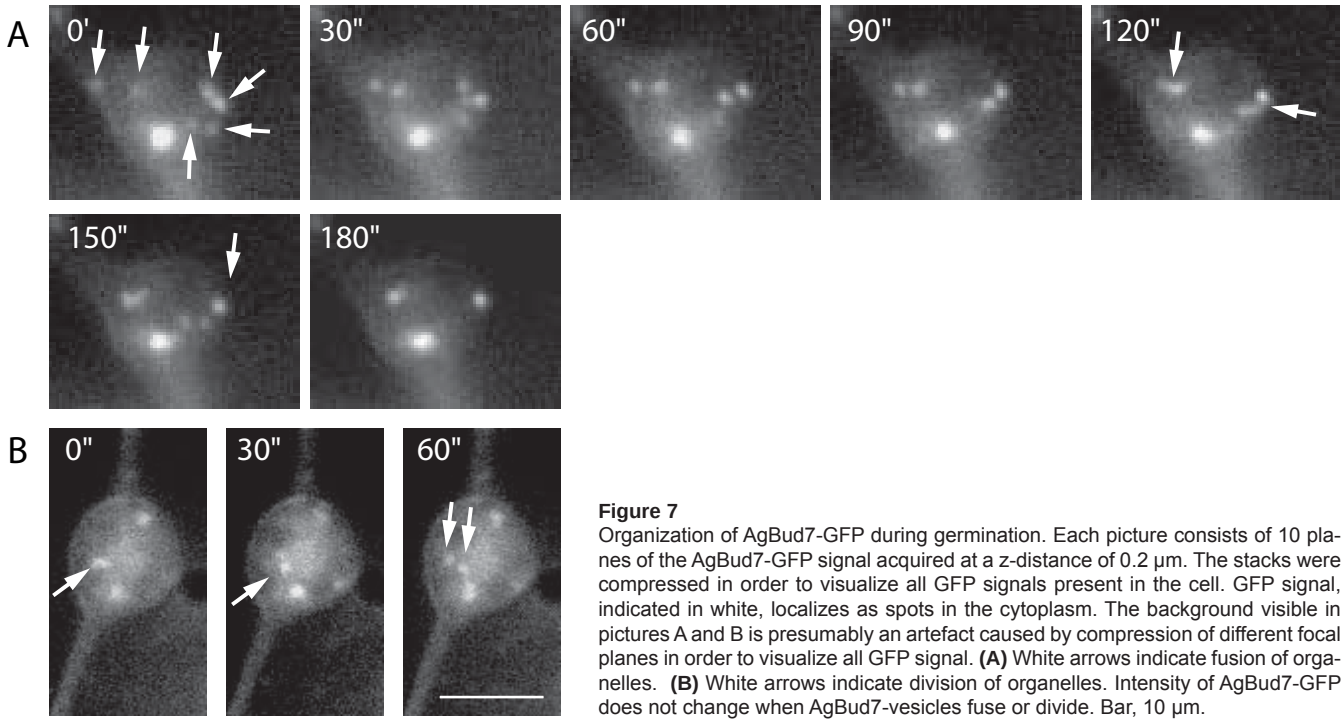

Figure 7
Organization of AgBud7-GFP during germination. Each picture consists of 10 planes of the AgBud7-GFP signal acquired at a z-distance of 0.2 µm. The stacks were compressed in order to visualize all GFP signals present in the cell. GFP signal, indicated in white, localizes as spots in the cytoplasm. The background visible in pictures A and B is presumably an artefact caused by compression of different focal planes in order to visualize all GFP signal. **(A)** White arrows indicate fusion of organelles. **(B)** White arrows indicate division of organelles. Intensity of AgBud7-GFP does not change when AgBud7-vesicles fuse or divide. Bar, 10 µm.

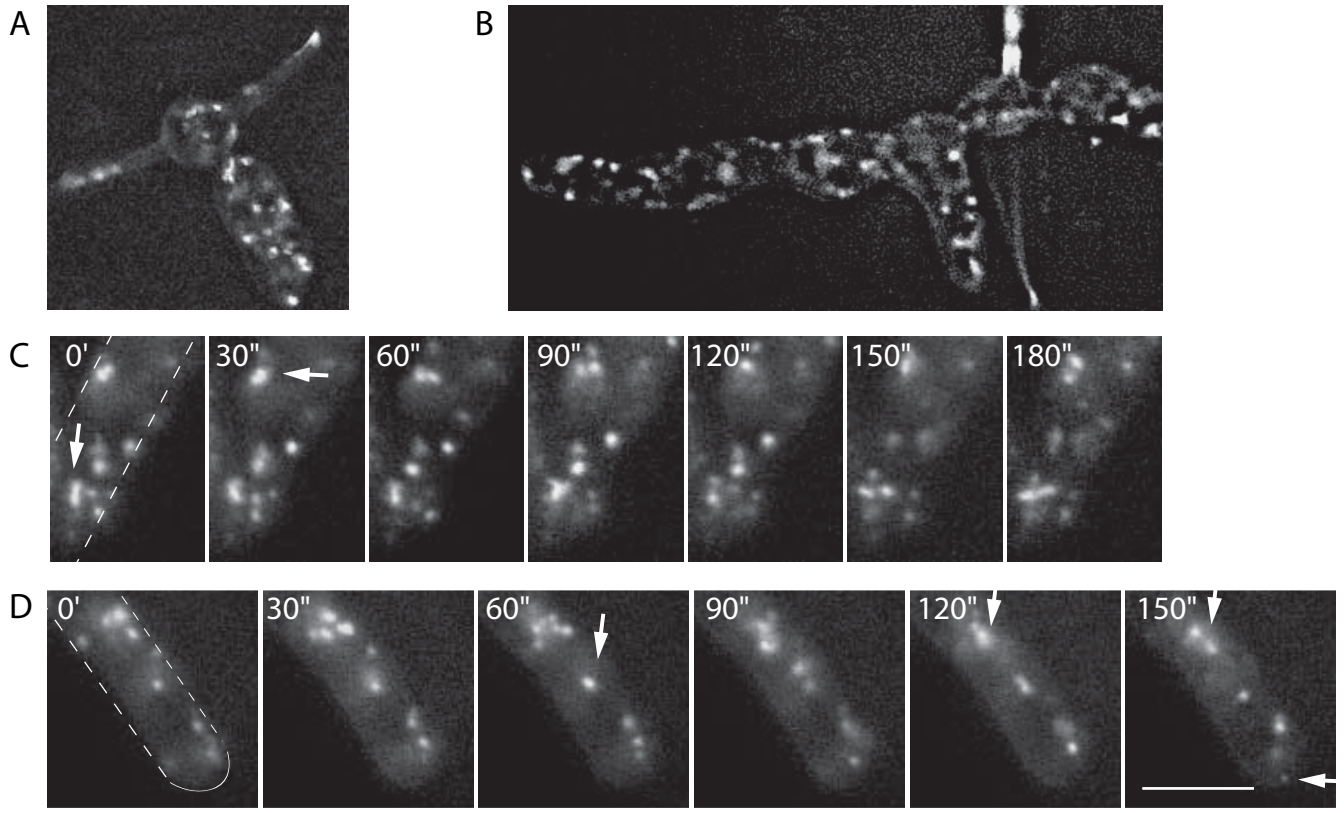

Figure 8
Organization of AgBud7-GFP during sustained polar growth. Each picture consists of 10 planes of the AgBud7-GFP signal acquired at a z-distance of 0.2 µm. The stacks were compressed in order to visualize all GFP signals present in the cell. Compression likely causes the high fluorescence background. GFP signal, indicated in white, localizes as spots in the cytoplasm. **(A, B)** Localization of AgBud7-GFP in young mycelium. The number of AgBud7-vesicles increases with time and size of the cell. **(C)** Localization and dynamic of AgBud7-GFP in internal parts of the mycelium. White arrows indicate movements of organelles. **(D)** Localization and dynamics of AgBud7-GFP close to the tip of hyphae. White arrows indicate organelles that fuse and divide. AgBud7-GFP intensity does not change during fusion or division process. Bar, 10 µm.

we performed the stack of pictures and compressed them in order to record all existing GFP signals per hyphal segment. The estimated amount of vesicles per 20µm hyphal segment was 17-20 and remained (n=32) constant in cells of different age.

AgBud7-GFP oscillations most probably depend on the flow of cytoplasm

Because AgBud7p appeared to be a rather dynamic protein to explore the role of actin in AgBud7p-GFP signal distribution we applied Latrunculin A (LatA). Addition of LatA disrupts actin structures, abolishes the vesicular movement and apical localization, giving rise to a uniform fluorescence within hyphae.

First, we followed the AgBud7-GFP signal by video microscopy for about 10 min. Next, we applied 3µl of 2mM LatA directly under the cover slide, therefore, the final concentration of LatA in the agar was approximately 2mM.

When exposed to LatA, normally quite dynamic organelles slowed down their movements and stopped after 12 min. **(Fig. 9)**. Their intensity did not change during the course of the experiment demonstrating that the localization of AgBud7p does not rely on the actin cytosceleton.

Thus, the observed AgBud7-GFP movements rather depend on the flow of cytoplasm, than any actin dependent structures.

Part of AgBud7-GFP signal co-localizes with Spindle Pole Bodies

To examine the mechanism underlying the observed oscillations of AgBud7- vesicles, we tested if AgBud7-GFP co-localizes with secretory vesicles. We constructed and transformed the AgBud7-GFP strain with a plasmid carrying an amino-terminal fusion of *RFP* to *AgSEC4* under its native promoter. In budding yeast, the gene product of *SEC4* fused to GFP localizes to secretory vesicles. Although we were able to visualize AgSec4-RFP in the control strain, the intensity of the AgBud7-GFP was to strong to accurately co-localize it with AgSec4-RFP signal.

Consequently, to verify with what kind of cellular structures AgBud7p is associated we performed nuclei staining. AgBud7-GFP spores were grown for 16 hours, fixed and stained with DAPI in order to visualize nuclei and AgBud7-GFP.

Unlikely, due to the fixation procedure, we lost small part of the AgBud7-GFP signal. Because some of the remaining AgBud7-GFP signal appeared to co-localize with Spindle Pole Bodies (SPB) **(Fig. 10)**, we performed a tubulin co-staining of the AgBud7-GFP strain. The AgBud7-GFP spores were grown for 16 h and fixed according to a standard protocol. A small number (less than 10 %, however a precise number is not available due to the fixation that disrupts part of the signal) of AgBud7p vesicles co-localized with SPB **(Fig. 11)**.

We propose that the presence of AgBud7-GFP at the SPB could be related to the sporulation defect. The SPB plague in *S.cerevisiae* was shown to be involved in spore formation. Moreover, one of the *AgBUD7* homologues *ScBCH1* was shown in *S.cerevisiae* to be expressed during the first hours of sporulation, whereas expression level of the second *ScBUD7* dropped down immediately after cells were shifted to sporulation medium (Chu S, et al 2000, Primig et al., 2003, Wiederkehr et al., 2004a and Wiederkehr et al., 2004b). Consequently, deficient expression of *AgBUD7* during sporulation could be due to the observed sporulation defect in *Agbud7Δ.*

Since we were able to co-localize only part of the AgBud7-GFP signal, some further co-localization studies should be done to verify with what cellular structures AgBud7p is associated. Studies done in *S.cerevisiae* indicated co-localization of ScBud7p with late golgi. Because we lack golgi marker in *A.gossypii* we are currently not able to confirm such localization in *A.gossypii*.

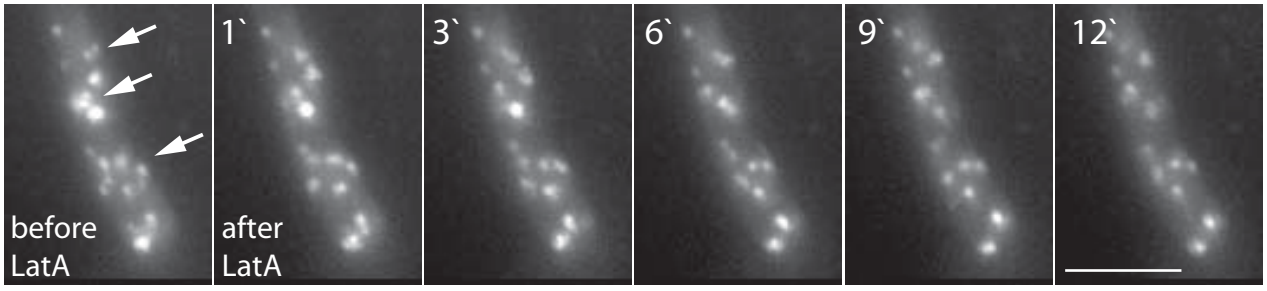

Figure 9
Organization of AgBud7-GFP before and after LatA treatment. Each picture consists of 10 planes of the AgBud7GFP signal acquired at a z-distance of 0.2 µm. The stacks were compressed in order to visualize all GFP signals present in the cell. The time elapsed between two frames is indicated. White arrows indicate oscillating organells. When exposed to LatA AgBud7-vesicels slow down and stop their movements after 12 min. Bar, 10 µm.

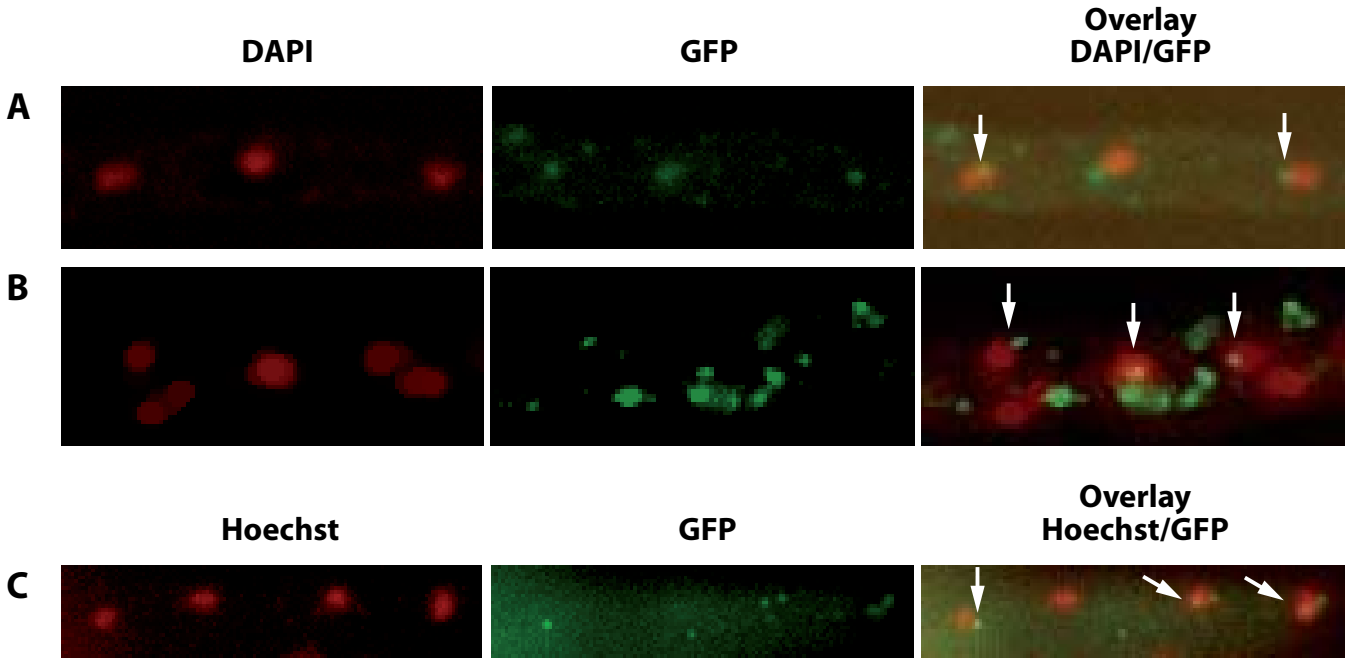

Figure 10
Part of AgBud7-GFP signals co-localize with nuclei. **(A, B)** Nuclei were visualized with DAPI staining. *A.gossypii* was cultured in AFM for 17 hours, fixed with 70% ethanol and stained with DAPI. In green: AgBud7-GFP; in red:nuclei DAPI staining. Right panels show overlay of Bud7-GFP with nuclei. Weak GFP signal is probably due to the fixation with ethanol. **(C)** Nuclei were visualized with Hoechst staining. *A.gossypii* was cultured in AFM for 17 hours, fixed with formaldehyde and stained with Hoechst. In green: AgBud7-GFP: in red: nuclei Hoechst staining. Right panel shows overlay of AgBud7-GFP with nuclei. Weak GFP signal is probably due to the fixation with formaldehyde.

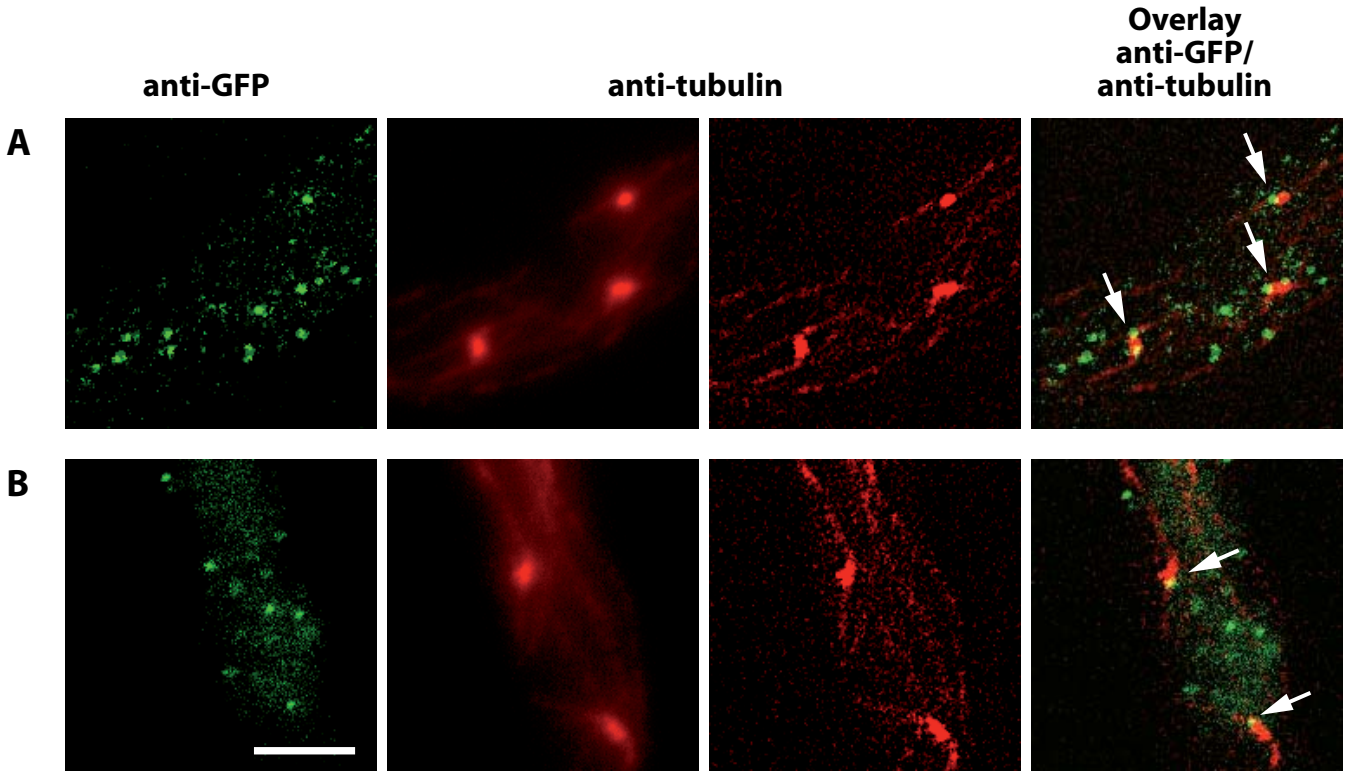

Figure 11
(A-B) Small part (less than 10%) of AgBud7-GFP signals co-localizes with Spindle Pole Bodies (SPB). Visualization of the microtubules cytoskeleton and GFP was done using anti-tubulin and anti-GFP antibody. *A.gossypii* was cultured in AFM for 20 hours, predigested and treated with primary and secondary antibodies according to the protocol (Materials and Methods). The slides were mounted in mounting media and analyzed by microscopy. In green: AgBud7-GFP; in red: tubulin staining. Right panels: overlay of green and second red panel. The weak GFP signal is probably due to the quality of antibodies and fixation protocol.

Discussion

ScBud7p and ScBch1p are involved in the budding pattern of *S.cerevisiae*

ScBUD7 was previously identified in a visual screen for mutants with a defect in the bipolar budding pattern; it was described as having a heterogeneous budding pattern phenotype (Zahner *et al*., 1996). Snyder (Snyder *et.al*., 2001) found that *Scbud7Δ/ bud7Δ* cells exhibit an axial-like phenotype. This pattern differs from the unipolar pattern in that the cells had long chains of bud scars, very similar to those seen on axial budding cells (Chant and Pringle, 1995). However, in contrast to normal axially budding cells the *Scbud7Δ/bud7Δ* mutant produced chains of bud sites starting at either the distal pole or the proximal pole, as well as in the equatorial region, although there was a strong bias in most cases for one end of the chain to originate from the proximal pole. 75% of the *Scbud7Δ/bud7Δ* deletion mutants used the proximal pole for the first two divisions (Snyder *et al.*,2001).
Cullen and Sprague (Cullen and Sprague, 2002) showed that the disruption of *ScBUD7* in haploid *S.cerevisiae* caused an invasive growth defect. The mutant also exhibited a distal pole bud site selection defect. 78% of the haploid Sc*bud7Δ* cells budded exclusively at the proximal pole versus 17 % that formed buds at the distal pole. Moreover, they suggested that ScBud7p and ScBud8p might be components of the same pathway.

Many details of the role of ScBud7p remained unclear, including the relationship between its function and the function of its twin ORF ScBch1p. The studies reported here have now clarified several of the beforehand unanswered issues.
First, both proteins ScBud7p and ScBch1p have the same ancestor that diverged during evolution. This way one function could be shared between two proteins.
Careful analysis of the single and double mutants showed that although a deletion of one or the other protein does not seem to affect the budding pattern of *S.cerevisiae* haploid cells the double deletion *Scbud7Δ/bch1Δ* seems to affect their development in subsequent cell cycles.
Partial loss of proximal-pole budding in haploid a*Scbud7Δ/bch1Δ* mutant suggests that there is another not yet identified protein that may function at proximal poles in the absence of ScBud7p and ScBch1p.
The homozygous double deletion *Scbud7Δ/ bud7Δbch1Δ/ bch1Δ* strain showed predominantly a randomised budding pattern in subsequent cell cycles. The occurrence of some apparent chains of bud scars and a tendency to bud at the proximal pole suggested that under these conditions (i.e., the putative absence of both types of bipolar-budding markers), a diploid strain might show some ability to use axial cues for bud-site selection.
Moreover, our results allow the conclusion that both investigated *S.cerevisiae* proteins are part of two different pathways, however they may act together in order to select budding pattern in haploid and diploid cells.
Analysis of the haploid *Scbud7Δ/bch1Δ and diploid Scbud7Δ/bud7Δbch1Δ/ bch1Δ* revealed elongated mother-daughter necks, problems with cytikinesis and some decreased sensitivity to calcofluor. All this observations suggest that chitin deposition may be disturbed in both investigated strains. Thus we propose that both proteins are required for the proper chitin deposition. Indeed, in *S.cerevisiae* J. Pringle proposed that the vesicular trafficking of ScBud8p and ScBud9p appears to involve ScBud7p, a member of a protein family that includes ScChs6p, which is itself involved in vesicular trafficking of the chitin synthase ScChs3p (J.Pringle, personal communication Gothenburg symposium 2003).

AgBud7p maintains polar growth likely by supporting the cell wall construction

The above observations highlight the role of ScBud7p and ScBch1p in polar growth of *S.cerevisiae* and are raising many questions considering the role of their homologue in the filamentous fungus *A.gossypii.*
Our functional analysis of *Agbud7Δ* revealed that the maximal speed determined from radial growth colonies was on average 40% slower.
Furthermore, the AgBud7p protein appears to play an important role in cell morphogenesis. During germination AgBud7p may be involved in the selection of new polar sites. Additionally, we found that in absent of AgBud7p hyphae and branches exhibits deviations from the growth direction, thus it may be required to maintain polarity at the hyphal tip.
These findings together with the localization of AgBud7-GFP put forward a possible role of AgBud7p in maintenance of polar growth, e.g. by supporting cell wall synthesis. According to our theory AgBud7p may be involved in transport of AgChs6 in order to synthesize extending cell walls. Similar function was proposed and discussed above for the homologues of AgBud7p in *S.cerevisiae*.
Furthermore, a recommended function would be in agreement with the *Agbud7Δ* deletion phenotype and would explain changes in the growth direction of mutant hyphae.
However, some additional studies have to be done to confirm this suggestion. If Agbud7p is involved in the maintenance of polar growth by substantial support,

then all polarity markers sitting at the tip or close to the hyphal tip should be continuously present there in the absence of the AgBud7p protein.

Therefore, we propose the following experiments: localization of AgSpa2-GFP and AgRax2-GFP in the absence of AgBud7p. If any of the investigated markers will change the localization it will clearly show that the role of *Agbud7*Δ is not only restricted to delivering building materials to the cell wall but as well that AgBud7p may be a landmark protein recruiting other proteins in order to establish polar growthMoreover, we observed a delay in actin ring formation in the apical part of the mycelium.

Consequently, to verify if this delay is due to a delay in placement of other proteins marking the sites for actin ring formation, localization of some known septum site markers, like Ag Sep7p, AgCyk1p or AgBud3p should be tested in the *Agbud7*Δ mutant.

Our further studies will address above mentioned experiments.

Furthermore, *Agbud7*Δ displayed a sporulation defect. Considering the nuclear alignment failure and partial co-localization of AgBud7p with SPB (should be proven with life marker) we hypothesized that SPB extension into the spore wall structure, which is important for the attachment of microtubules, could be defective in Agbud7Δ.

Moreover, if SPB plaque extension into the spore wall structure is defective, the cell wall around nuclei is not formed. In *S.cerevisiae* many proteins were found to interact with ScBud7p (YPD data), for example ScSmkp that is involved in sporulation. It is still not clear which proteins are important for sporulation in *A.gossypii*. We suggest that AgBud7p could be one of them.

Considering the hypothetical function of AgBud7p in AgChs6 trafficking a sporulation defect could be equally due to a defect in the chitin pathway.

Heterologous complementation in *S.cerevisiae* by *A.gossypii* genes

Introduction

The filamentous fungus *A.gossypii* is closely related to yeasts, as shown by its genome organization. Based on the phylogeny of genes such as rDNA, *A. gossypii* belongs to the family of *Saccharoyceta-ceae*. The uninucleate spores of *A.gossypii* carry a haploid genome and are similar in cell wall carbohydrate and di-tyrosine composition to *S.cerevisiae* ascospores but differ in their morphologyies. About 95% of all *A. gossypii* genes have a homologue in *S. cerevisiae*, which indicates that the basic cellular functions and morphogenetic machineries are well conserved between these species.

The *A.gossypii* genome sequence is now publicly available and is one of the best-annotated eukaryotic genome sequences, largely owing to an in depth analysis of the high degree of synteny with the *S.cerevisiae* genome and to the relative compactness of the *A.gossypii* genome (Dietrich 2004). Based on the genome size it represents the simplest free-living filamentous fungal species with only 4700 protein-coding genes.The *A. gossypii* genome sequence was also used to reanalyse the genome annotation of *S.cerevisiae* which provides strong evidence for ancient genome duplication in the *Saccharomyces* lineage (Brachat, S. *et al*., Dietrich, F. S. *et al*.,).

Therefore, *A.gossypii* is a very good model for comparing the cell biology of filamentous fungi and yeasts.

Because of the genome duplication, the *S. cerevisiae* genome frequently contains two homologues of a single *A.gossypii* gene, which might be relevant for morphogenesis.

For example, *A. gossypii* has only one homologue of the *S. cerevisiae RAS1/RAS2* pair, one homologue of the *SPA2/SPH1* (Spa2 homologue) twins, and one homologue of the GTPase-activating proteins *RGA1/ RGA2*.

Furthermore it has only one homologue of the *S.cerevisiae BUD8/BUD9* genes, which encode bipolar landmark proteins. ScBud8p and ScBud9p localize to the distal and proximal pole in diploid *S. cerevisiae* cells, respectively and are important for determining bud-site selection in (a/alpha) cells (Madden, K. & Snyder). Equally discussed in this PhD-work, two genes *ScBUD7 and ScBCH1*, which are involved in the bud site selection and according to Trautwein (unpublished) they are most likely required for transport at the trans Golgi network, are having only one homologue in the filamentous fungus *A.gossypii.*

Functional analyses of morphogenetic genes in yeast and a closely related filamentous fungus such as *A. gossypii* will provide new details on the general mechanisms of growth and may also contribute to our understanding how these processes evolved.

A.gossypii RAX1, *RAX2* and *BUD8* complement deletions of *S.cerevisiae RAX1*, *RAX2* and *BUD8* genes

RAX1, RAX2, BUD8 and *BUD9* in *S.cerevisiae* are crucial for the bipolar budding pattern observed in diploid cells. To answer the question whether *A.gossypii* genes are able to complement deletions of *S.cerevisiae* homologues we created plasmids carrying WT copies of *A.gossypii* genes (see Materials and Methods) and transformed them into the *S.cerevisiae* proper deletion strains indicated in the

Name		Genotype	Plasmid used for complementation
YEF473	a/α	*Wild type*	-
YEF473 A	a	*Wild type*	-
YEF473 B	α	*Wild type*	-
HH391	a	*bud8-Δ::TRP1*	pAgBUD8
HH399	α	*bud8-Δ::TRP1*	pAgBUD8
HH615	a/α	*bud8-Δ::TRP1/ bud8-Δ::TRP1*	pAgBUD8, pAgBUD8_CTGFP
HH613	a	*bud9-Δ::HIS3*	pAgBUD8
HH614	α	*bud9-Δ::HIS3*	pAgBUD8
HH615	a/α	*bud9-Δ::HIS3/ bud9-Δ::HIS3*	pAgBUD8,
AM365	α	*rax1-Δ::KAN*	pRS415RAX1
AM366	a	*rax1-Δ::KAN*	pRS415RAX1
AM377	a/α	*rax1-Δ::KAN/ rax1-Δ::KAN*	pRS415RAX1
AM474	a	*rax2-Δ::HIS3*	pRS415RAX2
AM475	α	*rax2-Δ::HIS3*	pRS415RAX2
AM476	a/α	*rax2-Δ::HIS3/ rax2-Δ::HIS3*	pRS415RAX2, pRS415RAX2_CTGFP

Table 1
Complementation of *S.cerevisiae* deletions with *A.gossypii* homologues genes.

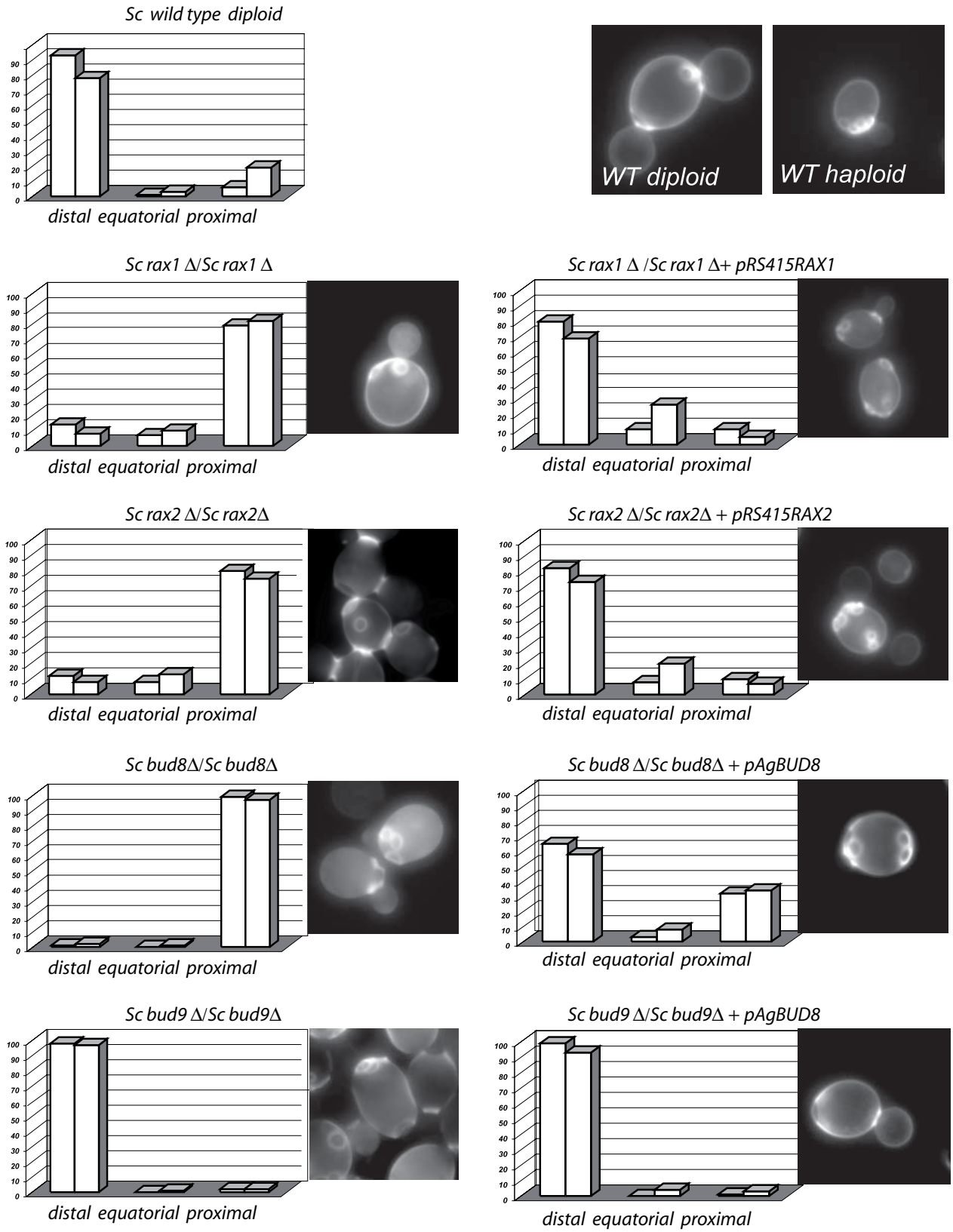

Figure 1
Complementation of *S.cerevisiae* deletions with *A.gossypii* homologues genes. The deletion of *ScBUD9*, the twin of *ScBUD8*, could not be complemented by the *A.gossypii AgBUD8* gene. All others *A.gossypii* homologues were able to complement *S.cerevisiae* deletions, however not to 100%. 100 cells with one bud scar (left column) and 100 cells with 3 bud scars (right column) were monitored. Bud scars were scored as distal, equatorial (middle section), or proximal. For each strain the average value from three independent experiments are shown.

table below **(Table1)**. The *S.cerevisiae* strains used in these studies were provided by Laura Schenkman.
As the deletion of *S.cerevisiae* genes led to a change in the budding pattern we could determine whether an *A.gossypii* homologue gene was able to complement a *S.cerevisiae* deletion by comparing the budding pattern of the deletion strain and the same strain carrying a plasmid expressing an *A.gossypii* homologue of the deleted *S.cerevisiae* gene.
We have tested the complementation of *S.cerevisiae* deletions in haploid and diploid strains also in those cases where genes exclusively act in diploid *S.cerevisiae* strains.
Phenotypes of the *RAX1, RAX2, BUD8* and *BUD9* null mutation in wild type haploid cells were indistinguishable from those of wild type cells; both budded in an "axial" fashion. Moreover, none of the plasmids carrying the homologues of *A.gossypii* corresponding genes was able to influence a budding pattern typical for haploid cells.
Therefore, we present here only data concerning complementation of the deletions of *RAX1, RAX2, BUD8* and *BUD9* genes in diploid a/alpha cells with *A.gossypii* homologues genes **(Fig 1)**.

As previously observed in *S.cerevisiae* diploid cells, nearly all first buds (>98%) emerged at the distal pole of the daughter cells. Whereas mother cells that had budded multiple times displayed most or all of the bud scars clustered around the two poles of the cell (Chant and Pringle, 1995 ; Harkins *et al*., 2001). The *Scrax1*Δ*/Scrax1*Δ and *Scrax2*Δ*/Scrax2*Δ mutants displayed a severe disruption of the bipolar budding, but their phenotypes were strikingly different from those of the *Scbud8*Δ*/Scbud8*Δ and *Scbud9*Δ*/Scbud9*Δ mutants.
The *Scrax1*Δ*/Scrax1*Δ diploid mutant did not exhibit a complete axial budding pattern. *Scrax1*Δ*/Scrax1*Δ cells showed a rather non-random budding pattern (heterogeneous), however there was a strong bias in most cases for one end of the chain of bud scars to originate from the proximal pole.
A very similar phenotype was observed for the *Scrax2*Δ*/Scrax2*Δ diploid mutant. Mother cells displayed a wide variety of bud-scar patterns.
For the *Scbud8*Δ and *Scbud9*Δ mutants we confirmed the phenotypes reported previously by Zahner and Harkins. In the *Scbud8*Δ*/Scbud8*Δ mutant, nearly all first buds and most subsequent buds, were at the proximal pole, whereas in the *Scbud9*Δ*/Scbud9*Δ mutant, nearly all first buds, and most subsequent buds, were at the distal pole (Zahner *et al*., 1996 ; Harkins *et al*., 2001).

A.gossypii AgRAX1, AgRAX2 and *AgBUD8* were able to complement the deletion of *S.cerevisiae* homologues, however, not to 100%.
The presence of plasmid pRS415_RAX1 rescued the deletion phenotype observed for the diploid *Scrax1/Scrax1* strain. The majority of the cells carrying this plasmid exhibited the first bud at the distal position. Interestingly, in almost 25% of cells the third bud appeared in the equatorial region, which is slightly different from the wild type pattern. A similar budding pattern was observed for the *Scrax2*Δ*/Scrax2*Δ deletion strain carrying the plasmid pRS415_RAX2.
To verify whether the obtained budding pattern was due to the incomplete complementation or for example insufficient selection for the plasmid containing *A.gossypii* wild type gene, we introduced into the *Scrax2*Δ*/Scrax2*Δ strain a plasmid carrying a C-terminal GFP fusion to the wild type copy of the *AgRAX2* gene. Consequently, the cells that displayed the GFP signal (indication for the proper function of the AgRax2p) showed a wild-type like budding pattern.
The *AgBUD8* gene was able to complement the *Scbud8*Δ*/Scbud8*Δ deletion, however only in 65% of the cells analyzed. We also repeated this experiment using an *A.gossypii* plasmid carrying C-terminal GFP fusions to the wild type copy of the *AgBUD8* gene. We found that cells carrying the GFP signal showed in the majority a wild-type like budding pattern. Thus, incomplete complementation could be due to to plasmid instability, or the presence of the twin gene-*ScBUD9*.

The evolutionary rearranged *ScBUD9* promoter does not allow complementation of the *ScBUD9* deletion by the *A.gossypii* homologue

A.gossypii AgBUD8 was not able to complement the deletion of the *S.cerevisiae BUD9* gene. During evolution, in order to specialize cell function, *S.cerevisiae* genes diverged after duplication, giving rise to *ScBUD8* and *ScBUD9* genes. Promoter studies reveal that the *ScBUD8* gene very likely has a similar promoter as its *A.gossypii* homologues and that the *ScBUD9* promoter potentially has rearranged during evolution compared to its *A.gossypii* homologue **(Fig. 2)**.
ScBud8p localizes to the distal pole and ScBud9 to

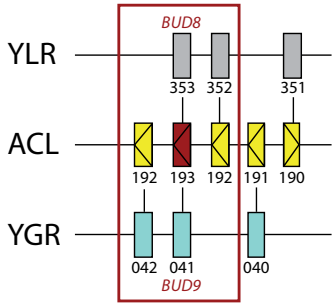

Figure 2
Rearangments of the *S.cerevisiae ScBUD8* and *ScBUD9* promoters during evolution.

the proximal pole in diploid *S. cerevisiae* cells. Hyphae of a filamentous fungus have unipolar (unidirectional) growth and therefore may not need to mark distal regions.
To verify this hypothesis a localization study of AgBud8p was performed. Unfortunately, C-terminal GFP fusion to the endogenous copy of the gene, although grew wild-type like have not shown any signal. Furthermore, N-terminal GFP fusion to AgBud8p introduced on plasmid into the *Agbud8*Δ strain have not displayed any signal, most likely due to a to weak signal intensity.
The *Agbud8*Δ displayed a decrease in the average colony growth speed and detailed studies indicated no switch from a slow to a fast growing mode, although we observed dichotomous branch formation, typical for a fast growing hyphae.
Moreover, chitin staining pointed to an altered chitin distribution in the subapical regions of the hyphae. We still could observe a proper septation, though produced compartments exhibited a similar size in the hyphae of different age. It is still not clear if observed comparable size of sections was a direct consequence of the AgBud8p deletion or the consequence of a lack of increase in the growth speed. Currently AgBud8p is under further investigation.

To summarize, homologue genes originating from the haploid filamentous fungus *A.gossypii* can replace *S.cerevisaie* diploid specific genes.
Thus *A.gossypii* proteins function in *S.cerevisiae* although they seem to play a slightly different role in the polar growth of filamentous fungus, than the one described for unicellular yeast.
Future work should focus on the complementation of the deletion of *ScBUD7* and its twin *ORF YMR237w/BCH1* to complete these studies on the role of diploid specific genes in haploid filamentous fungus *A.gossypii*.

Materials and Methods

A.gossypii and *E. coli* strains

The *A. gossypii* wild-type strain (ATCC 10895) and wild-type strain (ATCC 10895) in which the *AgLEU2* and *AgTHR4* genes were deleted were used (Altmann-Johl and Philippsen, 1996) and Ch. Mohr Ph.D thesis University of Basel (1997).
Escherichia coli XL1-blue was used as plasmid host.

Growth conditions

A.gossypii was grown in liquid AFM (*Ashbya* Full Medium, 10 g/l yeast extract, 10 g/l Select Peptone 140 (Gibco BRL / LIFE TECHNOLOGIES), 20g/l glucose, 1 g/l myo-Inositol) using shake flasks or on solid medium (AFM + 12 g/l agar granulated). For selection on the dominant drug resistance markers Geneticin (Calbiochem, 100% efficacy) or clonNat (WERNER Bio AGENTS, Jena, Germany) was added to the medium at concentrations of 200 µg/ml and 50 µg/ml, respectively. For auxotrophic selection using the LEU2 marker ASD drop out medium was prepared (*Ashbya* Synthetic Dextrose, 1.7 g/l YNB w/o amino acids and ammoniumsulfate (Difco), 0.78 g/l CSM-ADE / 0.69 g/l CSM-LEU (Bio101), 1 g/l Asn, 1 g/l myo-Inositol, 20 g/l Glucose, 12 g/l agar). Standard incubation temperature was 30°C.
To isolate spores an AFM plate was inoculated with *A.gossypii* spores or mycelium in the centre. After growth for 7 days the mycelium was harvested with a sterile loop and resuspended in 1 ml of 2 mg/ml aqueous Zymolyase solution (Seikagaku, 20 U/µg) and incubated at 37°C for 1 h. The suspension was centrifuged at 3000 x g and the supernatant decanted. Three washing steps with 0.03 % Triton X-100 were applied. Finally, spores were resuspended in 20 % glycerol and frozen at -70°C. The concentration was 1-2x10^7 spores/ml.

Genomic DNA isolation

The mycelium of a 50 ml o/n culture was harvested by filtration and washed once with water. 1 g of mycelium was incubated in 10 ml SPEZ (1 M Sorbitol, 10mM NaP pH 5.8, 10mM EDTA, 1 mg/ml Zymolyase) at 37°C for 1 h or until protoplastation. 1 ml 10 % SDS was added and the suspension was incubated at 37°C for 15 min. SDS was precipitated on ice for 30 min with 3.6 ml 3 M KAc. The suspension was centrifuged at 15000 x g for 15 min and the supernatant precipitated with 1 vol. of isopropanol. The solution was centrifuged at 15000 x g, the pellet washed with cold 70 % EtOH and dried. The pellet was resuspended in 1 ml TE containing 0.5 mg/ml RNase A (Roche) and incubated at 37°C for 1 h. The solution was phenol-chlorophorm extracted, precipitated, washed and resuspended in Tris pH 8.0 (Wright and Philippsen, 1991).

Cytoskeletal staining

Visualization of the actin cytoskeleton was done using Rhodamine- Phalloidine coupled fluorophores (acc. to Amberg, 1998, modified).
A.gossypii was cultured in AFM to the desired stage. All subsequent steps were performed on ice and without centrifugation to assure maximum preservation of the delicate actin cytoskeleton. After letting mycelia settle to the ground 1 ml of the culture was mixed with 100 µl 37 % formaldehyde (Fluka puriss. p.a.) and fixed for 10 min. Mycelia were centrifuged at 2000 x g, resuspended in PBS containing 4 % formaldehyde and incubated for 1 h. Mycelia were washed twice with PBST (PBS containing 0.03 % Triton X-100) and resuspended in 100 µl PBST. 10 µl Rhodamine-Phalloidin (6.6 µM in MeOH, Molecular Probes Inc.) was added and the mycelia were incubated for 1 h in the dark. Mycelia were washed 5 times in PBST and resuspended in 50 µl mounting medium (50 mg p-phenylenediamine in 5 ml PBS, adjust pH to 8.0 with 0.5 M Na_2CO_3 pH 9.0, bring volume to 50 ml with glycerol). Alternatively, cells were fixed with paraformaldehyde (Fluka) if the fluorescence of GFP should be maintained. 1 ml of a cell culture was fixed for 30 min. with 1 ml of 4 % paraformaldehyde (Sambrook *et al*., 2001). Mycelia were washed twice with PBST and resuspended in mounting medium or stained for actin using Rhodamine-Phalloidin according to the above protocol.

Tubulin staining

Visualization of the microtubule cytoskeleton was done using anti-tubulin antibody. *A.gossypii* was cultured in AFM to the desired stage. 10 ml of culture was mixed with 1ml 37 % formaldehyde (Fluka puriss. p.a.) and fixed for 1 hour.
Mycelia were centrifuged at 2000 x g and wash twice with PBS. After the PBS wash, the cell pellet was resuspended in 2 ml Solution A (0.1 M potassium phosphate buffer pH 7.5, 1.2 M sorbitol, H_2O). 1 ml of these cells were transferred to a new eppendorf tube and was mixed with 150 µl, 10 mg/ml zymolyase, 10 µl mercaptoethanol and incubated with gentle rotation at 37 °C.
This step is performed to permeabilize the cell to enable the antibody to cross the cell wall and to bind

to tubulin. The cells were checked microscopically in order to stop the digestion process at the right time. The digested cells were centrifuged at low speed 3000 rpm in small bench top centrifuge, washed and resuspended in 1 ml solution A.
The immunoflurescence slides were treated with poly-lysine to help cells to attach to the glass surface (10 µl/well, for 5 minutes, aspirate, let air dry, wash 1 time with H_2O, aspirate and let air dry). 20 µl of cells were dropped onto a poly-lysine treated well of a multi-well slide. They were allowed to settle for 15 minutes and washed 2 times with PBS.
In order to block cells 10 µl 1xPBS+1mg/ml BSA (IgG free) was added. Cells were washed 2 times with PBS+BSA. 10 µl primary anti-tubulin antibody (Rat anti-alpha tubulin YOL34 from Serotec were added at 1/50 dilution in PBS+BSA incubated for 2 hours in a humid chamber to avoid evaporation. After the incubation time, the slide was washed 10 times with PBS+BSA and the cells were incubated for 1 hour with the secondary antibody (mouse anti Rat antibody) 1 mg/ml at 1/200 dilution+1 mg/ml DAPI at 1/200 dilution, washed after the incubation time 10 times with PBS+BSA.
The slides were then mounted in mounting media and analysed under the fluorescence microscope.

Hoechst staining

Hoechst is a fluorescent dye that interacts with DNA and was used for visualisation of the nuclei. A PBS (potassium phosphate buffer pH 7.5) solution containing 1:500 Hoechst 1 mg/ml was prepared for staining. The cells were resuspended and incubated for 1 hour in this solution.
After the incubation time the cells were washed two times in PBS to remove the additional dye and resuspended in mounting media (500 µl 1.0 M phosphate buffer pH 7.5, 2,5 ml glycerol 100 %, 5 mg p-pheniylendiamine, 5 ml H_2O).

Calcofluor staining

For characterization of budding patterns of *S.cerevisiae* and chitin deposition in *A.gossypii,* unfixed cells were stained with 0.1–1 mg/ml Calcofluor as described by Zahner *et al*. (1996).

FM 4-64 staining

For co-localization of the Spitzenkorper with GFP signal cells were stained with the endocytic livedye FM4-64 at a final concentration 2µM.
The samples could quickly be analyzed.

Image acquisition and processing

The microscopy units used (as described in Hoepfner *et al*., 2000, modified) consisted of two, 'Axioplan 2 imaging' microscopes (Carl Zeiss, Feldbach, Switzerland). One was equipped with the objectives Plan Neofluar 100x Ph3 N.A. 1.3, Plan Neofluar 63x Ph3 N.A. 1.3, Plan Neofluar 40x Ph3 N.A. 1.3 and the illumination sources 75 W XBO, HBO and 100 W halogen. The other, with the objectives Plan Apochromat 100x DIC N.A. 1.4, Plan Apochromat 63x DIC N.A. 1.4, Plan Neofluar 40x Ph3 N.A. 1.3 and the illumination sources 75 W XBO and 100 W halogen. The UV illumination source was controlled by a MAC2000 shutter and filter wheel system (Ludl Electronics, Hawthorne, NY, USA). The cameras were a TE/CCD-1000PB and an NTE/CCD back-illuminated cooled charge-coupled device (Princeton Instruments, Trenton, NJ). Phase contrast and DIC filters for Nomarski illumination were used for brightfield imaging, according to the manufacturer (Carl Zeiss). Following filter sets were applied for different fluorophores: DIC filter for Nomarski Illumination and #41018 for GFP with excitation spectrum at 450-490nm and a longpass emission at 500+ (Chroma Technology Corp, Rockingham, VT); for rhodamine-phalloidin double stainings with GFP, Chroma filter #41025 Piston GFP with a bandpass emission of 500-530nm (excitation at 450-490) for GFP and Zeiss Filter #15 for rhodamine (ex: 540-552, em: 590+). The FM4-64 live dye was recorded with the same double labelling filter set. Excitation intensity was controlled with different neutral density filters (Chroma Technology). The setup, including microscope, camera, and Ludl controller, was controlled by MetaMorph 4.1.7 software (Universal Imaging Corporation, Downingtown, PA).

For time-lapse acquisition spores were cultured on a slide with a cavity (time-lapse slide, Merck) that was filled with medium (AFM, for fluorescent acquisitions 0.25 x AFM in respect to peptone, yeast extract and myo-Inositol, 1 x in respect to glucose). Spores were pre-incubated in a humid chamber without cover slip until they reached the required developmental stage. Then a cover slip was applied. An acquisition set consisted of a brightfield image with optional three fluorescent images. Alternatively, streaming movies of a single focal plane of a specimen provided temporal resolution of three images per second.
The exposure time for the fluorescent images was reduced to 0.2-0.5 sec at 50% excitation intensity. The z-distance in stack acquisitions was set to 0.3 µm. For multiple exposures of the same sample bleaching of the sample had to be taken into account.
The time lapse picture series were processed in MetaMorph and converted to a QuickTime Movie. Brightfield single plane fluorescent images were scaled

using the „scaling“ dropin in MetaMorph. Stacks were deblurred with MetaMorphs „remove shading“ drop-in, flattened by „stack arithmetic“ and scaled with the „scale Image“. Fluorescent picture sets of two labels were combined using Meta-Morph‘s „Color overlay“ and „Color align“ drop-in.
For brighfield time-lapse acquisitions with a frequency of 0.5 h-1 spores were cultured on AFM plates and allowed to germinate for 8-10h in RT. After the plates have been placed under the objective, covered with foil to be protected against drying, pictures were acquired.

Analysis of sequences and standard procedures

The sequences of gene of interest were retrieved from the Ashbya genome database, generated from the complete genome sequencing approach by Dietrich *et al*., 2004. The resulting amino acid sequences were used for analysing similarity to the homologous genes in *S. cerevisiae*. Regions of identity were defined using the CLUSTALW module of the (*www.ebi.ac.uk/clustalw*). To define the percentage of identity in similar regions the clonManager 7.03 suite (Scientific & Educational Software, Cary, NC) „Align two sequences“ in the global alignment mode was used. Potential domains were predicted using the SMART software packag (Single Modular Architecture Research Tool), (http://smart.embl-heidelberg.de/); TMpred-Prediction of Transmembrane Regions and Orientation (http://www.ch.embnet.org) and CBS Prediction Servers (http://www.cbs.dtu.dk/services/).

Construction of the deletion mutants ;Transformation of *A. gossypii* strains

A.gossypii was either transformed replicative (Wright and Philippsen, 1991) or integrative (Steiner *et al*., 1995). In replicative transformation pRS415 (Sikorski and Hieter, 1989) and pAG503 served as shuttle vectors. pRS415 carries a CEN/ARS element and the LEU2 gene from *S.cerevisiae* and complements *Agleu2* strains (Mohr, 1997).
Integrative transformants were obtained by transformation of cloned and linearised DNA fragments or via PCR based gene targeting (Wendland *et al*., 2000). The deletions were made in the wild type and in some cases in *A. gossypii* ∆*leu2* ∆*thr4* strains.
GEN3 served as resistance marker against Geneticin. It encodes a phosphotransferase that is controlled by ScTEF2 promoter and terminator.
Alternatively the NAT1 ORF alone amplified from pAG36 (Goldstein and McCusker, 1999) was used as resistance marker. A selected ORF was exchanged with the NAT1 ORF by PCR based gene targeting. The NAT1 ORF was then under the control of the endogenous promoter. NAT1 encodes a N-acetyltransferase that was used as a resistance marker against clonNat.
Than again the pScLEU2 plasmid was used as a template to generate the ScLEU2 deletion cassette (Wendland *et al*., 2000, Bauer *et al*.2001). Since pGEN3 and pScLEU2 share the same vector backbone, we were able to use the same primer pair to generate a ScLEU2 disruption cassette as to generate GEN3 cassette.
Oligonucleotides used for PCR based gene targeting are listed in **Table 1** and created strains are listed in **Table 2**. The homology regions were selected to delete if possible the whole ORFs.

For transformation of *A.gossypii* 200 ml of AFM were inoculated with spores to a concentration of ~$7.5x10^4$ spores/ml. After 16-18 h the mycelium was harvested by filtration and washed with water once. It was incubated in 40 ml PD (50mM Phosphate-buffer pH 7.4, 25mM DTT) at 30°C with soft shaking for 30 min. The mycelium was filtrated again and washed with 40 ml of cold STM (270mM Sucrose, 10 mM Tris pH 7.5, 1 mM $MgCl_2$).
The competent mycelium was resuspended in 1-2 ml cold STM. 1-10 µg DNA resuspended in 50 µl of water was mixed with 150 µl of competent mycelium and transferred into a cold 4 mm electroporation cuvette (BioRad). The mycelium was electroporated (Gene Pulser, BioRad) at 100, 25 µF and 1.5 kV and resuspended in 1 ml AFM.
Using the dominant drug resistance markers GEN3 or NAT1 the transformed mycelium was resuspended in 5 ml AFM liquid medium and incubated for 5 h at 30°C to recover and after was streaked on pre-dried AFM plates containing 250 µg/ml Geneticin or 75 µg/ml clonNat, respectively. Primary transformants appeared after 2-3 days.
Using auxotrophic markers the mycelium was allowed to recover for 5 h in 5 ml AFM. The mycelium was then washed twice with water and streaked onto the appropriate ASD drop out plates.
Primary transformants appeared after 3-5 days. Primary heterokaryotic transformants were transferred onto selective plates and allowed to sporulate.
The transformation of young multinucleate mycelia produces heterokaryotic transformants that carry the wild type and the mutant allele. Therefore spores were prepared and separated on selective plates using a micromanipulator (Singer Instruments) to obtain homokaryotic transformants. Isolation of spores containing a single haploid nucleus from heterokaryotic transformants on G418/Geneticin-containing, clonNat-containing medium or on minimal medium gives rise to homokaryotic transformants in which all nuclei carry the mutant allele.

Correct genomic integration was verified by analytical PCR (Wendland *et al*., 2000). The newly generated links at the transformed loci were amplified from genomic DNA and the size verified on agarose gels. Oligonucleotides used for verification are listed in **Table 1**.
Standard oligonucleotides for verification of deletions generated with GEN3 are G3_2.1 and G3_3.2, for deletions generated with NAT1 are V2*NAT1 and V3*NAT1 were used. They bind in the 5'-region and in the 3'-region of the respective marker. After PCR verification of the resulting homokaryotic transformants a phenotypic analysis was initiated.
Homokaryotic spores of deletion mutants were germinated on selective medium containing plates and incubated for 5 days at 20, 30 and 37°C to analyse radial growth speeds.
A minimum of three independent homokaryotic transformants was claimed for each transformation. Experimental analysis was always done on at least two isolates demanding the same results.

Generation of C-Terminal GFP fusions to different genes

We were interested in the localization pattern and the dynamics of AgRax1p, AgRax2p, AgBud7p and AgBud8p. Therefore pGUG was amplified with specific oligonucleotides, listed in the **Table 1**, for the selected ORFs.
For AgRax2p and AgBud7p the GFP module was directly fused to endogenous copy of protein. The PCR products for an AgRax2-GFP and AgBud7-GFP fusion were transformed directly into *A.gossypii*. Isolates were verified by PCR for correct integration of the module. The transformants showed specific fluorescence and the fusion protein complemented the endogenous copy.
C-terminal GFP fusions to AgRax1p was not fully functional and although C-terminal GFP fusion to AgBud8p was functional we could not detect any signal. Therefore, we decided to integrate GFP into N-terminal part of both proteins. In both cases the approach via the yeast detour was followed. Please see cloning chapter.

Yeast strains, growth conditions, and genetic methods

Culture conditions, transformation methods and DNA isolation were performed as described by Burke *et al*., 2000. The oligonucleotides used to create *S.cerevisiae* strains and yeast strains used in these studies are listed in **Table 3** and **Table 4**, respectively.
Cells were grown at 30°C on YPD rich solid/ liquid medium, or synthetic complete (SC) medium lacking appropriate nutrients as needed to maintain plasmids (Lillie and Pringle, 1980; Guthrie and Fink, 1991). All media contained 2% glucose as carbon source. Cells to be examined for GFP fluorescence were grown in the dark to minimize photobleaching.

Cloning

General molecular cloning was done according to Sambrook *et al*., 2001. *E.coli* DH5 (Hanahan, 1983) was used as a host strain for all plasmid work.
Bacteria were grown at 37°C in LB medium (1.6g/l Tryptone, 1g/l yeast extract and 0.5g/l NaCl) supplemented with 100 µg/ml ampicillin for selection.
Sequencing was performed on an ABI 377 automated sequencer using the BigDye Terminator Sequencing Kit.
Enzymes for cloning were purchased at NEB, polymerases for PCR at NEB (Vent DNA polymerase), Pharmacia (Taq DNA polymerase) and Roche (Pwo DNA polymerase).
For plasmid isolation 5 ml LB media with 5 µl ampicilin solution (100mg/ml stock solution) was inoculated with a single *E. coli* colony containing the plasmid of interest, and was grown overnight (16 hours) at 37°C.
The plasmids were extracted from the host *E.Coli* cells using the Kits from Roche which is based on DNA denature–renature reaction due to the different pH of the solutions.
For DNA extraction from agarose gels Kits from Roche were used.
Oligonucleotides used for cloning are listed in **Table 5**; plasmids and pAgs are listed in **Table 6**. All maps of cloned plasmids for the purpose of this work are listed in the end of this chapter.

Cloning of pRS*415_RAX1*

The sequence of the homologue of ScRax1p was retrieved from the *A. gossypii* genome database. Primers Rax1_vectorS1BamHi and Rax1_vectorPsiI were designed and used for PCR amplification with genomic *A. gossypii* DNA as template.
Obtained fragment had length of 2768bps and additional BamHI site. Obtained PCR product was cut with XbaI and BamHI and ligated into pRS415 cut with the same restriction enzymes.
The resulting vectors were dubbed pRS415_*RAX1*. Constructed clones were partially sequenced.

Construction of N-terminal GFP fusion to pRS415_*RAX1*

As C-terminus GFP(S65T) was not functional we decided to attach the GFP into N-terminal part of the *AgRAX1* gene. Primers Rax1NTGFP_S1 and Rax1NTGFP_S2 were used to obtain the CORE fragment carrying resistance marker G418 from pCORE plasmid. Co-transformation of this fragment into N-terminal part of pRS415_*RAX1* was performed in *S.cerevisiae* Dhd5 and transformants subsequently grown under selective pressure by G418. Growing colonies were picked and the pRS415_*RAX1*_CORE plasmid was isolated. The generated plasmids were amplified in *E.coli*. Verification of plasmids extracted from *E.coli* for a correct recombination was done by digestion.
Obtained plasmid was cut with PacI inside the pCORE region and dephosphorylated. Co-transformation of cut plasmid together with PCR fragment obtained by amplification of GFP cassette with two primers Rax1NTGFP_S3 and Rax1NTGFP_S4 was done in *S. cerevisiae* and transformants subsequently grown on YPD leu(-) plates. The resulting vectors were dubbed pRSRAX1_NTGFP. Verification for a correct recombination was done by PCR using oligonucleotides Rax1G1 x Rax1I1.
The generated plasmid was amplified in *E.coli*. 10µg of plasmid was then transformed via electrophoresis into *A. gossypii* ∆*leu2* ∆*thr4*. The resulting strains carrying pRS415*RAX1*_NTGFP did not show specific fluorescence.

Cloning of pRS415_*RAX2*

The sequence of the homologue of ScRax2p was retrieved from the *A. gossypii* genome database. The Ag*RAX2* ORF was 3606 bp in length. Primers Rax2vector_S1 and Rax2vector_S2 were designed and used for PCR amplification with genomic *A. gossypii* DNA as template. Obtained fragment had length of 4642bps and additional BamHI site. Obtained PCR product was cut with NotI and BamHI and ligated into pRS415 cut with the same restriction enzymes. The resulting vectors were dubbed pRS415_*RAX2*. Constructed clones were partially sequenced.

Construction of pRS415_*RAX2_GFP*

The C terminus of AgRax2p was tagged with GFP (S65T), in order to localize AgRax2p, using PCR-based insertion into a plasmid pRS415_*RAX2*.
Primers Rax2GFP_S1 and Rax2GFP_S2.1 and resistance marker fragment from pGUG (Knechtle *et al*., PhD Thesis) were used to obtain the GFP. Co-transformation of this fragment together with pRS415_*RAX2* was performed in *S.cerevisiae* and transformants subsequently grown under selective pressure by G418. Growing colonies were picked and the pRS415_*RAX2*_GFP plasmid was isolated. Verification for a correct recombination was done by PCR using oligonucleotides Rax1_I2 x Green2 and G3.2 x Rax2_G4. The plasmid was then transformed via electrophoresis into *A. gossypii* ∆*leu2* ∆*thr4* and the resulting strain grown under G418 selective conditions. Since integration is of plasmidic nature, hyphae with strong signals were chosen directly with the microscope under weak UV illumination (10%) and then recorded.

Construction of pRS415_*RAX2_DSP* and pRS415_*RAX2_DSP-GFP*

In order to investigate the localization pattern of AgRax2p in absence of the 21 aa after the start codon (potential signal peptide) two vectors pRS415_*RAX2*_DSP and pRS415_*RAX2*_DSP-GFP were constructed.
Primers Rax2_signaling_S1 and Rax2_signaling_S2 were used to obtain the CORE fragment carrying resistance marker G418 from pCORE plasmid. Co-transformation of this fragment together with pRS415_*RAX2* was performed in *S.cerevisiae* and transformants subsequently grown under selective pressure by G418. Growing colonies were picked and the pRS415_*RAX2*_CORE plasmid was isolated. Verification of plasmids extracted from *E.coli* for a correct recombination was done by digestion.
Obtained plasmid was cut with BglI inside the pCORE region and dephosphorylated. Co-transformation of cut plasmid together with PCR fragment obtained by amplification of 2 overlapping primers Rax2_over_S1 and Rax2_over_S2 was done in *S. cerevisiae* and transformants subsequently grown on YPD leu(-) plates. The resulting vectors were dubbed pRS415_*RAX2*_DSP. Constructed clones were sequenced to prove absence of the 21 aa after the start codon.
The C terminus of pRS415_*RAX2*_DSP was tagged with GFP(S65T) like described above for the C-terminus GFP fusion. The plasmid were then transformed via electrophoresis into *Agleu2.thr4* . Hyphae with strong signals were chosen directly with the microscope under weak UV illumination (10%) and then recorded.

Cloning of pRS415_*BUD7*

The sequence of the homologue of ScBud7p was retrieved from the *A. gossypii* genome database. Primers Bud7_vector_S1 and Bud7_vector_S2 were

designed and used for PCR amplification with genomic *A. gossypii* DNA as template. Obtained fragment had length of 4124 bps.
Obtained PCR product was cut with HpaI and NotI and ligated into pRS415 cut with the same restriction enzymes. For the time beeing the resulting vectors dubbed pRS415_*BUD7* are still under construction.

Construction of a N-terminal GFP fusion to pAgBUD8 and cloning of pRS415_*BUD8_NTGFP*

As with C-terminus GFP (S65T) we could not visualize the AgBud8-GFP signal we decided to fuse the GFP into the N-terminal part of the AgBud8p protein. The sequence of the *AgBUD8* homologue of *ScBUD8* gene was present on pAG19946 clone (plate 198 G20/red; 9023bps). Primers Bud8NTGFP_S1 and Bud8NTGFP_S2 were used to obtain the CORE fragment carrying resistance marker G418 from pCORE plasmid (cytat). Co-transformation of this fragment into N-terminal part of pAG19946 was performed in *S.cerevisiae* and transformants subsequently grown under selective pressure by G418. Growing colonies were picked and the pAG19946_CORE plasmid was isolated. Verification of plasmids extracted from *E.coli* for a correct recombination was done by digestion.
The plasmid was then cut with PacI inside the pCORE region and dephosphorylated. Co-transformation of cut plasmid together with PCR fragment obtained by amplification GFP cassette with primers Bud8NTGFP_S3 and Bud8NTGFP_S4 was done in *S. cerevisiae* and transformants subsequently grown on YPD ura(-) plates. The resulting vectors were dubbed pAG_*BUD8*_NTGFP. Verification for a correct recombination was done by PCR using oligonucleotides Bud8-G1 x Bud8-I1.
The plasmid was then cut with XmaI and SacII and ligated into pRS415 cut with the same restriction enzymes. The resulting vectors were named pRS15_*BUD8*_NTGFP and transformed via electrophoresis into *A. gossypii* ∆*leu2* ∆*thr4*. The resulting strains carrying pRS15_*BUD8*_NTGFP did not show specific fluorescence.

Cloning of pRS415_*SEC4_RFP*

In order to investigate if AgBud7-GFP co-localize with secretory vesicles we constructed pRS415_*SEC4*_RFP. An amino-terminal fusion of *AgSEC4* to RFP was constructed by a sequential series of PCR amplification and cloning steps. The dsRFD module was amplified by PCR from pRS415_*SPC42* with primers redSEC4EcoRI and redSEC4BamHI. Obtained fragment had length of 672bps bps. Obtained PCR product was cut with EcoRI and BamHI and ligated into pRS415_*SEC4* cut with the same restriction enzymes. The resulting vectors were dubbed pRS415_*SEC4*_RFP and transformed via electrophoresis into *Agbud7*∆.

Oligonucleotides	Sequence
Rax2_S1	GAATACCGAGAGACATAGAGACATAACAAATAGGCGGACGGGACGgctagggataacagggtaatacagat
Rax2_S2	GCTTATTTTATACAATTTAATCACTTCCTATTTTCAGACCCCGTTaggcatgcaagcttagatctgatga
Rax2_G1	CATCAAGAACATTGCTATATTAT
Rax2_G4	CAAAGATACAATTTACAATAGTAC
Rax2_I1	GCATAAGTGGGCACCACGCGTCACAAGTAG
Rax2_I2	GTGGCCGAAGACGGCAAACAAGTGTGGCAC
ver G 2.1	CTCCAACTCGGCACTATTTTAC
ver G 3.2	TGCCTCCAGCATAGTCGAAG
Rax2_GFP_S1	GAAATGTTAAAGACAGTACCGCCAGAAAAGTTGATGAAATTTATTggtgcaggcgctggagctggc
Rax2_GFP_S2.1	ACAATTTACAATAGTACACTAATATAACAATATTTGATGCTACACagggacctggcacggagctcg
ver green 2.1	GCATCACCTTCACCCTCTCCAC
Rax2::clon_N1	GAATACCGAGAGACATAGAGACATAACAAATAGGCGGACGGGACGccagtgaattcgagctcgg
Rax2::clon_N1	GCTTATTTTATACAATTTAATCACTTCCTATTTTCAGACCCCGTTtacgccaagcttgcatgcct
Rax1_S1	CAAAGATATAGAGGGCGCACGAGCTGACAAGGAAAAGgctagggataacagggtaat
Rax1_S2	GACGAAGTTAGAAAGTCCGATAACATGTTTCCTGGGATGaggcatgcaagcttagatct
Rax1_I1	GGAGCGACTGGCCTTCTGTGATAGTGAAATG
Rax1_I2	GAGCGCAAACACAATTGTCGACCGCTACTTGG
Rax1_G1	CCTTGTGGCACCTCATCTCTCTTATCAATAGCGG
Rax1_G4	GGATAAGATGAGGAGATTTGCACTAATGGCACTCG
Rax1_clon_S1	CAAAGATATAGAGGGCGCACGAGCTGACAAGGAAAAGccagtgaattcgagctcgg
Rax1_clon_S2	GACGAAGTTAGAAAGTCCGATAACATGTTTCCTGGGATGtacgccaagcttgcatgcct
Bud10_clon_S1	GCTCTGTGCAGTAGCAGGTGTGTACTATTGCTACCAAGAACAGACccagtgaattcgagctcgg
Bud10_clon_S2	CTTTTAATTATGTATATAATATGCAGGGGACGCTGTGTGGACTAGtacgccaagcttgcatgcct
Bud10_ G1	CGGTCACGTGGCAATCCG
Bud10_ G4	GAGAGTGAAGCGCCAGAG
Bud10_I1	CTGGCGCCGCCGACAATC
Cdc24_clon_S1	CGAACGAGAGCAAAGAACAGCCACACAGTCAAGCGGGATAccagtgaattcgagctcgg
Cdc24_clon_S2	GTCGCTCCTACATAGTCTGCACATTTGTTAATACCTCTCCtacgccaagcttgcatgcct
Cdc24_G1	GATCACCCGAACACCGTGCATTTCCGTG
Cdc24_G4	GATATCGATTGGGTGGTGCCAGAAGGTAG
Cdc24-I1	CCTCGTCGTTGAACGCAAAATGCAGCTTC
Cdc24-I2	CAAAGGCGCACGGAGAATCATGAGGTGG
Cyk1_clon_S1	ACTCGAGTTGGCAGCTGGTAATTCAATGCGCGACGGCTATTTTTTccagtgaattcgagctcgg
Cyk1_clon_S2	CGCCTACCAAATCCATCAGCGAAAAAAAAGCATTAATATTCTGTGtacgccaagcttgcatgccT
Cyk1_G1	GAATTTCTCTGTAGAGTTGG
Cyk1_G4	TCTTTCTTCTCGTATAGGTC
bni1-11.2 C1	GGGGTTCAAGTTGAGTACATTGCAGAGGCTCACCTTCATTgagctcgttttcgacactgg
bni1-11.2 C2	GTTCCACGTAGTTCAAGAAAGTCATGCTGTTTTTCTCGTCtccttaccattaagttgatc
Bud7_S1	CTCGAAGTACCTGTCGACGAGCGGCAAAAACGGGTCACACATGCGGACGGGgctagggataacagggtaatacagat
Bud7_S2	GTATAGAGAGCACTATAGGTACATAATCTATGCAAAAAGGCTTAGAGATCGGaggcatgcaagcttagatctgatga
Bud7_G1	GGTCGTGGCCGGGCGCTGCTCCAGTTCAG
Bud7_G4	CCTCGTTTCCCCGCGCGGTATTCCCCAGA
Bud7_I1	CGTCGCCGATGTCGCTCGACGTGAACGGG
Bud7_I2	GCGTCGAGACAGAGTTCCTCTTGGAGCGC
Bud7GFP_S1	CAAATGTGCTTGACTTTTTCGCTGAACATACTCGTGGTGAGTACGACCAAggtgcaggcgctggagctggc
Bud7GFP_S2	CTGTAGATGAAGTTGACGTATAGAGAGCACTATAGGTACATAATCTATGCagggacctggcacggagctcg
Bud8/9_S1	CATCACACTCTTTTAAACACCGCAAACTCTAGACGCTGAACTATGgctagggataacagggtaatacagat
Bud8/9_S2	CCAGTGCTAAATTGCGGTAAGTACAGAATCGAAGCGCCACGATGCaggcatgcaagcttagatctgatga
Bud8/9_G1	GATACCGTAGGCGTATGCAGGGGATTCGCAGC
Bud8/9_G4	CTCAGGCCGCTGGCGATACGTGTTCGACCG
Bud8/9_I1	GCTGGTGCACAGGCACATGGGACTCAAGG
Bud8/9_I2	CGGCACGGTAGCCGCGACCTCAACGTGCAC
Bud8GFP_S1	GCGCTGATAGGCGTGGGCTTCGGCCTGGGCCTCGCCACAGAAggtgcaggcgctggagctggc
Bud8GFP_S2	CGACGGGCGGGCGAGCCGTAAACCCTGCCTGCAGGCGCGGCGagggacctggcacggagctcg

Table 1. Oligonucleotides used for the construction of the deletions and GFP fusions in *A.gossypii*.

Name	Genotype	Source
Wild type		ATCC10895
*Agleu2*Δ	*leu2 thr4a*	Altman-Johl and Philippsen
AKB 001	*Ag rax1::GEN3; RAX1*	This work
AKB 002	*Ag rax1::GEN3; RAX1*	This work
AKB 003	*Ag rax1::GEN3; RAX1*	This work
AKB 004	*Ag rax1::GEN3; RAX1*	This work
AKB 005	*Ag rax1::GEN3*	This work
AKB 006	*Ag rax1::GEN3*	This work
AKB 007	*Ag rax1::GEN3*	This work
AKB 008	*Ag rax1::GEN3*	This work
AKB 009	*Ag rax2::GEN3; RAX2*	This work
AKB 010	*Ag rax2::GEN3; RAX2*	This work
AKB 011	*Ag rax2::GEN3; RAX2*	This work
AKB 012	*Ag rax2::GEN3; RAX2*	This work
AKB 013	*Ag rax2::GEN3*	This work
AKB 014	*Ag rax2::GEN3*	This work
AKB 015	*Ag rax2::GEN3*	This work
AKB 016	*Ag rax2::GEN3*	This work
AKB 017	*Ag Rax2GFP::GEN3; RAX2*	This work
AKB 018	*Ag Rax2GFP::GEN3; RAX2*	This work
AKB 019	*Ag Rax2GFP::GEN3; RAX2*	This work
AKB 020	*Ag Rax2GFP::GEN3*	This work
AKB 021	*Ag Rax2GFP::GEN3*	This work
AKB 022	*Ag Rax2GFP::GEN3*	This work
AKB 023	*Ag Rax2GFP::GEN3, rax1::clonNat, RAX1*	This work
AKB 024	*Ag Rax2GFP::GEN3, rax1::clonNat, RAX1*	This work
AKB 025	*Ag Rax2GFP::GEN3, rax1::clonNat, RAX1*	This work
AKB 026	*Ag Rax2GFP::GEN3, rax1::clonNat*	This work
AKB 027	*Ag Rax2GFP::GEN3, rax1::clonNat*	This work
AKB 028	*Ag Rax2GFP::GEN3, rax1::clonNat*	This work
AKB 029	*Ag Rax2GFP::GEN3, bni1::clonNat, BNI1 myc*	This work
AKB 030	*Ag Rax2GFP::GEN3, bni1::clonNat, BNI1 myc*	This work
AKB 031	*Ag Rax2GFP::GEN3, bni1::clonNat, BNI1 myc*	This work
AKB 032	*Ag Rax2GFP::GEN3, bni1::clonNat, BNI1 myc*	This work
AKB 033	*Ag Rax2GFP::GEN3, bni1::clonNat, BNI1*	This work
AKB 034	*Ag Rax2GFP::GEN3, bni1::clonNat, BNI1*	This work
AKB 035	*Ag Rax2GFP::GEN3, cdc24::clonNat, CDC24 myc*	This work
AKB 036	*Ag Rax2GFP::GEN3, cdc24::clonNat, CDC24 myc*	This work
AKB 037	*Ag Rax2GFP::GEN3, cdc24::clonNat, CDC24 myc*	This work
AKB 038	*Ag Rax2GFP::GEN3, cdc24::clonNat, CDC24*	This work
AKB 039	*Ag Rax2GFP::GEN3, cdc24::clonNat, CDC24*	This work
AKB 040	*Ag Rax2GFP::GEN3, cdc24::clonNat, CDC24*	This work
AKB 041	*Ag Rax2GFP::GEN3, cyk1::clonNat, CYK1 myc*	This work
AKB 042	*Ag Rax2GFP::GEN3, cyk1::clonNat, CYK1 myc*	This work
AKB 043	*Ag Rax2GFP::GEN3, cyk1::clonNat, CYK1 myc*	This work
AKB 044	*Ag Rax2GFP::GEN3, cyk1::clonNat, CYK1*	This work
AKB 045	*Ag Rax2GFP::GEN3, cyk1::clonNat, CYK1*	This work
AKB 046	*Ag Rax2GFP::GEN3, cyk1::clonNat, CYK1*	This work
AKB 047	*Ag Rax2GFP::GEN3, bud10::clonNat, BUD10*	This work
AKB 048	*Ag Rax2GFP::GEN3, bud10::clonNat, BUD10*	This work
AKB 049	*Ag Rax2GFP::GEN3, bud10::clonNat, BUD10*	This work
AKB 050	*Ag Rax2GFP::GEN3, bud10::clonNat*	This work
AKB 051	*Ag Rax2GFP::GEN3, bud10::clonNat*	This work
AKB 052	*Ag Rax2GFP::GEN3, bud10::clonNat*	This work
AKB 053	*Ag rax2::GEN3, rax1::clonNAt, RAX1*	This work
AKB 054	*Ag rax2::GEN3, rax1::clonNAt, RAX1*	This work
AKB 055	*Ag rax2::GEN3, rax1::clonNAt, RAX1*	This work
AKB 056	*Ag rax2::GEN3, rax1::clonNAt*	This work
AKB 057	*Ag rax2::GEN3, rax1::clonNAt*	This work
AKB 058	*Ag rax2::GEN3, rax1::clonNAt*	This work
AKB 134	*Agrax1::GEN3, rax2::clonNat, 1A*	This work
AKB 135	*Agrax1::GEN3, rax2::clonNat, 2B*	This work
AKB 071	*Agrax1::GEN3, Ag Sep7GFP::clonNAT, SEP7 (SEP7 on plasmid)*	This work
AKB 072	*Agrax1::GEN3, Ag Sep7GFP::clonNAT, SEP7 (SEP7 on plasmid)*	This work
AKB 073	*Agrax1::GEN3, Ag Sep7GFP::clonNAT, SEP7 (SEP7 on plasmid)*	This work

AKB 074	*Agrax2::GEN3, Ag Sep7GFP::clonNAT, SEP7 (SEP7 on plasmid)*	This work
AKB 075	*Agrax2::GEN3, Ag Sep7GFP::clonNAT, SEP7 (SEP7 on plasmid)*	This work
AKB 076	*Agrax2::GEN3, Ag Sep7GFP::clonNAT, SEP7 (SEP7 on plasmid)*	This work
AKB 077	*Ag Spa2GFP::GEN3, rax1::clonNat, RAX1*	This work
AKB 078	*Ag Spa2GFP::GEN3, rax1::clonNat, RAX1*	This work
AKB 079	*Ag Spa2GFP::GEN3, rax1::clonNat, RAX1*	This work
AKB 080	*Ag Spa2GFP::GEN3, rax1::clonNat*	This work
AKB 081	*Ag Spa2GFP::GEN3, rax1::clonNat*	This work
AKB 082	*Ag Spa2GFP::GEN3, rax1::clonNat*	This work
AKB 083	*Ag Spa2GFP::GEN3, rax2::clonNat, RAX2*	This work
AKB 084	*Ag Spa2GFP::GEN3, rax2::clonNat, RAX2*	This work
AKB 085	*Ag Spa2GFP::GEN3, rax2::clonNat, RAX2*	This work
AKB 086	*Ag Spa2GFP::GEN3, rax2::clonNat*	This work
AKB 087	*Ag Spa2GFP::GEN3, rax2::clonNat*	This work
AKB 088	*Ag Spa2GFP::GEN3, rax2::clonNat*	This work
AKB 154	*Ag bud8::GEN3; BUD8*	This work
AKB 155	*Ag bud8::GEN3; BUD8*	This work
AKB 156	*Ag bud8::GEN3; BUD8*	This work
AKB 157	*Ag bud8::GEN3*	This work
AKB 158	*Ag bud8::GEN3*	This work
AKB 159	*Ag bud8::GEN3*	This work
AKB 160	*Ag Bud8GFP::GEN3, BUD8*	This work
AKB 161	*Ag Bud8GFP::GEN3, BUD8*	This work
AKB 162	*Ag Bud8GFP::GEN3, BUD8*	This work
AKB 163	*Ag Bud8GFP::GEN3*	This work
AKB 164	*Ag Bud8GFP::GEN3*	This work
AKB 165	*Ag Bud8GFP::GEN3*	This work
AKB 166	*Ag bud7::GEN3, BUD7*	This work
AKB 167	*Ag bud7::GEN3, BUD7*	This work
AKB 168	*Ag bud7::GEN3, BUD7*	This work
AKB 169	*Ag bud7::GEN3*	This work
AKB 170	*Ag bud7::GEN3*	This work
AKB 171	*Ag bud7::GEN3*	This work
AKB 172	*Bud7GFP::GEN3, BUD7*	This work
AKB 173	*Bud7GFP::GEN3, BUD7*	This work
AKB 174	*Bud7GFP::GEN3, BUD7*	This work
AKB 175	*Bud7GFP::GEN3*	This work
AKB 176	*Bud7GFP::GEN3*	This work
AKB 177	*Bud7GFP::GEN3*	This work
AKB 201	*Ag bud7::GEN3, myc*	T Gaffney
AKB 202	*Ag bud7::GEN3, myc*	T Gaffney
AKB 181	*Ag bud10::GEN3, rax2::clonNAt, RAX2*	This work
AKB 182	*Ag bud10::GEN3, rax2::clonNAt, RAX2*	This work
AKB 183	*Ag bud10::GEN3, rax2::clonNAt, RAX2*	This work
AKB 184	*Ag bud10::GEN3, rax2::clonNAt*	This work
AKB 185	*Ag bud10::GEN3, rax2::clonNAt*	This work
AKB 186	*Ag bud10::GEN3, rax2::clonNAt*	This work
AKB 187	*Ag bud10::GEN3, BUD10*	This work
AKB 188	*Ag bud10::GEN3, BUD10*	This work
AKB 189	*Ag bud10::GEN3, BUD10*	This work
AKB 190	*Ag bud10::GEN3*	This work
AKB 191	*Ag bud10::GEN3*	This work
AKB 192	*Ag bud10::GEN3*	This work
AKB 193	*Ag bud10::GEN3*	This work
AKB 196	*Ag spa2del C::GEN3*	P. Knechtle
AKB 197	*Ag spa2del C::GEN3*	P. Knechtle
AKB 203	*Ag Spa2::GEN3,rax1::clonNat, RAX1, myc*	This work
AKB 204	*Ag Spa2::GEN3,rax1::clonNat, RAX1, myc*	This work
AKB 205	*Ag Spa2::GEN3,rax1::clonNat, RAX1, myc*	This work
AKB 206	*Ag Spa2::GEN3,rax1::clonNat, RAX1*	This work
AKB 207	*Ag Spa2::GEN3,rax1::clonNat, RAX1*	This work
AKB 208	*Ag Spa2::GEN3,rax1::clonNat, RAX1*	This work
AKB 209	*Ag Spa2::GEN3,rax2::clonNat, RAX2, myc*	This work
AKB 210	*Ag Spa2::GEN3,rax2::clonNat, RAX2, myc*	This work
AKB 211	*Ag Spa2::GEN3,rax2::clonNat, RAX2, myc*	This work
AKB 212	*Ag Spa2::GEN3,rax2::clonNat, RAX2*	This work
AKB 213	*Ag Spa2::GEN3,rax2::clonNat, RAX2*	This work

AKB 214	*Ag Spa2::GEN3,rax2::clonNat, RAX2*	This work
AKB 218	*Ag del lt+prs415 Rax2GFP_delSP*	This work
AKB 219	*Ag del lt+prs415 Rax2GFP_delSP*	This work
AKB 220	*Ag del lt+prs415 Rax2GFP*	This work
AKB 221	*Ag del lt+prs415 Rax2GFP*	This work
AKB 222	*Ag del lt+prs415 Rax1 NTGFP*	This work
AKB 223	*Ag del lt+prs415 Rax1 NTGFP*	This work

Table 2. *A.gossypii* strains created for the purpose of these studies
For most of the constructs the *A.gossypii* wild type strain was used , however the genotype of the background strain should be verify again before use.

Oligonucleotides	**Sequence**
ScBUD7_his_S1	CCCTCAGATGATTACGCAGAATTCTATACCAGAGGTAAAAGcggatccccgggttaattaa
ScBUD7_his_S2	CGTATTAATGTCTTTTTATCGTATTTATGCATCGTAGCATCCgaattcgagctcgtttaaac
ScBUD7G1	GAGCATTGCCTTAAGATTCTGTCATGC
ScBUD7G4	AGGTCGTTGTGCACAATGAATTTCCCG
ScBUD7I1	CTCGCTGATGACCTCTGAAATCTCCTT
ScBUD7I2	CCGAACAACTGTACATGGATGCACAGA
ScYMR237W_kan_S1	AGAACGTGAAAAGGATAAACTGAAAACTTGAAGTCCTAACCcggatccccgggttaattaa
ScYMR237W_kan_S2	TTGTATTCATCTTTTTCTAATTATCGAAAGTGTCATTCGTGgaattcgagctcgtttaaac
ScYMR237WG1	GCGCTAGTCGTGTATCGTGATCATG
ScYMR237WG4	GTTTCGCTTTACGCGGATTACATTG
ScYMR237WI1	TACCAAACCAAATTTGGGGCGTGTC
ScYMR237WI2	AGGAGGGATTCAGTCTCAGCAAACT

Table 3. Oligonucleotides used to create the *S.cerevisiae* mutants

Name		Genotype	Source
YEF473	a/α	*trp-Δ3/ trp-Δ3, leu2-Δ1/ leu2-Δ1, ura3-52/ ura3-52, his3-Δ200/ his3-Δ200,lys2-801/ lys2-801*	Provided by L.Schenkman
YEF473 A	a	*trp-Δ3, leu2-Δ1, ura3-52, his3-Δ200, lys2-801*	Provided by L.Schenkman
YEF473 B	α	*trp-Δ3, leu2-Δ1, ura3-52, his3-Δ200, lys2-801*	Provided by L.Schenkman
HH391	a	*trp-Δ3, leu2-Δ1, ura3-52, his3-Δ200, lys2-801, bud8-Δ::TRP1*	Provided by L.Schenkman
HH399	α	*trp-Δ3, leu2-Δ1, ura3-52, his3-Δ200, lys2-801, bud8-Δ::TRP1*	Provided by L.Schenkman
HH615	a/α	*trp-Δ3/ trp-Δ3, leu2-Δ1/ leu2-Δ1, ura3-52/ ura3-52, his3-Δ200/ his3-Δ200,lys2-801/ lys2-801, bud8-Δ::TRP1/ bud8-Δ::TRP1*	Provided by L.Schenkman
HH613	a	*trp-Δ3, leu2-Δ1, ura3-52, his3-Δ200, lys2-801, bud9-Δ::HIS3*	Provided by L.Schenkman
HH614	α	*trp-Δ3, leu2-Δ1, ura3-52, his3-Δ200, lys2-801, bud9-Δ::HIS3*	Provided by L.Schenkman
HH615	a/α	*trp-Δ3/ trp-Δ3, leu2-Δ1/ leu2-Δ1, ura3-52/ ura3-52, his3-Δ200/ his3-Δ200,lys2-801/ lys2-801, bud9-Δ::HIS3/ bud9-Δ::HIS3*	Provided by L.Schenkman
AM365	α	*trp-Δ3, leu2-Δ1, ura3-52, his3-Δ200, lys2-801, rax1-Δ::KAN*	Provided by L.Schenkman
AM366	a	*trp-Δ3, leu2-Δ1, ura3-52, his3-Δ200, lys2-801, rax1-Δ::KAN*	Provided by L.Schenkman
AM377	a/α	*trp-Δ3/ trp-Δ3, leu2-Δ1/ leu2-Δ1, ura3-52/ ura3-52, his3-Δ200/ his3-Δ200,lys2-801/ lys2-801, rax1-Δ::KAN/ rax1-Δ::KAN*	Provided by L.Schenkman
AM474	a	*trp-Δ3, leu2-Δ1, ura3-52, his3-Δ200, lys2-801, rax2-Δ::HIS3*	Provided by L.Schenkman
AM475	α	*trp-Δ3, leu2-Δ1, ura3-52, his3-Δ200, lys2-801, rax2-Δ::HIS3*	Provided by L.Schenkman
AM476	a/α	*trp-Δ3/ trp-Δ3, leu2-Δ1/ leu2-Δ1, ura3-52/ ura3-52, his3-Δ200/ his3-Δ200,lys2-801/ lys2-801, rax2-Δ::HIS3/ rax2-Δ::HIS3*	Provided by L.Schenkman
KB001	a	*trp-Δ3, leu2-Δ1, ura3-52, his3-Δ200, lys2-801, bud7-Δ::HIS3*	This work
KB002	α	*trp-Δ3, leu2-Δ1, ura3-52, his3-Δ200, lys2-801, bud7-Δ::HIS3*	This work
KB003	a/α	*trp-Δ3/ trp-Δ3, leu2-Δ1/ leu2-Δ1, ura3-52/ ura3-52, his3-Δ200/ his3-Δ200,lys2-801/ lys2-801, bud7-Δ::HIS3/ bud7-Δ::HIS3*	This work
KB004	a	*trp-Δ3, leu2-Δ1, ura3-52, his3-Δ200, lys2-801, bch1-Δ::KAN*	This work
KB005	α	*trp-Δ3, leu2-Δ1, ura3-52, his3-Δ200, lys2-801, bch1-Δ::KAN*	This work
KB006	a/α	*trp-Δ3/ trp-Δ3, leu2-Δ1/ leu2-Δ1, ura3-52/ ura3-52, his3-Δ200/ his3-Δ200,lys2-801/ lys2-801, bch1-Δ::KAN/ bch1-Δ::KAN*	This work
KB007	a	*trp-Δ3, leu2-Δ1, ura3-52, his3-Δ200, lys2-801, bch1-Δ::KAN, bud7-Δ::HIS3*	This work
KB008	α	*trp-Δ3, leu2-Δ1, ura3-52, his3-Δ200, lys2-801, bch1-Δ::KAN, bud7-Δ::HIS3*	This work
KB008	a/α	*trp-Δ3/ trp-Δ3, leu2-Δ1/ leu2-Δ1, ura3-52/ ura3-52, his3-Δ200/ his3-Δ200,lys2-801/ lys2-801, bch1-Δ::KAN/ bch1-Δ::KAN,, bud7-Δ::HIS3/ bud7-Δ::HIS3*	This work

Table 4. *S.cerevisiae* strains used in these studies

Oligonucleotides	Sequence
Rax1vectorS1bamHI	gacgcggatccGCAGGACGAGCAGGCGTCCGGGGACTCCAGC
Rax1vector_S2psiI	TGTGTGAATTGGTGTGCTTGACAGAAGGATAAGATG
Rax1NtGFP_S1	CAAAGATATAGAGGGCGCACGAGCTGACAAGGAAAAGGGCAtccttaccattaagttgatc
Rax1NtGFP_S2	CGGTAGCCGCTCCGACTGCAACCTCCATTCTTCTGTCTCCATgagctcgttttcgacactgg
Rax1NtGFP_S3	CAGCAAAGCACCAGACGAGCAAAGATATAGAGGGCGCACGAGCTGACAAGGAAAAGGGCAagtaaaggagaagaacttttcactggag
Rax1NtGFP_S4	GTTATTCAACACTTCGAACAACGTCGGTAGCCGCTCCGACTGCAACCTCCATTCTTCTGTCTCctatttgtatagttcatccatg
Rax2 vector _S1	CGGGGCATCTTTGCGCAACCCCTGCTACGC
Rax2 vector _S2	ccgccgggatccTGGTAGTTCACGAGGAAAC
Rax2signalling_S1	GAGAGACATAGAGACATAACAAATAGGCGGACGGGACGATGgagctcgttttcgacactgg
Rax2signalling_S2	GGGACCCTCGTACAACGTCCCCGAGCGGCGCAAGTGCCGCtccttaccattaagttgatc
Rax2_I1	GAAGTAAACCATGTCGCCGTCG (for sequencing)
Rax2_overlap_S1	CTGCTTAAAGTGTGCTGCCAGAGTCTACCCGAGAATACCGAGAGACATAGAGACATAACAAATAGGCGGACGGGACGATG
Rax2_overlap_S2	CTGCGCCACGCTCTCCAGATGGGACCCTCGTACAACGTCCCCGAGCGGCGCAAGTGCCGCCATCGTCCCGTCCGCCTATTTG
Rax2GFP_S1	GAAATGTTAAAGACAGTACCGCCAGAAAAGTTGATGAAATTTATTggtgcaggcgctggagctggc
Rax2GFP_S2	ACAATTTACAATAGTACACTAATATAACAATATTTGATGCTACACagggacctggcacggagctcg
Bud7vector_S1notI	CTGGCCGATGACCGTGTTGGTGTCCCAGTCCGATG
Bud7vectorS2bamHI	ccgccgggatccGGATAAACCCTGCTATGCTAAGCAATGGAAG
Bud8NtGFP_S1	CACACTCTTTTAAACACCGCAAACTCTAGACGCTGAACTtccttaccattaagttgatc
Bud8NtGFP_S2	GGCTATCCTGCTGGTCTAACAGTGACCTTATGTACGACATgagctcgttttcgacactgg
Bud8NtGFP_S3	CAAAATCCTCGAACCTTCCAACATCACACTCTTTTAAACACCGCAAACTCTAGACGCTGAACTagtaaaggagaagaacttttcactggag
Bud8NtGFP_S4	GTTTCAGGGTCAGTAGAGTCTTCTTGGCTATCCTGCTGGTCTAACAGTGACCTTATGTACGActatttgtatagttcatccatg
RedSEC4EcoRI	CCCGCTGGACGACGACACCGTTCTTAGCCCCGAGAATTCCAAGAACAAGTGGTGTCTAC
RedSEC4BamHI	TGACATAGTTGCCACGCAGCAGTACAGTAGCTATAATGGGATCCAGTGCTTCTTCTGAA

Table 5. Oligonucleotides used for cloning

Name	Comments
pRS415RAX1	This work
pRS415RAX1_NTGFP	This work
pRS415RAX2	This work
pRS415RAX2_CTGFP	This work
pRS415RAX2_deltaSP	This work
pRS415RAX2_deltaSP_GFP	This work
pRS415BUD7	Unfinished
pAgBUD8	This work
pAgBUD8_CTGFP	This work
pAgBUD8_NTGFP	This work
pRS415BUD8_NTGFP	This work
PHPS236 (PRS415_SEC4GFP)	Provided by H-P Schmitz
pAgRedStarGEN	Provided by A.GLatfelter
pRS415SEC4_RFP	This work
pGUG	Prof. P.Philippsen lab colection
PUCC19NATPS	Prof. P.Philippsen lab colection
PGEN3	Prof. P.Philippsen lab colection
PLEU2	Prof. P.Philippsen lab colection
pGUG	Prof. P.Philippsen lab colection
PFA6a-HIS3MX6	Wach *et al*; used for the deletion in *S.cerevisiae*
PFA6a-KANMX	Wach *et al*; used for the deletion in *S.cerevisiae*
PRS415_SEP7GFP	Provided by H-P. Helfer

Table 6. Plasmids used in these studies.

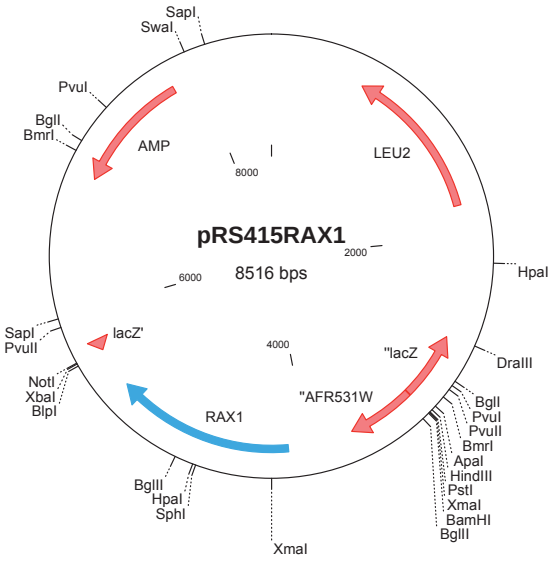
pRS415RAX1
8516 bps
AMP
LEU2
lacZ'
"lacZ
"AFR531W
RAX1
SapI
SwaI
PvuI
BglII
BmrI
HpaI
DraIII
NotI
XbaI
BlpI
BglII
HpaI
SphI
XmaI
BglI
PvuI
PvuII
BmrI
ApaI
HindIII
PstI
XmaI
BamHI
BglII

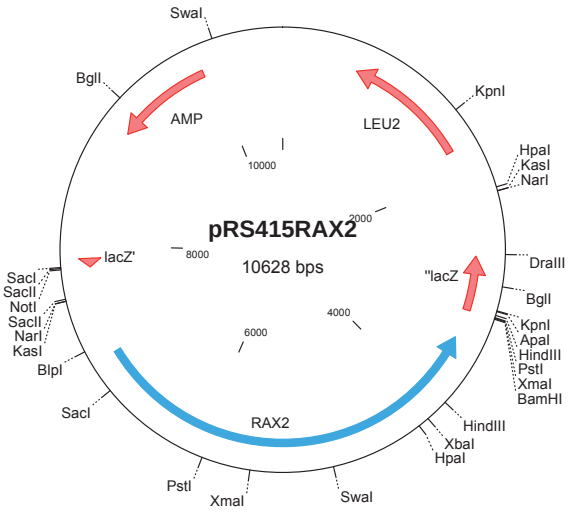
pRS415RAX2
10628 bps
AMP
LEU2
lacZ'
"lacZ
RAX2
SwaI
BglI
KpnI
HpaI
KasI
NarI
DraIII
BglI
KpnI
ApaI
HindIII
PstI
XmaI
BamHI
HindIII
XbaI
HpaI
SwaI
XmaI
PstI
SacI
BlpI
NarI
KasI
SacII
NotI

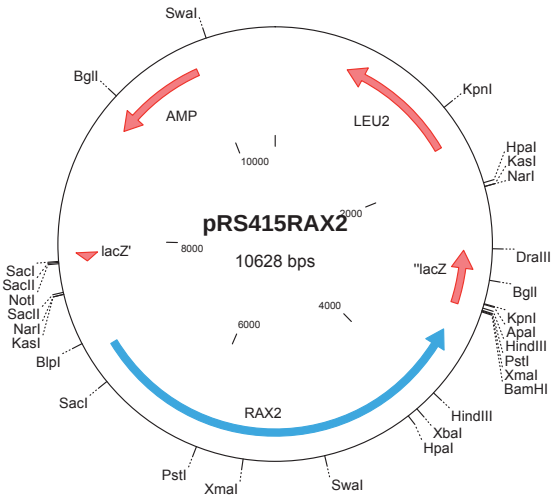
pRS415RAX2
10628 bps
AMP
LEU2
lacZ'
"lacZ
RAX2
SwaI
BglI
KpnI
HpaI
KasI
NarI
DraIII
BglI
KpnI
ApaI
HindIII
PstI
XmaI
BamHI
HindIII
XbaI
HpaI
SwaI
XmaI
PstI
SacI
BlpI
NarI
KasI
SacII
NotI
SacII

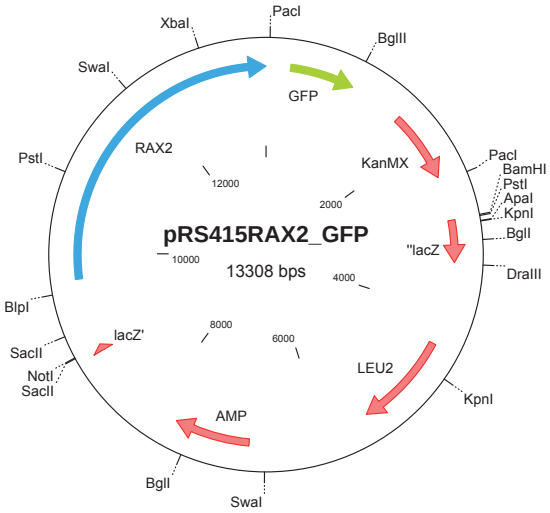
pRS415RAX2_GFP
13308 bps
GFP
KanMX
LEU2
AMP
lacZ'
"lacZ
RAX2
XbaI
PacI
BglII
SwaI
PstI
BamHI
PstI
ApaI
KpnI
BglI
DraIII
BglII
SwaI
BglI
AMP
KpnI
BlpI
SacII
NotI
SacII

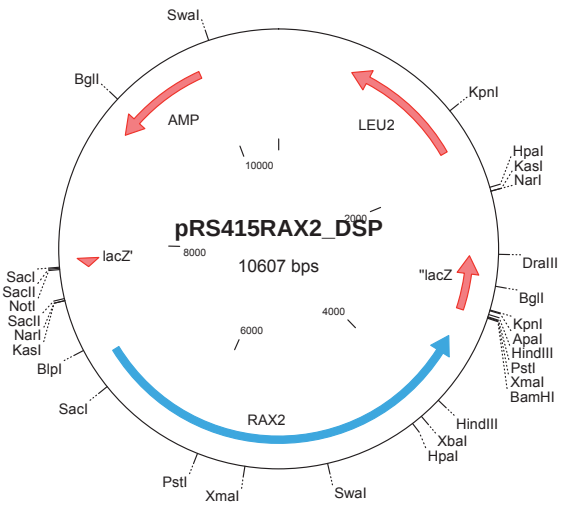
pRS415RAX2_DSP
10607 bps
AMP
LEU2
lacZ'
"lacZ
RAX2
SwaI
BglI
KpnI
HpaI
KasI
NarI
DraIII
BglI
KpnI
ApaI
HindIII
PstI
XmaI
BamHI
HindIII
XbaI
HpaI
SwaI
XmaI
PstI
SacI
BlpI
NarI
KasI
SacII
NotI
SacII

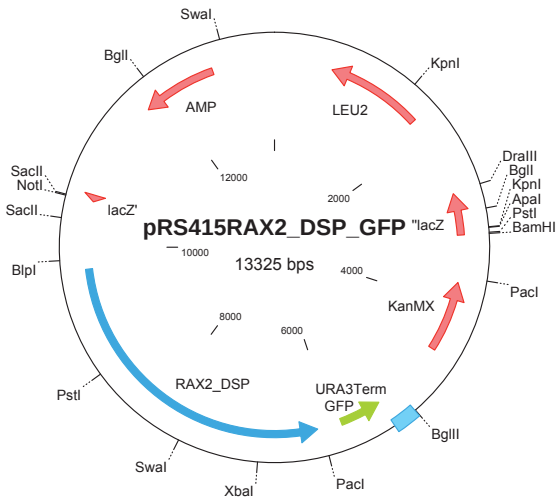
pRS415RAX2_DSP_GFP
13325 bps
AMP
LEU2
lacZ'
"lacZ
KanMX
RAX2_DSP
URA3Term
GFP
SwaI
BglI
KpnI
DraIII
BglI
KpnI
ApaI
PstI
BamHI
PacI
BglII
PacI
XbaI
SwaI
PstI
BlpI
SacII
NotI
SacII

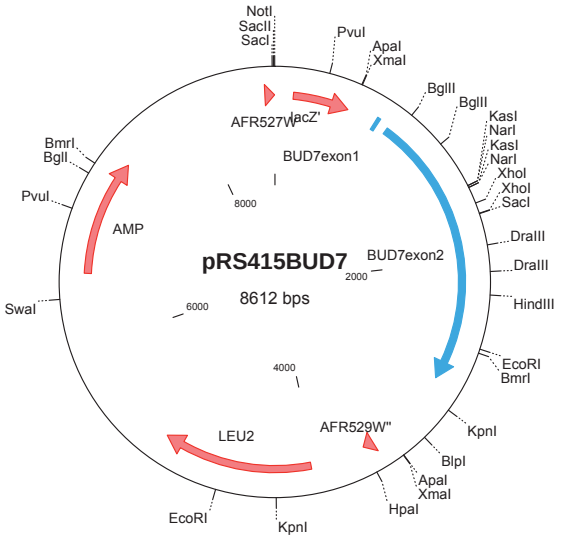
pRS415BUD7
8612 bps
BUD7exon1
BUD7exon2
AFR527W
lacZ'
AMP
LEU2
AFR529W"
NotI
SacII
SacI
PvuI
ApaI
XmaI
BglII
KasI
NarI
XhoI
DraIII
HindIII
EcoRI
BmrI
KpnI
BlpI
HpaI
BglI
SwaI

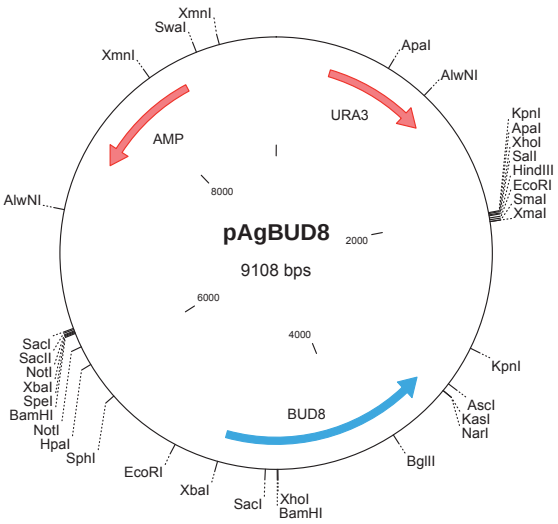
pAgBUD8
9108 bps
URA3
AMP
BUD8
AlwNI
XmnI
SwaI
ApaI
KpnI
XhoI
SalI
HindIII
EcoRI
SmaI
XmaI
SacI
SacII
NotI
XbaI
SpeI
BamHI
HpaI
SphI
EcoRI
XbaI
SacI
XhoI
BamHI
AscI
NarI
BglII

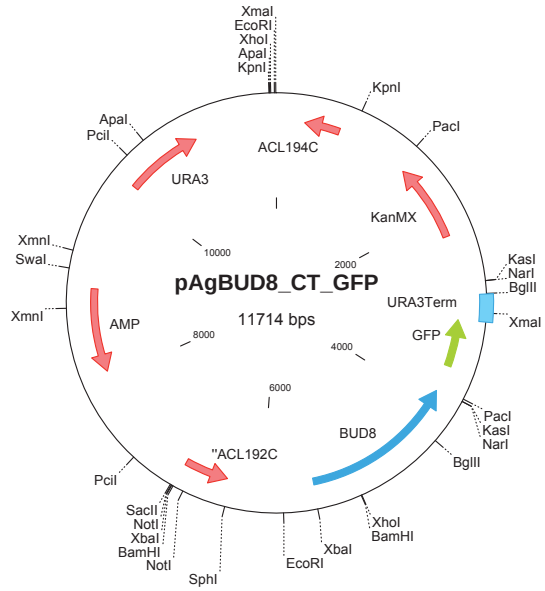
pAgBUD8_CT_GFP
11714 bps
ACL194C
URA3
KanMX
URA3Term
GFP
BUD8
"ACL192C
AMP
XmaI
EcoRI
XhoI
ApaI
KpnI
PacI
PciI
KasI
NarI
BglII
SacII
NotI
XbaI
BamHI
SphI

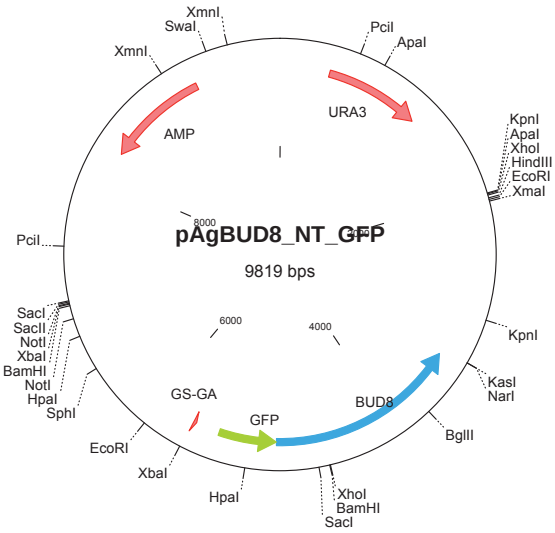
pAgBUD8_NT_GFP
9819 bps
URA3
AMP
GS-GA
GFP
BUD8
XmnI
SwaI
PciI
ApaI
KpnI
XhoI
HindIII
EcoRI
XmaI
SacI
SacII
NotI
XbaI
BamHI
HpaI
SphI
EcoRI
XbaI
XhoI
BamHI
SacI
KasI
NarI
BglII

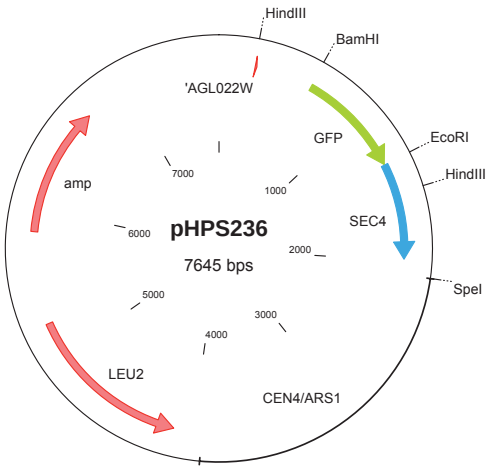
pHPS236
7645 bps
'AGL022W
GFP
SEC4
LEU2
CEN4/ARS1
amp
HindIII
BamHI
EcoRI
HindIII
SpeI

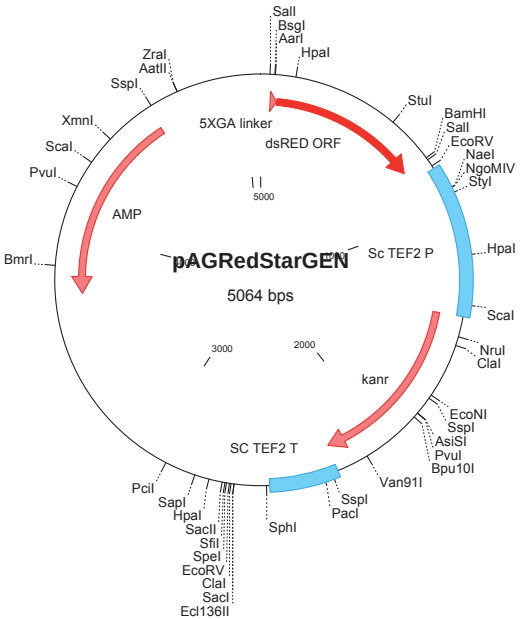
pAGRedStarGEN
5064 bps
5XGA linker
dsRED ORF
Sc TEF2 P
kanr
SC TEF2 T
AMP
SalI
BsgI
AarI
HpaI
ZraI
AatII
SspI
XmnI
ScaI
PvuI
BmrI
StuI
BamHI
SalI
EcoRV
NaeI
NgoMIV
StyI
HpaI
ScaI
NruI
ClaI
EcoNI
SspI
AsiSI
PvuI
Bpu10I
Van91I
SspI
PacI
SphI
PciI
SapI
HpaI
SacII
SfiI
SpeI
EcoRV
ClaI
SacI
Ecl136II

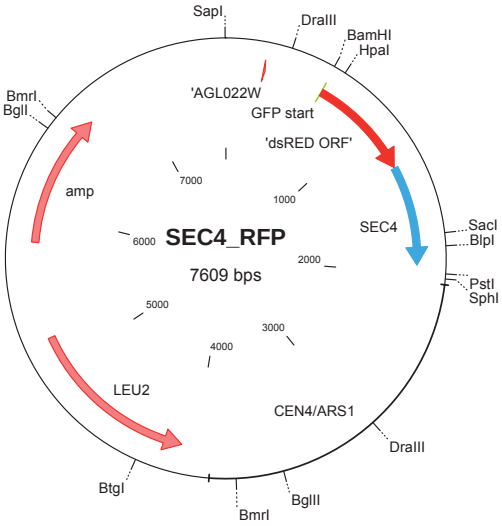
SapI
DraIII
BamHI
HpaI
BmrI
BglI
'AGL022W
GFP start
'dsRED ORF'
7000
1000
amp
SEC4_RFP
6000
SEC4
2000
SacI
BlpI
7609 bps
PstI
SphI
5000
3000
4000
LEU2
CEN4/ARS1
DraIII
BtgI
BmrI
BglII

Name:	**Kamila Dorota Boudier (born: Wojnowska)**
Nationality:	Polish
Marital status:	married
Date of birth/ place:	Dec. 29th 1976 in Gdynia/ Poland

Education

July 2005 - Oct. 2005	**Postdoctoral fellowship** in Molecular Microbiology with Prof. P. Philippsen Department of Applied Microbiology University of Basel, Switzerland
June 27th 2005	**PhD thesis in Microbiology**
June 2001 - June 2005	PhD with Prof. P. Philippsen Department of Applied Microbiology University of Basel, Switzerland
Oct. 2000 - Feb. 2001	First semester of 4 semesters **"Post-Graduate Studies in Management and Marketing"** Department of Management and Economics Gdansk University of Technology, Poland
June 28th 2000	**Master of Science/ Engineer Degree in Biotechnology**
Feb. 2000 - June 2000	Diploma thesis with Prof. S. Milewski Department of Pharmaceutical Technology and Biochemistry Gdansk University of Technology, Poland
Oct. 1995 - June 2000	5-year studies, field: Biotechnology Gdansk University of Technology, Poland
May 22nd 1995	**High School Diploma** (Matura exam)
Sept. 1991 - May 1995	Liceum VIII, Gdynia, Poland

Professional Experience

- **Teaching assistant** in undergraduate Microbiology Course for students of the European Biotechnology University Program („Ecole Supérieure de Biotechnologie de Strasbourg")
  Biozentrum, University of Basel, Switzerland
  September (2001, 2002, 2003, 2004); March (2002, 2003, 2004, 2005)

- **Instructor** in Summer Microbiology Course for students of the European Biotechnology University Program („Ecole Supérieure de Biotechnologie de Strasbourg")
  Biozentrum, University of Basel, Switzerland
  July-August 2004

- **PhD thesis** in Prof. P. Philippsen´s lab, University of Basel, Switzerland
  "The role of AgRax1p, AgRax2p, AgBud7p and AgBud10p in mycelial development of the filamentous fungus *Ashbya gossypii*"

- **Diploma thesis** in Prof. S. Milewski´s lab, Gdansk University of Technology, Poland
  "Investigation of the active center structure of glucosamine-6-phosphate (GlcN-6-P) synthase isolated from *S.cerevisiae"*

- **Bioprocess Project** with Prof. J. Hupka, Gdansk University of Technology, Poland
  "Collagenase production"

Publications

- Boudier K., Schmitz H. P., Philippsen P. "AgRax1p and AgRax2p are involved in controlling of branching pattern in filamentous fungus *A.gossypii*" (manuscript in preparation)
- Boudier K., Schmitz H. P., Philippsen P. "AgBud7p is involved in the maintaining of the sustained polar growth" (manuscript in preparation)

Conferences & Meetings

- **Swiss Yeast Meeting, Basel, Switzerland, Sept. 2006.**
  Poster presentation: "Homologues of *S.cerevisiae* proteins involved in the bipolar budding pattern are implicated in the morphogenesis of the filamentous fungus *A. gossypii*"

- **7th European Conference on Fungal Genetics, Copenhagen, Denmark, Apr. 2004.**
  Poster presentation: "*Ashbya gossypii* homologues of *S.cerevisiae* bud genes influence branching pattern and possibly septum biogenesis"

- **Swiss Yeast Meeting, Zurich, Switzerland, Sept. 2002.**
  Poster presentation: "AgRax1p and AgRax2p are involved in tip growth and septum formation in the filamentous fungus *Ashbya gossypii"*

- **6th European Conference on Fungal Genetics, Pisa, Italy, Apr. 2002.**
  Poster presentation: "AgRax1p and AgRax2p proteins are important for the mode of branching and growth in the filamentous fungus *Ashbya gossypii"*

- **Swiss Yeast Meeting, Geneva, Switzerland, Sept. 2001.**

Additional gene analyses

Strain number	**AKB 095-100**
Corresponding genotype	*AgCDC24-GFP::GEN3, Agrax2Δ1::clonNat,*
Primer S1	GAATACCGAGAGACATAGAGACATAACAAATAGGCGGACGGGACGccagtgaattcgagctcgg
Primer S2	GCTTATTTTATACAATTTAATCACTTCCTATTTTCAGACCCCGTTtacgccaagcttgcatgcct
Primer G1	CATCAAGAACATTGCTATATTAT
Primer G4	CAAAGATACAATTTACAATAGTAC
Marker	clonNat
Basic phenotype analysis	
Growth of deletion mutant on AFM at 30°C	As describe in this work
Chitin staining (Calcofluor)	As describe in this work
Actin staining (Rhodamine-Phalloidin)	As describe in this work
Comments	Localization of AgCdc24-GFP not changed in this mutant

Strain number	**AKB 089-094**
Corresponding genotype	*AgCDC24-GFP::GEN3, Agrax1Δ1::clonNat,*
Primer S1	CAAAGATATAGAGGGCGCACGAGCTGACAAGGAAAAGccagtgaattcgagctcgg
Primer S2	GACGAAGTTAGAAAGTCCGATAACATGTTTCCTGGGATGtacgccaagcttgcatgcct
Primer G1	CCTTGTGGCACCTCATCTCTCTTATCAATAGCGG
Primer G4	GGATAAGATGAGGAGATTTGCACTAATGGCACTCG
Marker	clonNat
Basic phenotype analysis	
Growth of deletion mutant on AFM at 30°C	As describe in this work
Chitin staining (Calcofluor)	As describe in this work
Actin staining (Rhodamine-Phalloidin)	As describe in this work
Comments	Localization of AgCdc24-GFP not changed in this mutant

Strain number	**AKB101-103**
Corresponding genotype	*AgSPA2-GFP::GEN3, Agrax1Δ1::clonNat, Agrax2Δ1::LEU2, leu2, thr4*
Primer S1	GAATACCGAGAGACATAGAGACATAACAAATAGGCGGACGGGACGccagtgaattcgagctcgg
Primer S2	GCTTATTTTATACAATTTAATCACTTCCTATTTTCAGACCCCGTTtacgccaagcttgcatgcct
Primer G1	CATCAAGAACATTGCTATATTAT
Primer G4	CAAAGATACAATTTACAATAGTAC
Marker	*LEU2*
Basic phenotype analysis	
Growth of deletion mutant on AFM at 30°C	
Chitin staining (Calcofluor)	
Actin staining (Rhodamine-Phalloidin)	
Comments	Unfinished

Strain number	**AKB 104-106**
Corresponding genotype	*AgRAX2-GFP::GEN3, Agbud3Δ1::clonNat,*
Primer S1	GTCACGGCCATATCAGATTTCAACGACGGGTAGTTGACTGAGCTccagtgaattcgagctcgg
Primer S2	GATAACTGGCTTACGGTGTAATATTAGTTGAGTATAATTATGATtacgccaagcttgcatgcct

Primer G1	CGACTAGAACGTTGGTATGCGTG
Primer G4	CATGGCATCGCGCCTGATGGTATG
Marker	*clonNat*

Basic phenotype analysis
Growth of deletion mutant on AFM at 30°C
Chitin staining (Calcofluor)
Actin staining (Rhodamine-Phalloidin)

Comments Unfinished

Strain number *AKB 107-109*

Corresponding genotype	*AgRAX2-GFP::GEN3, Agbud8Δ1::clonNat,*
Primer N1	CAACATCACACTCTTTTAAACACCGCAAACTCTAGACGCTGAACTCCAGTGAATTCGAGCTCGG
Primer N2	CCAGTGCTAAATTGCGGTAAGTACAGAATCGAAGCGCCACGATGTACGCCAAGCTTGCATGCCT
Primer G1	GATACCGTAGGCGTATGCAGGGGATTCGCAGC
Primer G4	CTCAGGCCGCTGGCGATACGTGTTCGACCG
Marker	*clonNat*

Basic phenotype analysis

Growth of deletion mutant on AFM at 30°C	Slower than the WT
Chitin staining (Calcofluor)	Indicates similar size of compartments for the hyphae of different age
Actin staining (Rhodamine-Phalloidin)	Wild type like
Comments	Finished

Strain number **AKB 110-115**

Corresponding genotype	*AgRAX2-GFP::GEN3, Agaxl1Δ1::clonNat,*
Primer S1	TTTAAGATAGCCAGTTTTCAAGTGCGAGCGTAGGCCTTCAGGCAAGCccagtgaattcgagctcgg
Primer S2	CAACTTCAGATTCTGAAGGGTTCTAGCATCTACGGGCTCATCGTCtacgccaagcttgcatgcct
Primer G1	GTAGAGTAACACATAACAAATTCCTCCCGG
Primer G4	GACTTGCTCTAAGGTTATCGCCGGAGTAAC
Marker	*clonNat*

Basic phenotype analysis

Growth of deletion mutant on AFM at 30°C	Wild type like
Chitin staining (Calcofluor)	Wild type like
Actin staining (Rhodamine-Phalloidin)	Wild type like
Comments	Finished

Strain number **AKB 116-121**

Corresponding genotype	*Agaxl1Δ1::GEN3, leu2,thr4*
Primer S1	TTTAAGATAGCCAGTTTTCAAGTGCGAGCGTAGGCCTTCAGGCAAGCgctagggataacagggtaatacagat
Primer S2	CAACTTCAGATTCTGAAGGGTTCTAGCATCTACGGGCTCATCGTCaggcatgcaagcttagatctgatga
Primer G1	GTAGAGTAACACATAACAAATTCCTCCCGG
Primer G4	GACTTGCTCTAAGGTTATCGCCGGAGTAAC
Marker	*GEN3*

Basic phenotype analysis

Growth of deletion mutant on AFM at 30°C	Wild type like
Chitin staining (Calcofluor)	Wild type like
Actin staining (Rhodamine-Phalloidin)	Wild type like
Comments	Finished

Strain number	**AKB 122-127**
Corresponding genotype	*Agbud4Δ1::GEN3, leu2,thr4*
Primer S1	CAGTGGAGCAGCCAGAGCCAGGCGACAGAGCTGAGTGAAGGCTAGgctagggataacagggtaatacagat
Primer S2	CTTTGCACAAAAGTTACTCTATGTAATCCTGTGGTCATGCTTTTCTaggcatgcaagcttagatctgatga
Primer G1	GTGCAGGCAAAATGCTCGAGAAGGCC
Primer G4	GCCTGCGTTTCCCATGGGTATGCCA
Marker	*GEN3*
Basic phenotype analysis	
Growth of deletion mutant on AFM at 30°C	Wild type like
Chitin staining (Calcofluor)	Wild type like
Actin staining (Rhodamine-Phalloidin)	Wild type like
Comments	Finished

Strain number	**AKB 128**
Corresponding genotype	*AgBUD10-GFP::GEN3, leu2,thr4*
Primer S1	GTTAACGTGAGCGATGCAAGTCTCATCGGCCAGGAGCCGGAGCGCGACggtgcaggcgctggagctggc
Primer S2	ATATTGTCTTTTAATTATGTATATAATATGCAGGGGACGCTGTGTGGAagggacctggcacggagctcg
Primer G4	GGACGACTTTCTGTCGTGTCCTGGC
Primer I2	GCAAACCGATCTCCGACGCCTCTAC
Marker	*GEN3*
Basic phenotype analysis	
Growth of deletion mutant on AFM at 30°C	
Chitin staining (Calcofluor)	
Actin staining (Rhodamine-Phalloidin)	
Comments	Unfinished

Strain number	**AKB 130-131**
Corresponding genotype	*AgBUD2-GFP::GEN3,BUD2 leu2,thr4*
Primer S1	CACCCGCAAGAAATACGAAACTTTCAAGATGGTTTAAAAAGGTCTCCTTCggtgcaggcgctggagctggc
Primer S2	ATAAATTATTACATATATATTTCAAGGGAGGACTTTGGCATCCTTCAAGGagggacctggcacggagctcg
Primer G4	GTACCGGCACAGCTCAATTCAAGGC
Primer I2	GCGTATACTACGATTCCCAGCGATC
Marker	*GEN3*
Basic phenotype analysis	
Growth of deletion mutant on AFM at 30°C	Wild type like
Chitin staining (Calcofluor)	Wild type like
Actin staining (Rhodamine-Phalloidin)	Wild type like
Comments	Finished, not functional

Strain number	**AKB 136-138**
Corresponding genotype	*AgRAX2-CFP, leu2,thr4*
Primer S1	GAAATGTTAAAGACAGTACCGCCAGAAAAGTTGATGAAATTTATTcggatccccgggttaattaa
Primer S2	GCTACACTTTCTAGTTTGCTTATTTTATACAATTTAATCACTTCCagggacctggcacggagc
Primer G4	CAAAGATACAATTTACAATAGTAC
Primer I2	GTGGCCGAAGACGGCAAACAAGTGTGGCAC

Marker	*GEN3*
Basic phenotype analysis	
Growth of deletion mutant on AFM at 30°C	Wild type like
Chitin staining (Calcofluor)	Wild type like
Actin staining (Rhodamine-Phalloidin)	Wild type like
Comments	Finished

Strain number	**AKB 139-144**
Corresponding genotype	*Agade2∆1::gen3,Aggal4 ∆1::clonNAT, leu2,thr4*
Primer S1	TTGGAACTCGAAAAGACGACACGCGGGCGGCGGCGGGGACACGGGccagtgaattcgagctcgg
Primer S2	CCAGCGGCGGAGGCTCGACGGAGCCGATACAAGGCGAGTGGCTACtacgccaagcttgcatgcct
Primer G1	CGTTACGGAGGAGCAGAGTTGCAGG
Primer G4	CTGATCTTCGCGCCCGCTTCTACC
Marker	*clonNAT*
Basic phenotype analysis	
Growth of deletion mutant on AFM at 30°C	Wild type like
Chitin staining (Calcofluor)	Wild type like
Actin staining (Rhodamine-Phalloidin)	Wild type like
Comments	Finished

Strain number	**AKB 145-150**
Corresponding genotype	*Agade2∆1::GEN33, Aggal4 ∆1::clonNAT, Aghis3::LEU2, leu2,thr4*
Primer S1	CGACCATCATACGACAGAAGACTGTGGTCTAGCCCTTGGTCAGGCgctagggataacagggtaat
Primer S2	AGATATAATGCTCAAATAAATATAAATTGTCGACTCACAGCGCTCaggcatgcaagcttagatct
Primer G1	CGCACGAAGTACTCGCGCCTGTTGC
Primer G4	GCGGCTCTGCGTCCTGCATTCAAG
Marker	*LEU2*
Basic phenotype analysis	
Growth of deletion mutant on AFM at 30°C	Slow
Chitin staining (Calcofluor)	Wild type like
Actin staining (Rhodamine-Phalloidin)	Wild type like
Comments	Finished

Strain number	**AKB 151-153**
Corresponding genotype	*AgBUD5-GFP:: GEN3,BUD5 leu2,thr4*
Primer S1	GAGCGTATAACTTGAGTACCGGCTTGAAACCTGCGACAAACggtgcaggcgctggagctggc
Primer S2	GTCCGCTAACGATTATAGCAAAACCGGAGAAATACATAGCTAagggacctggcacggagctcg
Primer G1	CTACCAGGGCTAACTAATAGCGTACA
Primer G4	CACACAATGTCAGAAATACAAGTAG
Marker	*GEN3*
Basic phenotype analysis	
Growth of deletion mutant on AFM at 30°C	
Chitin staining (Calcofluor)	
Actin staining (Rhodamine-Phalloidin)	

Abbreviations

LatA	Latrunculin A
GAP	GTPase activating protein
GEF	GDP-GTP exchange factor
CEN/ARS	centromer autrosomus replicative sequence
KDa	kilo Dalton
WT	wild type
TM	transmembrane domain
SP	signal peptide
N	number
DAPI	4', 6'-diamino-2-phenyldole dihydrochloride
AFM	ashbya full medium
AMM	ashbya minimal medium
aa	amino acid
NaCl	sodium chloride
ASD	ashbya synthetic dextrose
mM	millimolar
NaP	sodium phosphate
EDTA	ethylene diamine tetra acetate
SDS	dodecylsulfate
min	minute
h	hour
sec	second
M	molar
KAc	potassium acetate
vol.	volume
g	gram
EtOH	ethanol
acc.	according
MeOH	methanol
GFP	green fluorescent protein
rpm	rotations per min.
BSA	bovine synthetic albumin
DNA	deoxyribonucleinic acid
DIC	differential interference contrast
RT	room temperature
PCR	polymerase chain reaction
ORF	open reading frame
DTT	ditiotreidol
bp	base pair
µg/ml	microgram per milliliter
g/l	gram per liter
U/µg	unit/microgram
µF	micro Farad
kV	kilo Volt
et al.	and others

Acknowledgments

First, I would like to sincerely thank my thesis advisor Prof. Peter Philippsen for giving me the opportunity to perform my thesis in his lab. I deeply appreciate his support and guidance during the time we were analyzing and writing together, especially for a critical and time consuming reading of this manuscript. Thank you for all your comments. Without them I would not have achieved what I finally did.
I would also thank him for all his support in the very difficult moments for my family.

I would like to thank Dr Hans-Peter Schmitz, my “great supervisor” for introducing me into the methods of molecular genetics, for having always time and patience and for a very helpful discussions during the time of my thesis.

Further, I would like to thank the members of my thesis committee Marie-Pierre Gulli and Michael Primig for their time and suggestions on my project. Especially, I would like to say thank you to Marie-Pierre for the very motivating discussion at the time when I was lost.

I am also very thankful to Dr Yasmina Bauer and Dr Philippe Knechtle for giving me an introduction into *Ashbya gossypii* as a model organism.

Thank you to Dr Amy Glatfelter for careful listening of my seminars and helping me to improve them.

I am grateful to all present members of the lab, especially Katrin Hungerbuhler, Riccarda Rischatsch, Pesche Helfer and Michael Köhli, for all support during my entire PhD, all scientific and not scientific discussions and for all cakes that they brought to the lab. They all baked great! Thank you for your great sense of humor.

Thank you to Andreas Kaufmann, Dr Dominic Höpfner, Dr Pesche Helfer and Dr Philippe Laissue, for giving me an introduction into video-microscopy and for setting up hardware and software facilities used for the fluorescence microscopy. Without them costs of my PhD would definitely ebe levated and we would have to exchange microscopes.

I would like to thank the members of the sequencing group, Fred Dietrich, Anita Lerch, Dr Sophie Brachat and Sylvia Vögeli for providing me not only with excellent sequence information.

Doris Rossi and Sandra Götz-Krebs for taking care for all work that we in lab were not able to do.

Ulrike and Sylviane, two summer students who were working with me on some proteins involved in cell polarity, and whose work is mentioned in this thesis.

Leszek Wojnowski, for supporting me in the beginning of my scientific life and for all his help in starting up my PhD.

My family, here and in Poland.
Bez waszego wsparcia nie osiagnelabym tak wiele. Dziekuje moim rodzicom za uswiadomienie mi jak wazna jest nauka i wspieranie mnie w trudnych i wesolych chwilych. Za kazde 1600 km ktore pokonaliscie zeby sie ze mna zobaczyc. Dziekuje mojemu bratu Mackowi, ze zastapil mnie na korepetycjach jak jechalam na rozmowy kwalifikacyjne I za to ze odwiedzal mnie w Bazylei jak brkowalo mi rodziny.

I would like to thank my husband Andreas. Without his support I would not have gone through it how I finally did, especially last months…
I will never be able to thank him enough for all he did.

References

Ayad-Durieux, Y., P. Knechtle, et al. (2000). „A PAK-like protein kinase is required for maturation of young hyphae and septation in the filamentous ascomycete *Ashbya gossypii*.“ J Cell Sci **113** Pt 24: 4563-75.

Bender, A. and J. R. Pringle (1989). „Multicopy suppression of the cdc24 budding defect in yeast by CDC42 and three newly identified genes including the ras-related gene RSR1.“ Proc Natl Acad Sci U S A **86**(24): 9976-80.

Bocking, S. P., M. G. Wiebe, et al. (1999). „Effect of branch frequency in *Aspergillus oryzae* on protein secretion and culture viscosity.“ Biotechnol Bioeng **65**(6): 638-48.

Casamayor, A. and M. Snyder (2002). „Bud-site selection and cell polarity in budding yeast.“ Curr Opin Microbiol **5**(2): 179-86.

Caviston, J. P., S. E. Tcheperegine, et al. (2002). „Singularity in budding: a role for the evolutionarily conserved small GTPase Cdc42p.“ Proc Natl Acad Sci U S A **99**(19): 12185-90.

Chant, J. (1999). „Cell polarity in yeast.“ Annu Rev Cell Dev Biol **15**: 365-91.

Chant, J. and I. Herskowitz (1991). „Genetic control of bud site selection in yeast by a set of gene products that constitute a morphogenetic pathway.“ Cell **65**(7): 1203-12.

Chen, T., T. Hiroko, et al. (2000). „Multigenerational cortical inheritance of the Rax2 protein in orienting polarity and division in yeast.“ Science **290**(5498): 1975-8.

Christiansen, T., A. B. Spohr, et al. (1999). „On-line study of growth kinetics of single hyphae of *Aspergillus oryzae* in a flow-through cell.“ Biotechnol Bioeng **63**(2): 147-53.

Cullen, P. J. and G. F. Sprague, Jr. (2000). „Glucose depletion causes haploid invasive growth in yeast.“ Proc Natl Acad Sci U S A **97**(25): 13619-24.

Cullen, P. J. and G. F. Sprague, Jr. (2002). „The roles of bud-site-selection proteins during haploid invasive growth in yeast.“ Mol Biol Cell **13**(9): 2990-3004.

Dietrich, F. S., S. Voegeli, et al. (2004). „The *Ashbya gossypii* genome as a tool for mapping the ancient *Saccharomyces cerevisiae* genome.“ Science **304**(5668): 304-7.

Drubin, D. G. and W. J. Nelson (1996). „Origins of cell polarity.“ Cell **84**(3): 335-44.

Fujita, A., C. Oka, et al. (1994). „A yeast gene necessary for bud-site selection encodes a protein similar

to insulin-degrading enzymes.“ Nature **372**(6506): 567-70.

Guest, G. M., X. Lin, et al. (2004). „*Aspergillus nidulans* RhoA is involved in polar growth, branching, and cell wall synthesis.“ Fungal Genet Biol **41**(1): 13-22.

Gulli, M. P., M. Jaquenoud, et al. (2000). „Phosphorylation of the Cdc42 exchange factor Cdc24 by the PAK-like kinase Cla4 may regulate polarized growth in yeast.“ Mol Cell **6**(5): 1155-67.

Gulli, M. P. and M. Peter (2001). „Temporal and spatial regulation of Rho-type guanine-nucleotide exchange factors: the yeast perspective.“ Genes Dev **15**(4): 365-79.

Hall, A. (1998). „Rho GTPases and the actin cytoskeleton.“ Science **279**(5350): 509-14.

Halme, A., M. Michelitch, et al. (1996). „Bud10p directs axial cell polarization in budding yeast and resembles a transmembrane receptor.“ Curr Biol **6**(5): 570-9.

Harkins, H. A., N. Page, et al. (2001). „Bud8p and Bud9p, proteins that may mark the sites for bipolar budding in yeast.“ Mol Biol Cell **12**(8): 2497-518.

Harris, S. D., L. Hamer, et al. (1997). „The *Aspergillus nidulans* sepA gene encodes an FH1/2 protein involved in cytokinesis and the maintenance of cellular polarity.“ Embo J **16**(12): 3474-83.

Irazoqui, J. E., A. S. Gladfelter, et al. (2003). „Scaffold-mediated symmetry breaking by Cdc42p.“ Nat Cell Biol **5**(12): 1062-70.

Johnson, D. I. (1999). „Cdc42: An essential Rho-type GTPase controlling eukaryotic cell polarity.“ Microbiol Mol Biol Rev **63**(1): 54-105.

Kang, P. J., A. Sanson, et al. (2001). „A GDP/GTP exchange factor involved in linking a spatial landmark to cell polarity.“ Science **292**(5520): 1376-8.

Knechtle, P., F. Dietrich, et al. (2003). „Maximal polar growth potential depends on the polarisome component AgSpa2 in the filamentous fungus *Ashbya gossypii*.“ Mol Biol Cell **14**(10): 4140-54.

Kozminski, K. G., L. Beven, et al. (2003). „Interaction between a Ras and a Rho GTPase couples selection of a growth site to the development of cell polarity in yeast.“ Mol Biol Cell **14**(12): 4958-70.

Lengeler, K. B., R. C. Davidson, et al. (2000). „Signal transduction cascades regulating fungal development and virulence.“ Microbiol Mol Biol Rev **64**(4): 746-85.

Lord, M., F. Inose, et al. (2002). „Subcellular localization of Axl1, the cell type-specific regulator of polarity.“ Curr Biol **12**(15): 1347-52.

Madden, K. and M. Snyder (1998). „Cell polarity and morphogenesis in budding yeast.“ Annu Rev Microbiol **52**: 687-744.

Marston, A. L., T. Chen, et al. (2001). „A localized GTPase exchange factor, Bud5, determines the orientation of division axes in yeast.“ Curr Biol **11**(10): 803-7.

Michelitch, M. and J. Chant (1996). „A mechanism of Bud1p GTPase action suggested by mutational analysis

and immunolocalization.“ Curr Biol **6**(4): 446-54.

Momany, M. and J. E. Hamer (1997). „Relationship of actin, microtubules, and crosswall synthesis during septation in *Aspergillus nidulans*.“ Cell Motil Cytoskeleton **38**(4): 373-84.

Momany, M., R. Lindsey, et al. (2004). „The *Aspergillus fumigatus* cell wall is organized in domains that are remodelled during polarity establishment.“ Microbiology **150**(Pt 10): 3261-8.

Momany, M. and I. Taylor (2000). „Landmarks in the early duplication cycles of *Aspergillus fumigatus* and *Aspergillus nidulans:* polarity, germ tube emergence and septation.“ Microbiology **146 Pt 12**: 3279-84.

Park, H. O., J. Chant, et al. (1993). „BUD2 encodes a GTPase-activating protein for Bud1/Rsr1 necessary for proper bud-site selection in yeast.“ Nature **365**(6443): 269-74.

Pruyne, D. and A. Bretscher (2000). „Polarization of cell growth in yeast.“ J Cell Sci **113 (Pt 4)**: 571-85.

Pruyne, D. and A. Bretscher (2000). „Polarization of cell growth in yeast. I. Establishment and maintenance of polarity states.“ J Cell Sci **113 (Pt 3)**: 365-75.

Pruyne, D., A. Legesse-Miller, et al. (2004). „Mechanisms of polarized growth and organelle segregation in yeast.“ Annu Rev Cell Dev Biol **20**: 559-91.

Regalado, C. M. (1998). „Roles of calcium gradients in hyphal tip growth: a mathematical model.“ Microbiology **144 (Pt 10)**: 2771-82.

Riquelme, M. and S. Bartnicki-Garcia (2004). „Key differences between lateral and apical branching in hyphae of *Neurospora crassa*.“ Fungal Genet Biol **41**(9): 842-51.

Robson, G. D., E. Prebble, et al. (1996). „Polarized Growth of Fungal Hyphae Is Defined by an Alkaline pH Gradient.“ Fungal Genet Biol **20**(4): 289-98.

Roemer, T., L. G. Vallier, et al. (1996). „Selection of polarized growth sites in yeast.“ Trends Cell Biol **6**(11): 434-41.

Sanders, S. L. and I. Herskowitz (1996). „The BUD4 protein of yeast, required for axial budding, is localized to the mother/BUD neck in a cell cycle-dependent manner.“ J Cell Biol **134**(2): 413-27.

Spohr, A., C. Dam-Mikkelsen, et al. (1998). „On-line study of fungal morphology during submerged growth in a small flow-through cell.“ Biotechnol Bioeng **58**(5): 541-53.

Steiner, S., J. Wendland, et al. (1995). „Homologous recombination as the main mechanism for DNA integration and cause of rearrangements in the filamentous ascomycete *Ashbya gossypii*.“ Genetics **140**(3): 973-87.

Taheri, N., T. Kohler, et al. (2000). „Asymmetrically localized Bud8p and Bud9p proteins control yeast cell polarity and development.“ Embo J **19**(24): 6686-96.

That, T. C., C. Rossier, et al. (1988). „Induction of multiple germ tubes in *Neurospora crassa* by antitubulin agents.“ Eur J Cell Biol **46**(1): 68-79.

Virag, A. and A. J. Griffiths (2004). „A mutation in the *Neurospora crassa* actin gene results in multiple defects in tip growth and branching.“ Fungal Genet Biol **41**(2): 213-25.

Wedlich-Soldner, R., S. Altschuler, et al. (2003). „Spontaneous cell polarization through actomyosin-based delivery of the Cdc42 GTPase.“ Science **299**(5610): 1231-5.

Wendland, J., Y. Ayad-Durieux, et al. (2000). „PCR-based gene targeting in the filamentous fungus *Ashbya gossypii.*“ Gene **242**(1-2): 381-91.

Wendland, J. and P. Philippsen (2000). „Determination of cell polarity in germinated spores and hyphal tips of the filamentous ascomycete *Ashbya gossypii* requires a rho-GAP homolog.“ J Cell Sci **113 (Pt 9)**: 1611-21.

Wendland, J. and P. Philippsen (2001). „Cell polarity and hyphal morphogenesis are controlled by multiple rho-protein modules in the filamentous ascomycete *Ashbya gossypii*.“ Genetics **157**(2): 601-10.

Wright, M. C. and P. Philippsen (1991). „Replicative transformation of the filamentous fungus *Ashbya gossypii* with plasmids containing Saccharomyces cerevisiae ARS elements.“ Gene **109**(1): 99-105.

Zahner, J. E., H. A. Harkins, et al. (1996). „Genetic analysis of the bipolar pattern of bud site selection in the yeast *Saccharomyces cerevisiae*.“ Mol Cell Biol **16**(4): 1857-70.

Hoepfner, D., A. Brachat, and P. Philippsen. 2000. “Time-lapse video microscopy analysis reveals astral microtubule detachment in the yeast spindle pole mutant cnm67. Mol Biol Cell **11**:1197-211.

Ich erkläre, dass ich die Dissertation

„The role of AgRax1p, AgRax2p, AgBud7p and AgBud10p in mycelial development of the filamentous fungus Ashbya gossypii“

nur mit der darin angegebenen Hilfe verfasst und bei keiner anderen Fakultät eingereicht habe.

Basel, Juni 2005

Kamila Wojnowska-Boudier